Angewandte Chemie
Eine Zeitschrift der Gesellschaft Deutscher Chemiker

Supporting Information

Contorted Polycyclic Aromatic Hydrocarbons with Two Embedded Azulene Units

*Xuan Yang, Frank Rominger, and Michael Mastalerz**

anie_201908643_sm_miscellaneous_information.pdf

Supporting Information

Table of Contents

1. General remarks S3

2. Experimental part S4

3. NMR spectra S14

4. Mass spectra S40

5. FT-IR spectra S49

6. UV/vis and fluorescence spectra S54

7. Cyclovoltammograms S59

8. DFT calculations S64

9. X-ray crystallographic structure determination S73

10. Temperature dependant ^{1}H NMR of compound 13 ..... S76

11. Chiral HPLC chromatogram S77

12. References S79

1. General remarks

All reagents and solvents were obtained from Fisher Scientific, Alfa Aesar, Sigma-Aldrich or VWR and were used without further purification unless otherwise noted. For thin layer chromatography silica gel 60 F254 plates from Merck were used and examined under UV-light irradiation (254 nm and 365 nm). Flash column chromatography was performed on silica gel from Sigma-Aldrich (particle size: 0.04-0.063 mm) using petroleum ether, dichloromethane and/or ethyl acetate. Melting points (not corrected) were measured with a Büchi Melting Point B-545. IR-Spectra were recorded on a Bruker Lumos spectrometer on a Ge ATR crystal. NMR spectra were taken on Bruker Avance 300 (300 MHz) , Bruker Avance III 400 (400 MHz) or Bruker Avance III 600 (600 MHz) spectrometer. Chemical shifts (δ) are reported in parts per million (ppm) relative to traces of $CHCl_3$ (δ_H = 7.26 ppm, δ_C = 77.0 ppm), CH_2Cl_2 (δ_H = 5.32 ppm, δ_C = 54.0 ppm) or tetrachloroethane (δ_H = 5.963 ppm, δ_C = 73.78 ppm) in the corresponding deuterated solvent. Signals were assigned by 2D NMR experiments (^{1}H,^{1}H-COSY, ^{1}H,^{1}H-NOESY, ^{1}H,^{1}H-ROESY, ^{1}H,^{13}C-HSQC, ^{1}H,^{13}C-HMBC). HRMS experiments were carried out on a Fourier Transform Ion Cyclotron Resonance (FTICR) mass spectrometer solariX (Bruker Daltonik GmbH, Bremen, Germany) equipped with a 7.0 T superconducting magnet and interfaced to an Apollo II Dual ESI/MALDI source. Absorption spectra were recorded on a Jasco UV-VIS V-730. Emission spectra were recorded on a Jasco FP-8300. Quantum yields Φ were obtained by the absolute method[S1] using an PTI Quantum Master 40 with an Ulbricht sphere. Given Φ for solutions are average values of three independent measurements. Electrochemical data were obtained in dichloromethane or *o*-dichlorobenzene solution of *n*-Bu_4NClO_4 (0.1 M), as indicated. Ferrocene was used as an internal standard. Cyclic voltammagrams were obtained using a glassy carbon working electrode, a Pt counter electrode, and a Ag reference electrode. Elemental Analysis was performed by the Microanalytical Laboratory of the University of Heidelberg using an Elementar Vario EL machine. Crystal structure analysis was accomplished on a STOE Stadivari diffractometer with a copper source (Cu K_α = 1.54178Å). Dibromide **6** was synthesized via our previously reported synthetic route.[S2] The geometry optimizations were performed using DFT calculations at B3LYP/6-311G* using Spartan 14. Time-dependent DFT (TDDFT) calculation for the $S_0 \rightarrow S_n$ transitions using the same function and basis set were performed based on the optimized structures at ground states using Gaussian 09 package.[S3] Typically, the lowest 30 singlet roots of the nonhermitian eigenvalue equations were obtained to determine the vertical excitation energies.

2. Experimental part

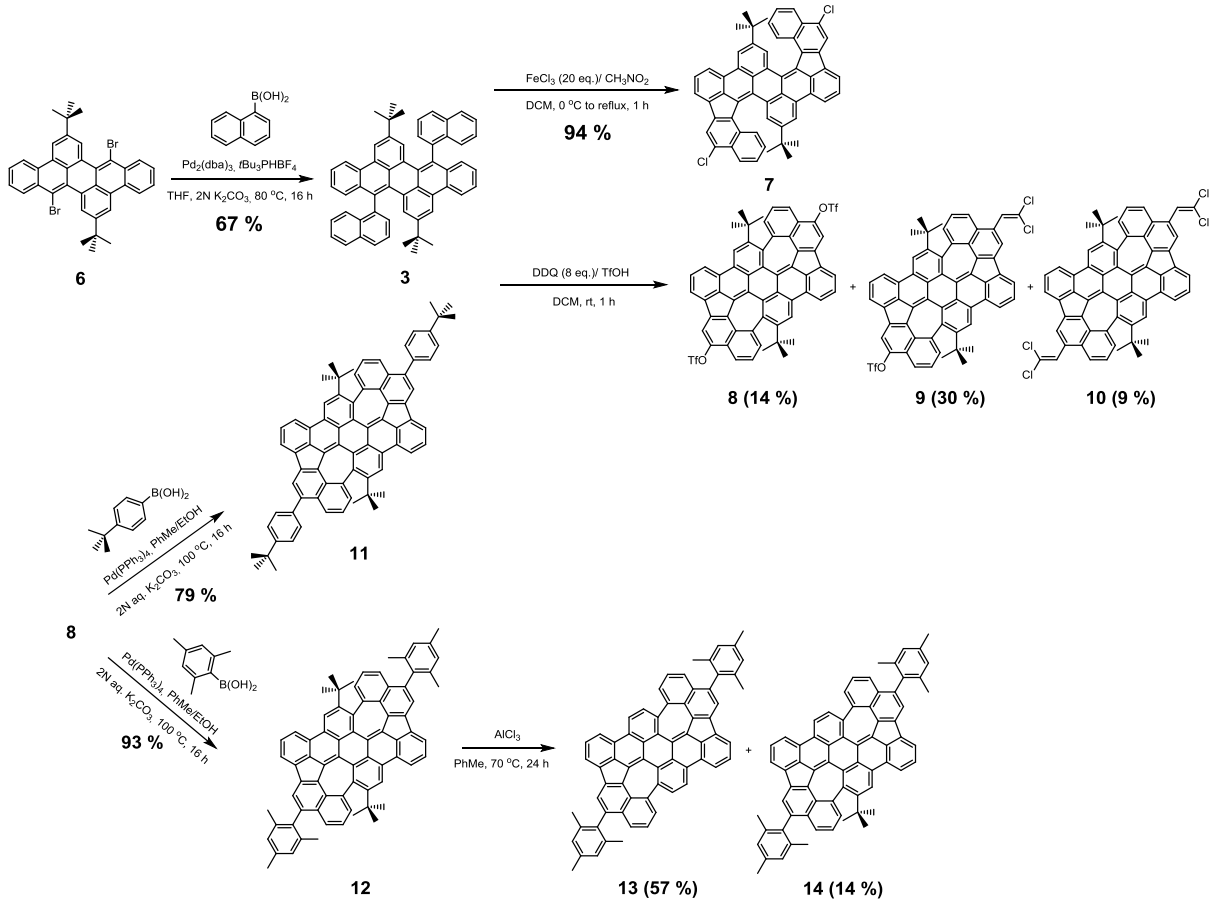

Scheme S1. Overview of the synthetic routes and isolated yields of all target molecules.

2,10-Di-*tert*-butyl-8,16-di(naphthalen-1-yl)dibenzo[*fg,qr*]pentacene (3)

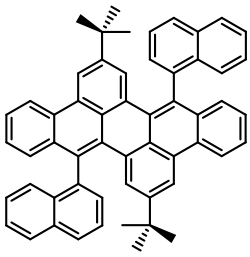

In a screw-capped vial a mixture of $Pd_2(dba)_3$ (68 mg, 0.075 mmol) and *t*-Bu_3PHBF_4 (68 mg, 0.237 mmol) was added to a suspension of dibromide **6** (468 mg, 0.75 mmol), 1-naphthaleneboronic acid (1.03 g, 6.0 mmol) and K_2CO_3 (332 mg, 2.4 mmol) in argon-degassed THF/water (4.5 mL/1.2 mL). The mixture was stirred vigorously at 80 ^oC overnight under argon atmosphere. After cooling to room temperature, the mixture was diluted with dichloromethane (100 mL), washed with water (3 × 50 mL) and the organic layer dried over Na_2SO_4. After removal of the solvent by rotary evaporation, the crude product was purified by silica gel column chromatography (petroleum ether/dicholomethane 10:1) to give after precipitation from dichloromethane/methanol and drying in vaccum the product **3** (as mixture of atropisomers) as yellow solid (362 mg, 67 %).

m.p.: 360 ^oC (dec.). ^1H NMR (600 MHz, $Cl_2CDCDCl_2$) δ (ppm) = 8.67 (d, *J*= 8.3 Hz, 1H), 8.63 (d, *J*= 8.3 Hz, 1H), 8.45 (d, *J*= 1.3 Hz, 1H), 8.40 (d, *J*= 1.3 Hz, 1H), 8.04 (d, *J*= 8.3 Hz, 1H), 7.97 (d, *J*= 8.2 Hz, 1H), 7.95 (d, *J*= 8.3 Hz, 2H), 7.74 (d, *J*= 1.6 Hz, 1H), 7.65 (d, *J*= 7.0 Hz, 1H), 7.62 (d, *J*= 7.1 Hz, 1H), 7.58 (d, *J*= 7.6 Hz, 2H), 7.57 - 7.52 (m, 3H), 7.48 (d, *J*= 1.6 Hz, 1H), 7.47 - 7.43 (m, 1H), 7.42 (d, *J*= 8.0 Hz, 1H), 7.41 - 7.38 (m, 1H), 7.29 (dd, *J*= 7.4, 6.9 Hz, 1H), 7.28 - 7.25 (m, 1H), 7.24 - 7.17 (m, 3H), 7.10 (d, *J*= 8.3 Hz, 1H), 0.77 (s, 10H), 0.68 (s, 8H). ^{13}C NMR (151 MHz, $Cl_2CDCDCl_2$) δ (ppm) = 148.60, 148.50, 139.60, 139.53, 134.51, 134.19, 133.94, 133.66, 133.15, 133.04, 132.73, 132.29, 130.88, 130.74, 129.80, 129.50, 129.32, 129.02, 128.96, 128.85, 128.80, 128.73, 128.36, 128.30, 128.05, 127.96, 127.92, 127.83, 127.43, 127.33, 127.19, 126.96, 126.93, 126.83, 126.70, 126.59, 126.44, 126.32, 126.30, 126.05, 125.94, 122.12, 122.09, 117.12, 117.03, 34.28, 34.23, 30.61, 30.49. FT-IR (ATR) $\tilde{\nu}$ (cm^{-1}) = 3061 (w), 3008 (w), 2960 (m), 2904 (w), 2866 (w), 1937 (w), 1823 (w), 1798 (w), 1703 (w), 1607 (w), 1573 (w), 1506 (w), 1475 (w), 1462 (w), 1446 (w), 1422 (w), 1395 (w), 1363 (m), 1318 (w), 1296 (w), 1273 (w), 1233 (w), 1215 (w), 1153 (w), 1123 (w), 1066 (w), 1038 (w), 1018 (w), 985 (w), 970 (w), 952 (w), 927 (w), 895 (m), 874 (m), 798 (w), 776 (s), 757 (s), 713 (s), 700 (w), 672 (w), 648 (m), 636 (m), 609 (w). UV/Vis ($CHCl_3$): λ_{max} (nm) (log ε) = 288 (4.57), 301 (4.64), 308 (4.66), 385 (4.22), 407 (4.46), 429 (4.47). Fluorescence ($CHCl_3$): λ_{em} (λ_{ex}) (nm) = 466 (407). Φ= 57.4±1.5%. HRMS-MALDI (DCTB) (*m*/*z*): $[M]^+$ calcd. for $C_{56}H_{44}$, 716.3443; found, 716.3432. Elemental anal. calcd. for $C_{56}H_{44}$: C 93.81, H 6.19, found: C 93.81, H 6.26.

11,23-di-*tert*-butyl-5,17-dichlorodibenzo[*hi*,*st*]benzo[4,5]indeno[1,2,3-*de*]benzo[4,5]indeno[1,2,3-*op*]pentacene (7)

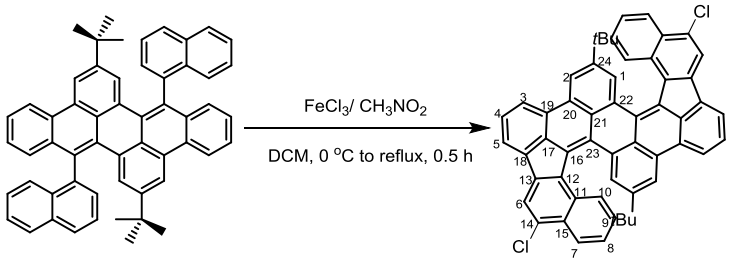

In a 250 mL Schlenk flask, a solution of **3** (115 mg, 0.16 mmol) in dry dichloromethane (150 mL) was purged with argon for 15 min. A solution of $FeCl_3$ (519 mg, 3.2 mmol) in nitromethane (1.2 mL) was then added dropwise at 0 °C. The mixture was stirred at 0 °C for 5 minutes while continuing to bubble argon gas through the mixture. The mixture was then heated up to reflux for 1 hour. The reaction was quenched by adding methanol (5 mL). The mixture was washed with water (3 × 50 mL) and dried over Na_2SO_4. After removal of the solvent by rotary evaporation, the residue was refluxed in 10 mL *n*-heptane for 10 minutes. After cooling down to room temperature, the suspension was filtered off and the solid was washed with *n*-hexane (2 × 5 mL). The product **7** was obtained as dark-purple solid (118 mg, 94 %) after drying in vacuum.

m.p.: >400 °C. ^{1}H NMR (600 MHz, $Cl_2CDCDCl_2$, 298 K) δ (ppm) = 8.60 (s, 2H, H-2), 8.53 (d, *J*= 8.1 Hz, 2H, H-3), 8.29 (d, *J*= 8.4 Hz, 2H, H-7), 8.22 (s, 2H, H-6), 8.06 (s, 2H, H-1), 8.06 (d, *J*= 4.3 Hz, 2H, H-5), 7.80 (dd, *J*= 12.4, 4.9 Hz, 4H, H-4, 10), 7.43 - 7.37 (m, 2H, H-8), 7.07 - 7.00 (m, 2H, H-9), 0.95 (s, 18H). ^{13}C NMR (151 MHz, $Cl_2CDCDCl_2$, 343 K) δ (ppm) = 149.54 (C-24), 140.34 (C-13), 135.78 (C-19), 134.63 (C-17), 133.76 (C-12), 133.07 (C-11), 132.36 (C-23), 131.66 (C-16), 131.20 (C-22), 131.15 (C-1), 130.54 (C-15), 130.17 (C-20), 129.72 (C-21), 129.49 (C-14), 128.38 (C-10), 127.88 (C-4), 126.91 (C-9), 126.70 (C-18), 126.01 (C-8), 125.52 (C-7), 122.26 (C-3), 120.27 (C-6), 120.09 (C-2), 120.04 (C-5), 34.72, 30.48. FT-IR (ATR) $\tilde{\nu}$ (cm^{-1}) = 3070 (w), 2961 (m), 2903 (w), 2867 (w), 1896 (w), 1779 (w), 1601 (w), 1575 (m), 1548 (w), 1514 (w), 1478 (w), 1460 (w), 1441 (w), 1414 (w), 1390 (m), 1360 (w), 1342 (w), 1305 (w), 1265 (w), 1244 (w), 1223 (w), 1198 (w), 1178 (w), 1146 (w), 1110 (w), 1030 (w), 949 (w), 933 (m), 878 (w), 867 (m), 823 (w), 810 (w), 784 (w), 757 (m), 742 (s), 707 (m), 675 (w), 658 (w), 638 (w), 620 (w). UV/Vis ($CHCl_3$): λ_{max} (nm) (log ε) = 270 (4.80), 308 (4.68), 324 (4.68), 423 (4.14), 509 (4.50), 542 (4.61). Fluorescence ($CHCl_3$): λ_{em} (λ_{ex}) (nm) = 570, 614 (509). Φ= 15.8±1.0%. HRMS-MALDI (DCTB) (*m*/*z*): $[M]^+$ calcd. for $C_{56}H_{38}Cl_2$, 780.2350; found, 780.2351. Elemental anal. calcd. for $C_{56}H_{38}Cl_2 \cdot 0.5CHCl_3$: C 80.64, H 4.61, found: C 80.61, H 4.89.

Scholl cyclization of PAH 2 using DDQ/TfOH

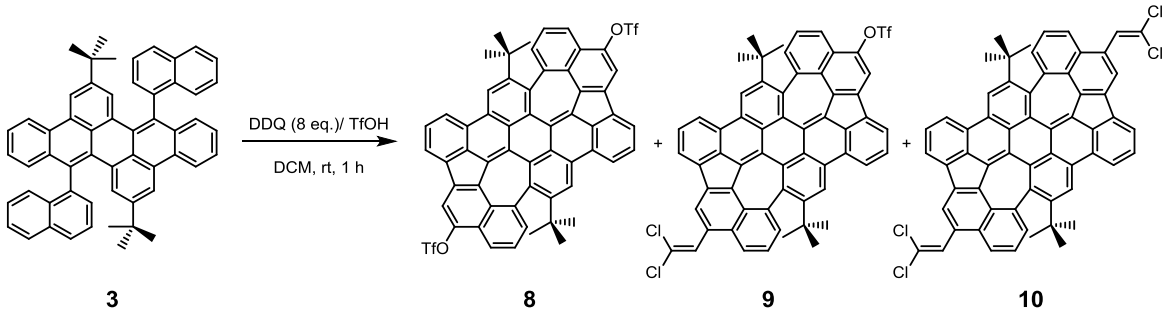

In a 100 mL Schlenk flask, a solution of PAH **3** (72 mg, 0.1 mmol) in dry dichloromethane (60 mL) was purged with argon for 15 min. 2,3-Dichloro-5,6-dicyano-1,4-benzoquinone (DDQ, 182 mg, 0.8 mmol) was added in one portion at room temperature. First portion (1 mL) of trifluoromethanesulfonic acid (TfOH) was then added dropwise. After stirring at room temperature for 5 minutes, another portion (2 mL) of TfOH was added dropwise. The mixture was stirred at room temperature for 1 hour. The reaction was quenched by pouring into saturated aq. $NaHCO_3$ (100 mL). After stirring vigorously for 15 minutes, the mixture was extracted with dichloromethane (3 × 50 mL) and the organic layers combinded. The organic phase was washed with aq. NH_4Cl (100 mL), water (100 mL) and dried over anhydrous Na_2SO_4. After removal of the solvent by rotary evaporation, the crude product mixture was separated by silica gel column chromatography (petroleum ether/chloroform/ethyl acetate 30:1:1 to 30:2:1). The three fractions were obtained after precipitation from dichloromethane/methanol and drying in vacuum, respectively, as dark-blue solid, with yields of product **8** (14 mg, 14%, third fraction, R_f= 0.25), product **9** (29 mg, 30%, second fraction, R_f= 0.30) and product **10** (8 mg, 9%, first fraction, R_f= 0.35).

Azulene-PAH 8

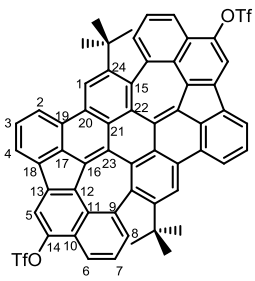

m.p.: > 400 °C. ^{1}H NMR (600 MHz, $CDCl_3$) δ (ppm) = 8.90 (s, 2H, H-1), 8.45 (d, *J*= 8.0 Hz, 2H, H-2), 8.12 (d, *J*= 7.0 Hz, 2H, H-4), 8.09 (d, *J*= 9.2 Hz, 4H, H-6,5), 7.87 - 7.83 (m, 2H, H-3), 7.45 - 7.40 (m, 2H, H-7), 7.05 (d, *J*= 7.0 Hz, 2H, H-8), 0.97 (s, 18H). ^{13}C NMR (151 MHz, $CDCl_3$) δ (ppm) = 153.91 (C-24), 143.81 (C-14), 135.72 (C-9), 135.06 (C-15), 135.04 (C-8), 134.94 (C-19), 134.70 (C-11), 134.09 (C-12), 133.71 (C-13), 133.21 (C-20), 131.49 (C-17), 130.65 (C-16), 130.34 (C-22), 129.80 (C-21), 128.08 (C-3), 126.16 (C-18), 125.66 (C-1), 125.48 (C-23), 125.00 (C-7), 124.71 (C-10), 120.81 (C-2), 120.75 (C-4), 120.45 (C-6), 118.89 (q, $J_{C\text{-}F}$= 320.6 Hz, -CF_3), 113.25 (C-5), 38.90, 33.47. FT-IR (ATR) $\tilde{\nu}$ (cm^{-1}) = 3066(w), 2963 (m), 2936 (w), 2911 (w), 2871 (w), 1928 (w), 1791 (w), 1744 (w), 1617 (w), 1585 (m), 1554 (w), 1478 (w), 1467 (w), 1424 (s), 1365 (w), 1347 (m), 1300 (w), 1244 (m), 1209 (s), 1136 (s), 1076 (w), 1057 (w), 1036 (w), 1001 (s), 973 (w), 947 (w), 927 (w), 892 (m), 862 (m), 840 (s), 821 (m), 806 (s), 780 (w), 757 (w), 714 (m), 690 (w), 670 (w), 658 (w), 636 (w), 608 (w). UV/Vis ($CHCl_3$): λ_{max} (nm) (log ε) = 280 (4.91), 329 (4.82), 377 (4.54), 397 (4.52), 424 (4.37), 460 (4.06), 500 (4.08), 546 (4.24), 582 (4.48), 628 (4.55). Fluorescence ($CHCl_3$): λ_{em} (λ_{ex}) (nm) = 648

(280). Φ= 19.8±1.0%. HRMS-MALDI (DCTB) (*m*/*z*): $[M]^+$ calcd. for $C_{58}H_{34}F_6O_6S_2$, 1004.1701; found, 1004.1704. Elemental anal. calcd. for $C_{58}H_{34}F_6O_6S_2 \cdot 0.5H_2O$: C 68.70, H 3.48, found: C 68.68, H 3.52.

Azulene-PAH 9

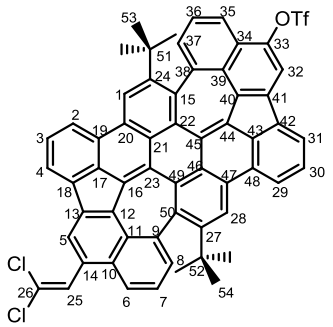

m.p.: > 400 °C. ^{1}H NMR (600 MHz, CD_2Cl_2) δ (ppm) = 8.78 (s, 1H, H-28), 8.77 (s, 1H, H-1), 8.33 (d, *J*= 8.0 Hz, 1H, H-29), 8.27 (d, *J*= 7.8 Hz, 2H, H-5,2), 8.02 (d, *J*= 7.0 Hz, 1H, H-31), 8.01 (s, 1H, H-32), 7.98 - 7.95 (m, 2H, H-35,4), 7.80 (d, *J*= 8.1 Hz, 1H, H-6), 7.77 (t, *J*= 7.4 Hz, 1H, H-30), 7.73 (t, *J*= 7.4 Hz, 1H, H-3), 7.38 (s, 1H, H-25), 7.30 (t, *J*= 7.7 Hz, 1H, H-36), 7.21 (t, *J*= 7.6 Hz, 1H, H-7), 7.00 (d, *J*= 7.1 Hz, 1H, H-37), 6.82 (d, *J*= 7.0 Hz, 1H, H-8), 0.89 (s, 9H, H-54), 0.88 (s, 9H, H-53). ^{13}C NMR (151 MHz, CD_2Cl_2) δ (ppm) = 154.43 (C-24), 154.15 (C-27), 144.30 (C-33), 136.73 (C-9), 136.51 (C-50), 136.33 (C-39), 136.17 (C-15), 135.71 (C-37), 135.62 (C-12), 135.42 (C-38), 135.29 (C-48), 135.11 (C-8), 135.07 (C-11), 135.03 (C-13), 134.67 (C-19), 134.62 (C-46), 134.04 (C-41), 133.99 (C-40), 133.62 (C-20), 132.37 (C-17), 131.95 (C-45), 131.86 (C-43), 131.10 (C-49), 130.64 (C-22), 130.40 (C-10), 130.24 (C-44), 130.20 (C-16), 130.18 (C-47), 128.51 (C-3), 128.43 (C-30), 128.31 (C-14), 128.06 (C-25), 126.72 (C-42), 126.50 (C-18), 126.41 (C-1), 126.14 (C-28), 126.01 (C-23), 125.83 (C-21), 125.61 (C-36), 125.20 (C-34), 124.73 (C-7), 124.02 (C-6), 123.74 (C-26), 122.22 (C-5), 121.35 (C-29), 121.12 (C-31), 120.91 (C-35), 120.88 (C-2), 120.76 (C-4), 119.48 (q, $J_{C\text{-}F}$= 320.5 Hz, $-CF_3$), 113.76 (C-32), 39.38 (C-51), 39.36 (C-52), 33.80 (C-54), 33.76 (C-53). FT-IR (ATR) $\tilde{\nu}$ (cm^{-1}) = 3064 (w), 2962 (w), 2932 (w), 2908 (w), 2869 (w), 1924 (w), 1789 (w), 1584 (m), 1552 (w), 1477 (w), 1467 (w), 1425 (m), 1364 (w), 1349 (w), 1299 (w), 1244 (m), 1209 (s), 1138 (m), 1094 (w), 1067 (w), 1008 (m), 987 (w), 972 (w), 949 (w), 930 (w), 912 (m), 876 (m), 834 (m), 808 (m), 779 (w), 755 (s), 732 (w), 713 (w), 694 (w), 677 (w), 653 (w), 636 (w). UV/Vis ($CHCl_3$): λ_{max} (nm) (log ε) = 280 (4.82), 331 (4.71), 383 (4.42), 404 (4.41), 427 (4.27), 468 (3.90), 506 (3.96), 552 (4.14), 590 (4.38), 636 (4.44). Fluorescence ($CHCl_3$): λ_{em} (λ_{ex}) (nm) = 662 (280). Φ= 26.5±1.0%. HRMS-MALDI (DCTB) (*m*/*z*): $[M]^+$ calcd. for $C_{59}H_{35}Cl_2F_3O_3S$, 950.1636; found, 950.1633. Elemental anal. calcd. for $C_{59}H_{35}Cl_2F_3O_3S$: C 74.45, H 3.71, found: C 74.61, H 4.14.

Azulene-PAH 10

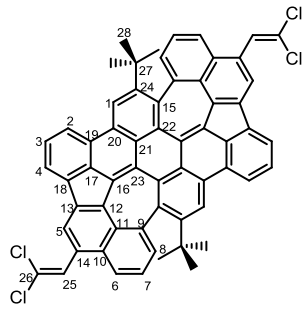

m.p.: > 400 °C. ^{1}H NMR (600 MHz, $CDCl_3$) δ (ppm) = 8.95 (s, 2H, H-1), 8.48 (d, *J*= 8.0 Hz, 2H, H-2), 8.39 (s, 2H, H-5), 8.15 (d, *J*= 7.0 Hz, 2H, H-4), 7.96 (d, *J*= 8.1 Hz, 2H, H-6), 7.84 (t, *J*= 7.5 Hz, 2H,

H-3), 7.49 (s, 2H, H-25), 7.39 (t, *J*= 7.7 Hz, 2H, H-7), 7.07 (d, *J*= 7.1 Hz, 2H, H-8), 1.06 (s, 18H, H-28). ^{13}C NMR (151 MHz, $CDCl_3$) δ (ppm) = 153.52 (C-24), 136.45 (C-9), 135.95 (C-19,15), 135.15 (C-12), 134.92 (C-11), 134.40 (C-8), 134.15 (C-13), 133.59 (C-20), 131.83 (C-17), 130.29 (C-22), 129.96 (C-10), 129.68 (C-16), 127.96 (C-3), 127.73 (C-14), 127.41 (C-25,23), 126.33 (C-18), 125.68 (C-21), 125.49 (C-1), 124.01 (C-7), 123.68 (C-6), 123.49 (C-26), 121.84 (C-5), 120.33 (C-2,4), 38.87 (C-27), 33.67 (C-28). FT-IR (ATR) $\tilde{\nu}$ (cm^{-1}) = 3064 (w), 3011 (w), 2962 (w), 2929 (w), 2908 (w), 2869 (w), 1927 (w), 1735 (w), 1622 (w), 1586 (m), 1548 (w), 1478 (w), 1428 (m), 1399 (w), 1383 (w), 1364 (w), 1352 (w), 1334 (w), 1297 (w), 1281 (w), 1245 (w), 1223 (w), 1178 (w), 1151 (w), 1134 (w), 1080 (w), 1065 (w), 1013 (w), 971 (w), 919 (m), 906 (m), 893 (w), 879 (m), 857 (w), 844 (w), 809 (m), 798 (w), 776 (w), 755 (s), 734 (m), 712 (m), 695 (m), 669 (w), 650 (w), 624 (w). UV/Vis ($CHCl_3$): λ_{max} (nm) (log ε) = 282 (4.97), 332 (4.84), 386 (4.57), 409 (4.55), 431 (4.41), 472 (4.04), 511 (4.11), 557 (4.28), 597 (4.52), 644 (4.58). Fluorescence ($CHCl_3$): λ_{em} (λ_{ex}) (nm) = 671 (282). Φ= 23.6±1.0%. HRMS-MALDI (DCTB) (*m*/*z*): $[M]^+$ calcd. for $C_{60}H_{36}Cl_4$, 898.1548; found, 898.1580. Elemental anal. calcd. for $C_{60}H_{36}Cl_4 \cdot 0.5H_2O$: C 79.39, H 4.11, found: C 79.08, H 4.32.

Azulene-PAH 11

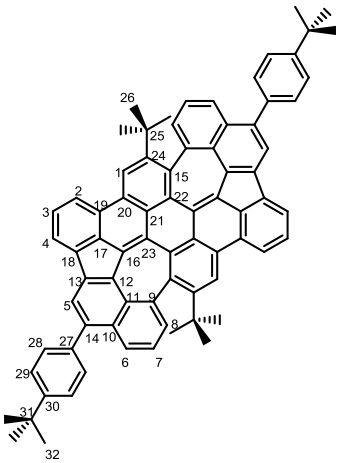

In a screw-capped vial, $Pd(PPh_3)_4$ (3.5 mg, 3 μmol) was added to a suspension of azulene bistriflate **8** (30 mg, 0.03 mmol), (4-(*tert*-butyl)phenyl)boronic acid (22 mg, 0.12 mmol) and 2M aq. K_2CO_3 (0.07 mL, 0.14 mmol) in argon-degassed toluene/ethanol (0.22 mL/0.07 mL). The mixture was stirred vigorously at 100 ^{o}C overnight under argon atmosphere. After cooling to room temperature, the mixture was diluted with dichloromethane (20 mL), washed with water (2 × 20 mL) and dried over Na_2SO_4. After removal of the solvent by rotary evaporation, the crude product was purified by silica gel column chromatography (petroleum ether/ethyl acetate 30:1). After precipitation from dichloromethane/methanol and drying in vaccum azulene PAH **11** was obtained as a dark-green to dark-blue solid (23 mg, 79%).

m.p.: >400 ^{o}C. ^{1}H NMR (600 MHz, CD_2Cl_2) δ (ppm) = 8.97 (s, 2H, H-1), 8.48 (d, *J*=8.1 Hz, 2H, H-2), 8.13 (s, 2H, H-5), 8.12 (d, *J*= 7.0 Hz, 2H, H-4), 8.02 (d, *J*= 8.2 Hz, 2H, H-6), 7.82 (t, *J*= 7.5 Hz, 2H, H-3), 7.65 - 7.60 (m, 8H, H-28,29), 7.24 (dd, *J*= 8.1, 7.2 Hz, 2H, H-7), 6.95 (d, *J*= 7.0 Hz, 2H, H-8), 1.46 (s, 18H, H-32), 1.09 (s, 18H, H-26). ^{13}C NMR (151 MHz, CD_2Cl_2) δ (ppm) = 154.04 (C-24), 151.20 (C-30), 138.67 (C-27), 138.36 (C-14), 136.96 (C-9), 136.89 (C-15), 136.84 (C-19), 136.32 (C-11), 135.19 (C-13), 134.95 (C-8), 134.66 (C-12), 134.38 (C-20), 132.52 (C-16), 132.43 (C-17), 131.16 (C-10), 130.52 (C-22), 130.32 (C-28), 130.06 (C-23), 128.45 (C-3), 126.90 (C-18), 126.46 (C-6), 126.33 (C-21), 126.26 (C-1), 126.02 (C-29), 124.26 (C-7), 122.20 (C-5), 120.82 (C-2), 120.78 (C-4), 39.35 (C-25), 35.16 (C-31), 33.97 (C-26), 31.77 (C-32). FT-IR (ATR) $\tilde{\nu}$ (cm^{-1}) = 3062 (w), 2957 (w),

2931 (w), 2902 (w), 2865 (w), 1912 (w), 1623 (w), 1586 (w), 1550 (w), 1511 (w), 1473 (w), 1462 (w), 1428 (m), 1386 (w), 1361 (w), 1299 (w), 1267 (w), 1244 (w), 1223 (w), 1200 (w), 1176 (w), 1149 (w), 1133 (w), 1117 (w), 1062 (w), 1019 (w), 954 (w), 933 (w), 909 (w), 887 (w), 836 (m), 809 (m), 777 (w), 755 (s), 732 (w), 713 (m), 698 (w), 671 (w), 652 (w), 644 (w), 629 (w), 608 (w). UV/Vis ($CHCl_3$): λ_{max} (nm) (log ε) = 281 (4.98), 332 (4.87), 380 (4.54), 409 (4.55), 432 (4.35), 470 (4.05), 506 (4.14), 557 (4.27), 594 (4.50), 641 (4.55). Fluorescence ($CHCl_3$): λ_{em} (λ_{ex}) (nm) = 667 (594). Φ= 28.4±1.0%. HRMS-MALDI (DCTB) (*m*/*z*): $[M]^+$ calcd. for $C_{76}H_{60}$, 972.4695; found, 972.4723. Elemental anal. calcd. for $C_{76}H_{60}$: C 93.79, H 6.21, found: C 93.53, H 6.48.

Azulene-PAH 12

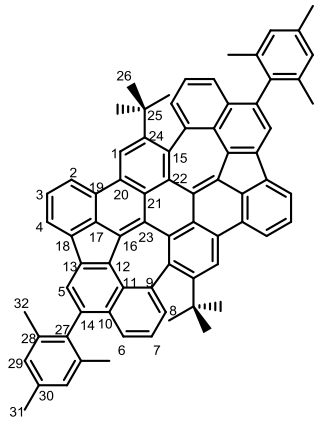

In a screw-capped vial, $Pd(PPh_3)_4$ (3.5 mg, 3 µmol) was added to a suspension of azulene bistriflate **8** (30 mg, 0.03 mmol), 2,4,6-trimethylphenylboronic acid (49 mg, 0.3 mmol) and 2M aq. K_2CO_3 (0.07 mL, 0.14 mmol) in argon-degassed toluene/ethanol (0.22 mL/0.07 mL. The mixture was stirred vigorously at 100 ^oC overnight) under argon atmosphere. After cooling to room temperature, the mixture was diluted with dichloromethane (20 mL), washed with water (2 × 20 mL) and the combinded organic layer dried over Na_2SO_4. After removal of the solvent by rotary evaporation, the crude product was purified by silica gel column chromatography (petroleum ether/dichloromethane/ethyl acetate 15:1:0 to 40:2:1). To give after precipitation from dichloromethane/methanol and drying in vacuum azulene PAH **12** as a dark-blue solid (26 mg, 93%).

m.p.: >400 ^oC. ^1H NMR (600 MHz, CD_2Cl_2) δ (ppm) = 9.03 (s, 2H, H-1), 8.56 (d, *J*= 8.0 Hz, 2H, H-2), 8.17 (d, *J*= 7.0 Hz, 2H, H-4), 8.02 (s, 2H, H-5), 7.86 (t, *J*= 7.5 Hz, 2H, H-3), 7.43 (d, *J*= 8.2 Hz, 2H, H-6), 7.32 - 7.26 (m, 2H, H-7), 7.10 (d, *J*= 2.3 Hz, 4H, H-29), 7.08 (d, *J*= 7.0 Hz, 2H, H-8), 2.43 (s, 6H, H-31), 2.04 (s, 6H, H-32), 2.02 (s, 6H, H-32), 1.11 (s, 18H, H-26). ^{13}C NMR (151 MHz, CD_2Cl_2) δ (ppm) = 154.04 (C-24), 137.94 (C-28), 137.68 (C-30), 137.52 (C-28), 137.36 (C-27), 137.11 (C-19), 137.06 (C-14), 136.98 (C-9), 136.93 (C-15), 136.23 (C-11), 135.44 (C-13), 134.79 (C-8), 134.50 (C-20), 134.35 (C-12), 132.70 (C-16), 132.50 (C-17), 131.58 (C-10), 130.57 (C-22), 130.10 (C-23), 128.80 (C-21), 128.74 (C-29), 128.53 (C-3), 127.07 (C-18), 126.44 (C-21), 126.22 (C-1), 125.76 (C-6), 124.56 (C-7), 122.21 (C-5), 120.96 (C-4), 120.88 (C-2), 39.40 (C-25), 33.83 (C-26), 21.48 (C-31), 20.55 (C-32), 20.53 (C-32). FT-IR (ATR) $\tilde{\nu}$ (cm^{-1}) = 3060 (w), 3032 (w), 3000 (w), 2962 (m), 2917 (w), 2863 (w), 1921 (w), 1730 (w), 1611 (w), 1587 (m), 1554 (w), 1469 (w), 1460 (w), 1428 (w), 1397 (m), 1383 (w), 1363 (w), 1353 (w), 1338 (w), 1296 (w), 1272 (w), 1246 (w), 1224 (w), 1201 (w), 1173 (w), 1150 (w), 1133 (w), 1102 (w), 1066 (w), 1032 (w), 1014 (w), 969 (w), 940 (w), 922 (w), 915 (w), 887 (w), 850 (m), 827 (m), 811 (m), 797 (w), 779 (w), 757 (s), 735 (w), 715 (m), 702 (w), 685 (w), 670 (w), 657 (w), 637 (w), 607 (w). UV/Vis ($CHCl_3$): λ_{max} (nm) (log ε) = 277 (4.88), 331 (4.78), 379 (4.44), 406 (4.46), 430 (4.23), 468 (3.99), 504 (4.06), 550 (4.18), 587 (4.39), 633 (4.43). Fluorescence

($CHCl_3$): λ_{em} (λ_{ex}) (nm) = 658 (277). Φ= 25.4±0.9%. HRMS-MALDI (DCTB) (*m*/*z*): $[M]^+$ calcd. for $C_{74}H_{56}$, 944.4382; found, 944.4398. Elemental anal. calcd. for $C_{74}H_{56}\cdot 0.5H_2O$: C 93.14, H 6.02, found: C 93.07, H 6.28.

Detert-butylation of azulene-PAH 12

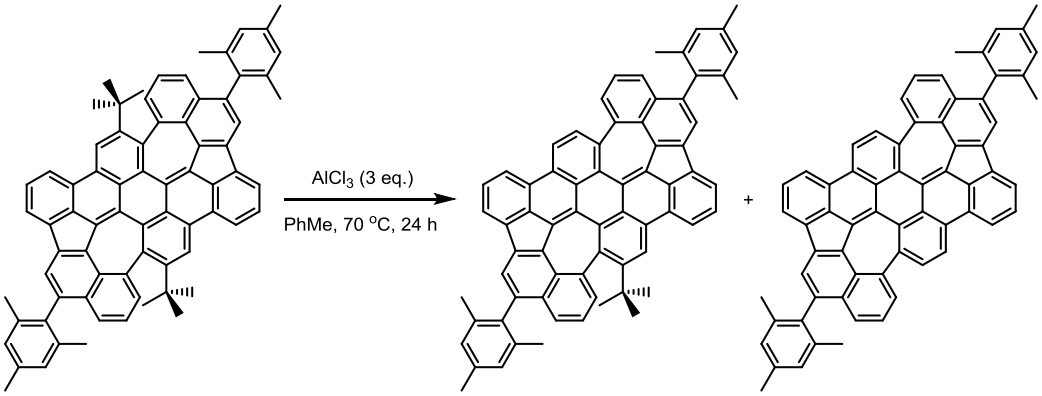

12 **14** **13**

To a suspension of azulene-PAH **12** (15 mg, 0.016 mmol) in 0.5 mL dry toluene $AlCl_3$ (6.4 mg, 0.048 mmol) was added in one portion under argon atmosphere. The mixture was stirred at 70 °C for 24 hours in a screw-capped glassy vial. After cooling down to room temperature, the mixture was diluted with dichloromethane (30 mL), washed with 2M aq. HCl (30 mL), and the organic layer dried over Na_2SO_4 before filtering through a short pad of Celite. After removal of the solvent by rotary evaporation, products **13** and **14** were separated by silica gel column chromatography (*n*-hexane /ethyl acetate 30:1 to 20:1 to collect **13**, then pure chloroform to collect **14**). The two fractions were obtained after precipitation from dichloromethane/methanol and drying in vacuum, respectively. Product **13** was obtained as dark-blue to black solid (7.5 mg, 57%). Product **14** was obtained as dark-blue solid (2 mg, 14%).

Azulene-PAH 13

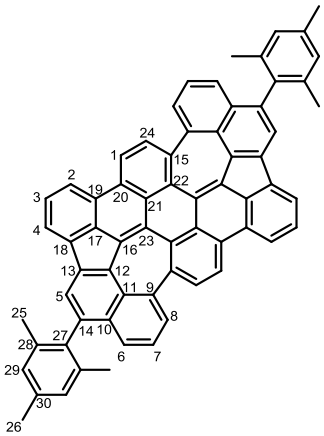

m.p.: >400 °C. ^{1}H NMR (600 MHz, CD_2Cl_2, 298 K) δ (ppm) = 8.09 (s, 2H, H-5), 8.02 (d, *J*= 6.8 Hz, 2H, H-2), 7.98 (br, 2H, H-1), 7.64 (br, 2H, H-4), 7.46 (d, *J*= 8.1 Hz, 2H, H-6), 7.43 - 7.37 (m, 2H, H-3), 7.30 (t, *J*= 7.5 Hz, 2H, H-7), 7.23 (d, *J*= 6.4 Hz, 2H, H-8), 7.15 (br, 6H, H-24,29), 2.47 (s, 6H, H-26), 2.15 (br, 12H, H-25). ^{13}C NMR (151 MHz, CD_2Cl_2, 298 K) δ (ppm) = 138.16 (C-9), 137.30 (C-14), 137.24 (C-27), 136.90 (C-30), 136.82 (C-28), 136.41 (C-15), 135.67 (C-19), 135.06 (C-11), 134.95 (C-24), 134.02 (C-20), 133.51 (C-12), 132.66 (C-13), 131.33 (C-16), 130.98 (C-8), 130.91 (C-

10), 130.32 (C-17), 130.10 (C-22), 129.44 (C-23), 128.47 (C-21), 128.38 (C-29), 127.55 (C-3), 125.14 (C-7), 124.93 (C-18), 124.77 (C-1), 124.44 (C-6), 121.15 (C-5), 119.97 (C-4), 119.55 (C-2), 21.29 (C-26), 20.36 (C-25). FT-IR (ATR) $\tilde{\nu}$ (cm^{-1}) = 3060 (w), 3032 (w), 2919 (w), 2919 (w), 2852 (w), 2731 (w), 1911 (w), 1783 (w), 1726 (w), 1633 (w), 1611 (w), 1594 (w), 1573 (w), 1549 (w), 1533 (w), 1475 (w), 1457 (w), 1431 (m), 1415 (w), 1377 (w), 1350 (w), 1304 (w), 1272 (w), 1257 (w), 1238 (w), 1220 (w), 1200 (w), 1178 (w), 1143 (w), 1127 (w), 1107 (w), 1065 (w), 1032 (w), 1013 (w), 958 (w), 941 (w), 893 (w), 849 (m), 827 (w), 800 (m), 778 (m), 752 (s), 729 (m), 716 (w), 684 (w), 643 (w), 628 (w). UV/Vis ($CHCl_3$): λ_{max} (nm) (log ε) = 260 (5.10), 319 (4.88), 328 (4.88), 353 (4.59), 372 (4.71), 390 (4.63), 423 (4.23), 449 (4.26), 476 (4.31), 540 (4.26), 574 (4.40), 615 (4.37). Fluorescence ($CHCl_3$): λ_{em} (λ_{ex}) (nm) = 646 (260). Φ= 17.9±0.2%. HRMS-MALDI (DCTB) (*m*/*z*): $[M]^+$ calcd. for $C_{66}H_{40}$, 832.3130; found, 832.3149. Elemental anal. calcd. for $C_{66}H_{40}\cdot 0.5H_2O$: C 94.14, H 4.91, found: C 94.05 H 5.12.

Azulene-PAH 14

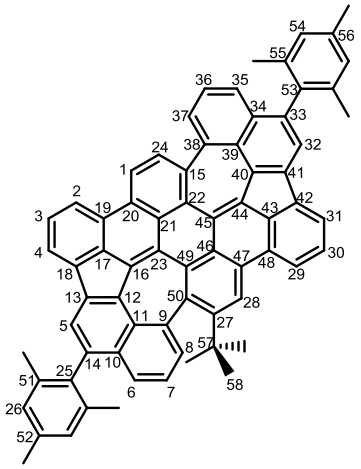

m.p.: >400 °C. ^{1}H NMR (600 MHz, CD_2Cl_2) δ (ppm) = 9.10 (s, 1H, H-28), 8.81 (d, *J*= 8.4 Hz, 1H, H-1), 8.63 (d, *J*= 8.0 Hz, 1H, H-29), 8.46 (d, *J*= 7.9 Hz, 1H, H-2), 8.22 (d, *J*= 7.0 Hz, 1H, H-31), 8.14 (d, *J*= 6.9 Hz, 1H, H-4), 8.08 (d, *J*= 8.5 Hz, 1H, H-24), 8.06 (s, 1H, H-32), 8.00 (s, 1H, H-5), 7.95 - 7.91 (m, 1H, H-30), 7.83 - 7.80 (m, 1H, H-3), 7.65 (d, *J*= 6.9 Hz, 1H, H-37), 7.53 - 7.50 (m, 1H, H-35), 7.48 (d, *J*= 7.5 Hz, 1H, H-36), 7.43 (d, *J*= 8.1 Hz, 1H, H-6), 7.33 - 7.29 (m, 1H, H-7), 7.14 (d, *J*= 7.0 Hz, 1H, H-8), 7.13 - 7.08 (m, 4H, H-26,54), 2.44 (s, 6H), 2.09 (s, 3H, H-Mes-CH_3), 2.04 (s, 3H, H-Mes-CH_3), 2.02 (s, 3H, H-Mes-CH_3), 1.98 (s, 3H, H-Mes-CH_3), 1.11 (s, 9H, H-58). ^{13}C NMR (151 MHz, CD_2Cl_2) δ (ppm) = 154.05 (C-27), 139.02 (C-33), 138.29 (C-51,55), 137.97 (C-52,56), 137.94 (C-15), 137.80 (C-52,56), 137.74 (C-38), 137.67 (C-51,55), 137.57 (C-53), 137.54 (C-14), 137.36 (C-11), 137.23 (C-25), 137.20 (C-50), 137.00 (C-19), 136.76 (C-9), 136.70 (C-48), 135.84 (C-13), 135.71 (C-24), 135.11 (C-39), 134.90 (C-41), 134.86 (C-12), 134.61 (C-8), 134.07 (C-40), 133.63 (C-20), 133.56 (C-47), 133.08 (C-44), 132.61 (C-17), 132.40 (C-37), 132.16 (C-16), 131.56 (C-43), 131.34 (C-22), 131.29 (C-10), 131.25 (C-34), 130.76 (C-23), 130.20 (C-45), 130.17 (C-49), 128.89 (C-3), 128.85 (C-26,54), 128.82 (C-26,54), 128.78 (C-30), 128.76 (C-26,54), 128.75 (C-26,54), 127.13 (C-42), 126.41 (C-18), 126.32 (C-46), 126.20 (C-28), 125.97 (C-35), 125.78 (C-1), 125.76 (C-6), 125.52 (C-36), 124.68 (C-7), 122.32 (C-5), 122.07 (C-32), 121.38 (C-4), 121.20 (C-2), 120.62 (C-29), 120.46 (C-31), 39.35 (C-57), 33.74 (C-58), 30.25 (C-Mes-CH_3), 21.48 (C-Mes-CH_3), 20.72 (C-Mes-CH_3), 20.56 (C-Mes-CH_3), 20.53 (C-Mes-CH_3), 20.45 (C-Mes-CH_3). FT-IR (ATR) $\tilde{\nu}$ (cm^{-1}) = 3064 (w), 2953 (w), 2921 (w), 2852 (w), 2731 (w), 1919 (w), 1626 (w), 1611 (w), 1587 (w), 1551 (w), 1458 (w), 1430 (m), 1405 (w), 1381 (w), 1363 (w), 1352 (w), 1303 (w), 1271 (w), 1239 (w), 1220 (w), 1203 (w),

1185 (w), 1172 (w), 1147 (w), 1130 (w), 1100 (w), 1032 (w), 1015 (w), 968 (w), 941 (w), 907 (w), 886 (w), 850 (m), 827 (w), 808 (m), 794 (w), 777 (w), 757 (s), 733 (w), 713 (w), 694 (w), 675 (w), 657 (w), 639 (w), 613 (w). UV/Vis ($CHCl_3$): λ_{max} (nm) (log ε) = 272 (4.98), 327 (4.82), 378 (4.55), 398 (4.52), 427 (4.21), 466 (4.08), 493 (4.15), 549 (4.23), 586 (4.39), 628 (4.39). Fluorescence ($CHCl_3$): λ_{em} (λ_{ex}) (nm) = 658 (272). Φ= 22.3±0.5%. HRMS-MALDI (DCTB) (*m*/*z*): $[M]^+$ calcd. for $C_{70}H_{48}$, 888.3756; found, 888.3750. Elemental anal. calcd. for $C_{70}H_{48}\cdot 0.5H_2O$: C 93.61, H 5.50, found: C 93.70, H 5.62.

3. NMR spectra

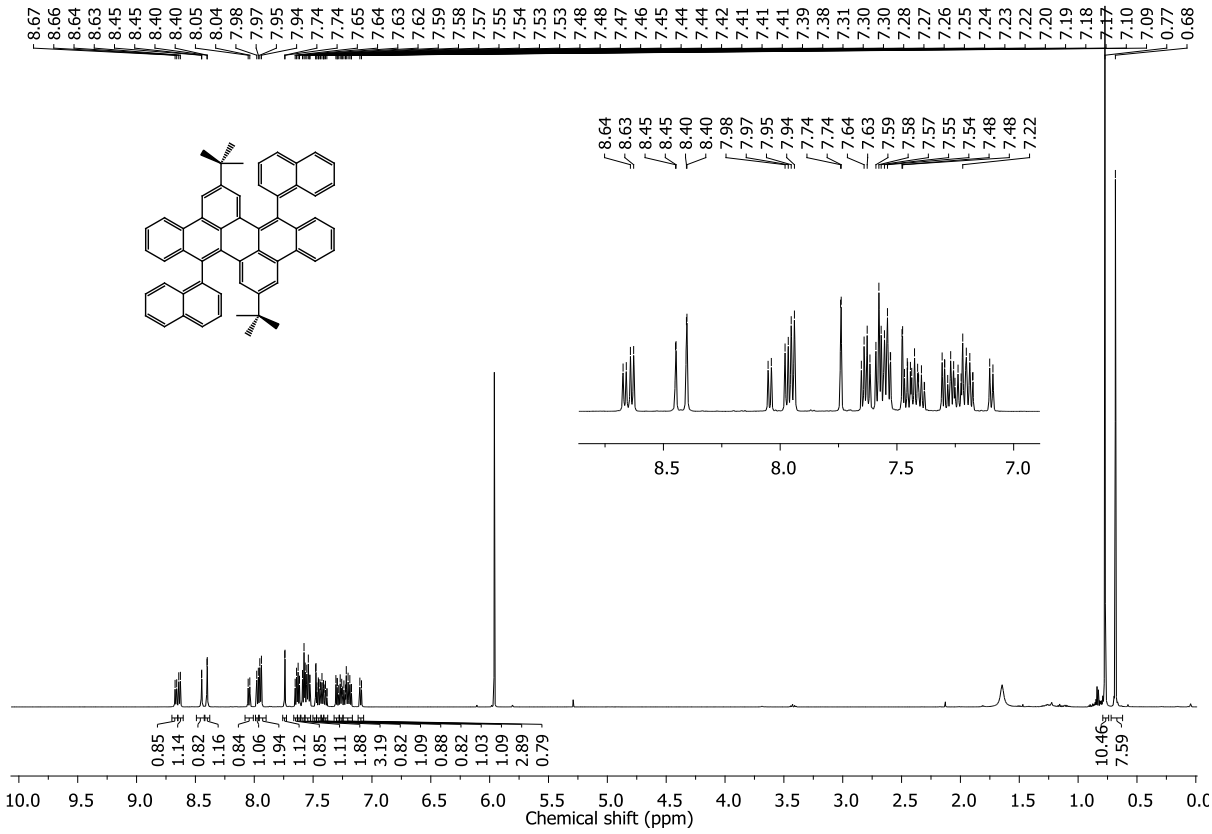

Figure S1. ^{1}H NMR spectrum (600 MHz, $Cl_2CDCDCl_2$) of **3**.

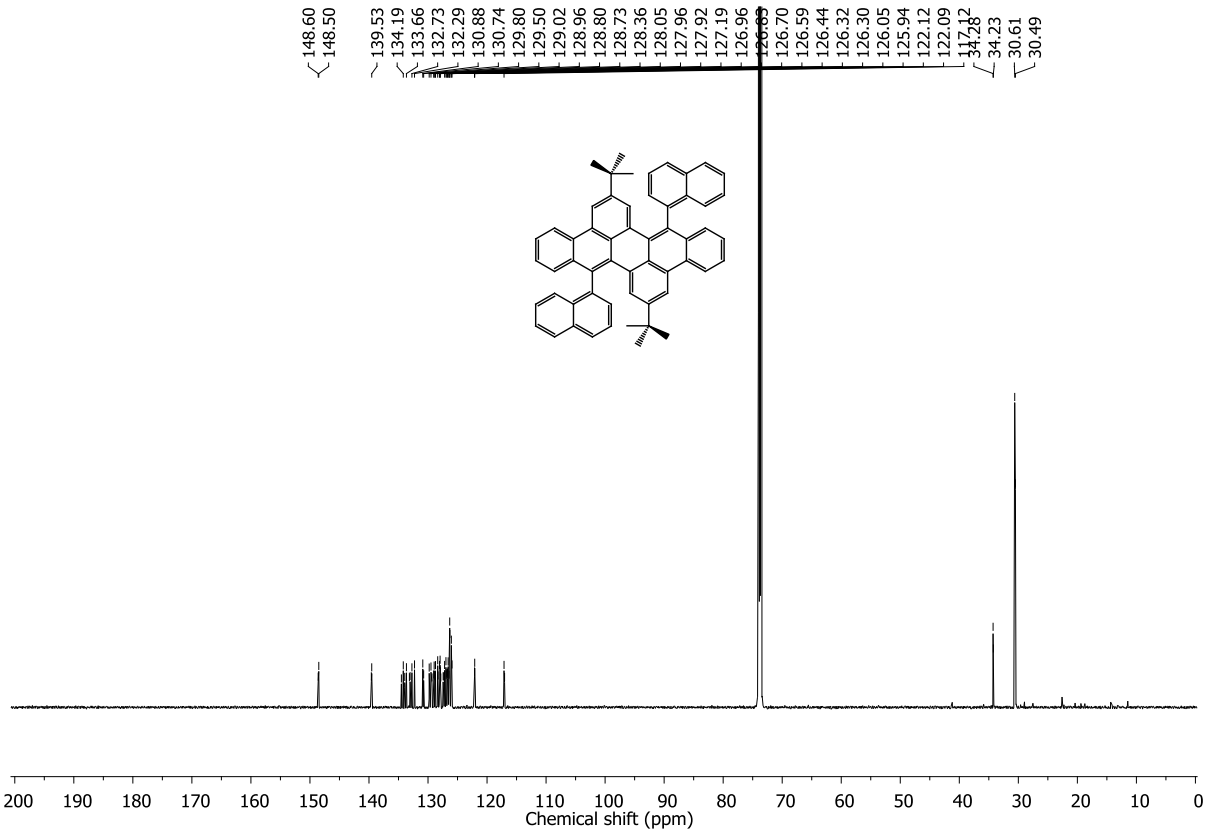

Figure S2. ^{13}C NMR spectrum (151 MHz, $Cl_2CDCDCl_2$) of **3**.

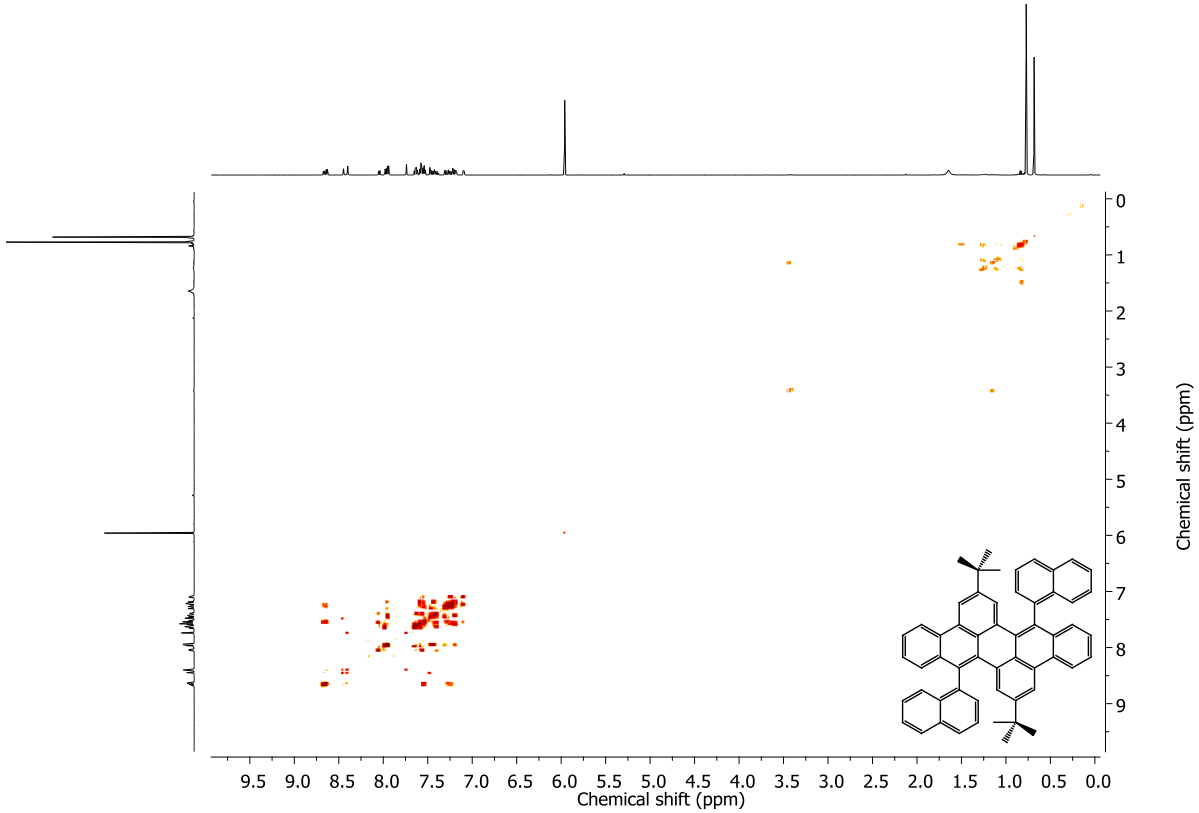

Figure S3. COSY NMR spectrum (600 MHz, $Cl_2CDCDCl_2$) of **3**.

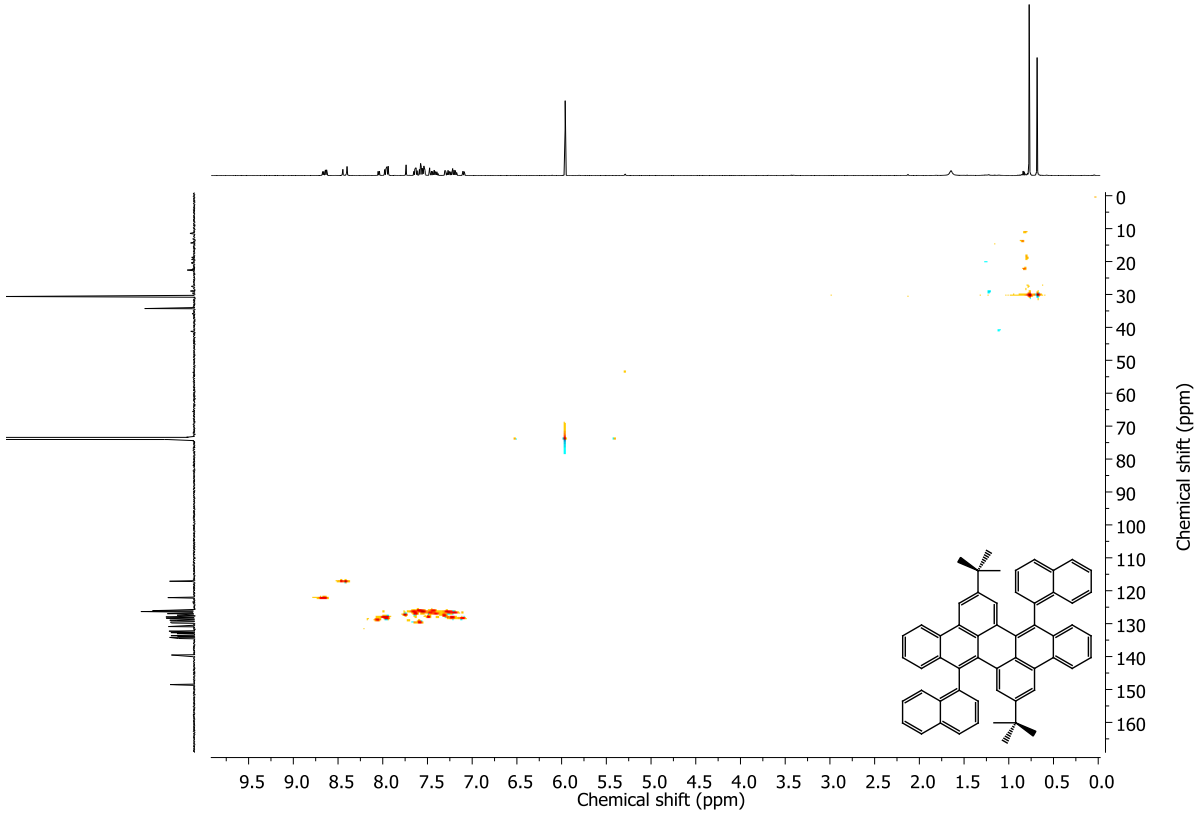

Figure S4. HSQC spectrum (600 MHz, $Cl_2CDCDCl_2$) of **3**.

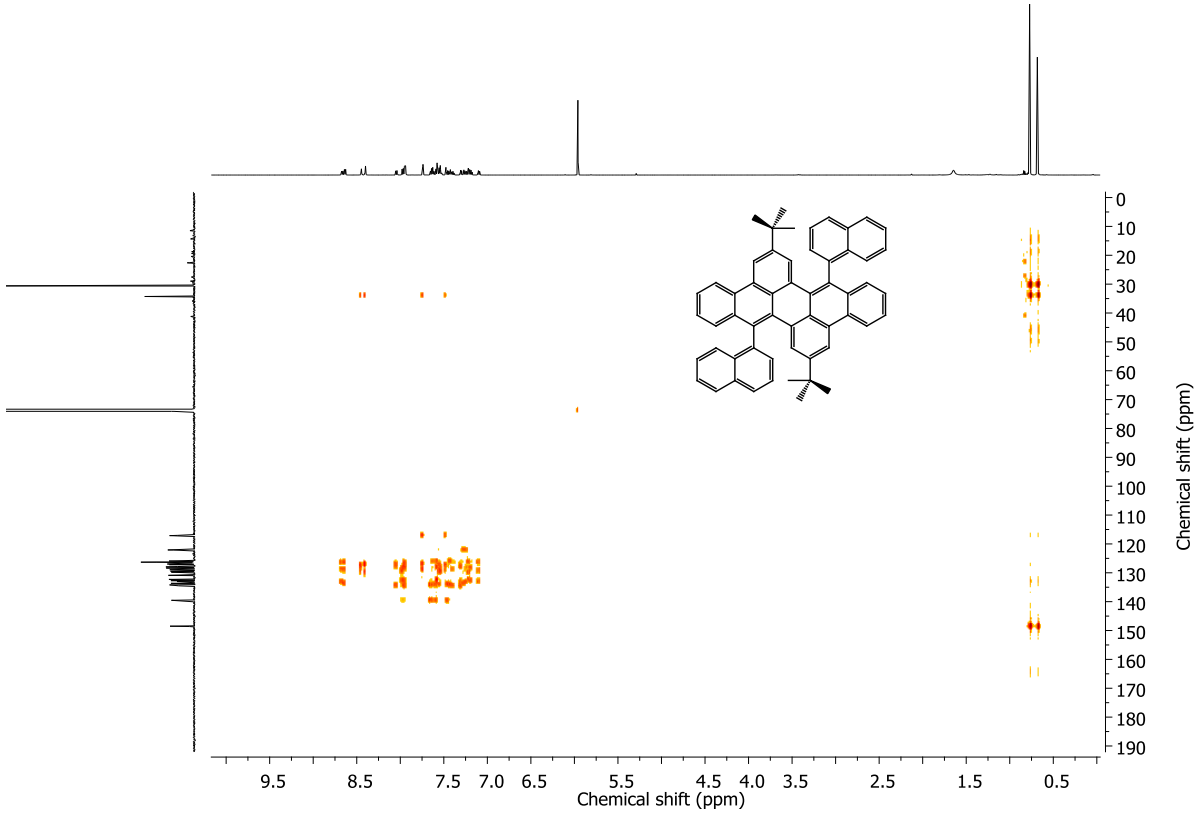

Figure S5. HMBC NMR spectrum (600 MHz, $Cl_2CDCDCl_2$) of **3**.

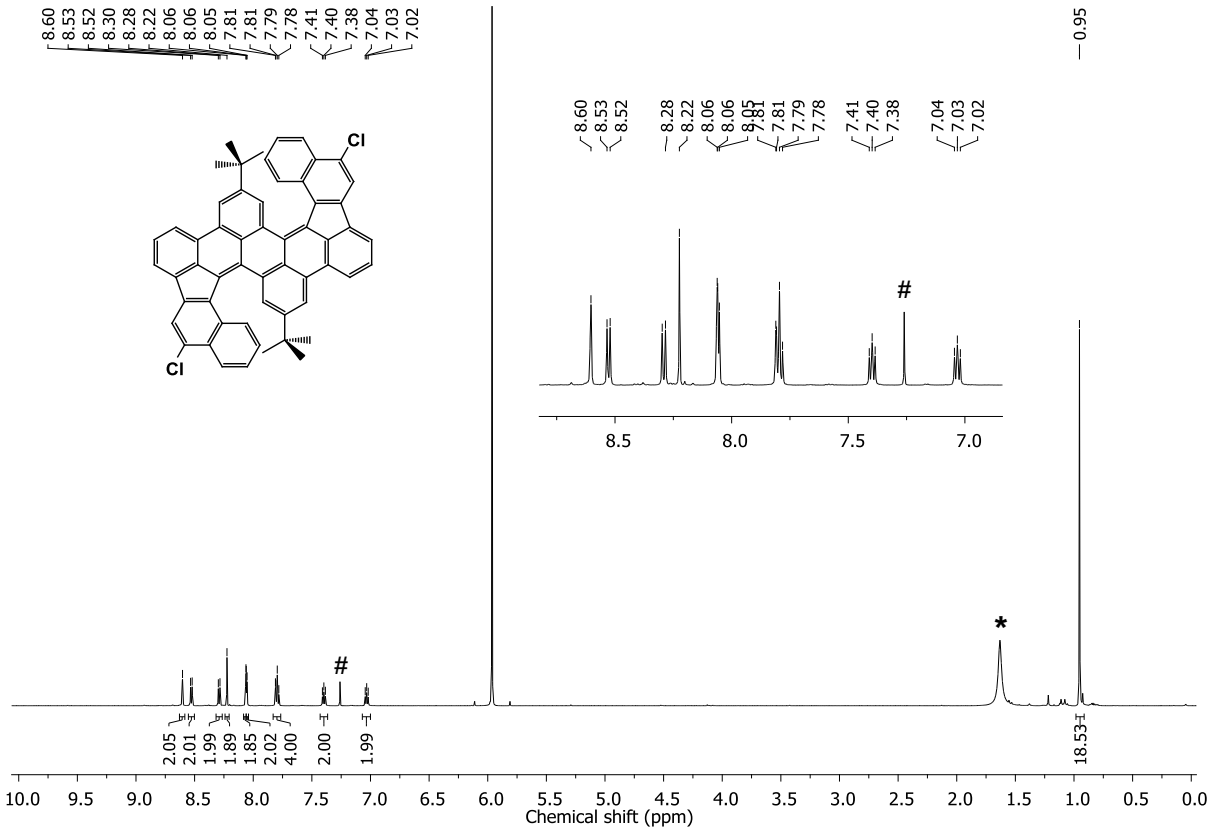

Figure S6. ^{1}H NMR spectrum (600 MHz, $Cl_2CDCDCl_2$, 298 K) of **7**. #$CHCl_3$, *H_2O.

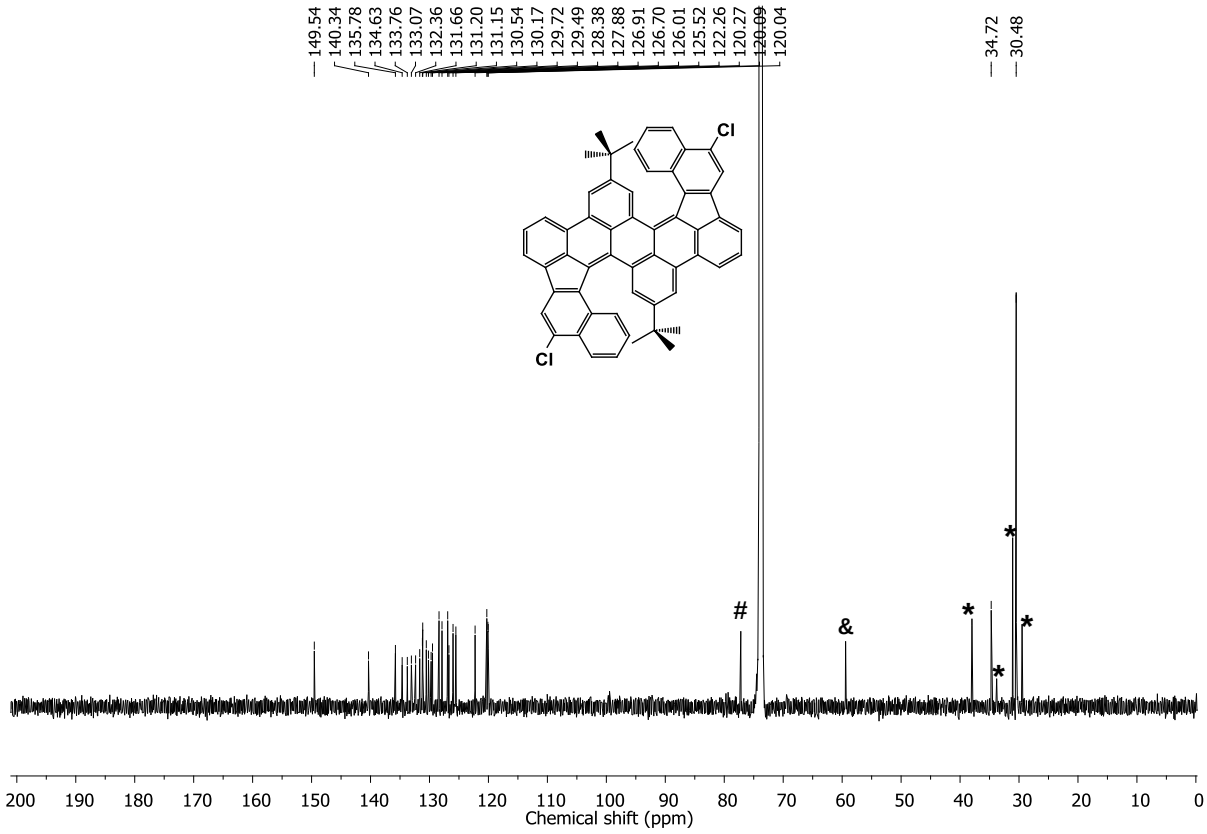

Figure S7. ^{13}C NMR spectrum (151 MHz, $Cl_2CDCDCl_2$, 343 K) of **7**. #$CHCl_3$, &ethanol, **n*-heptane.

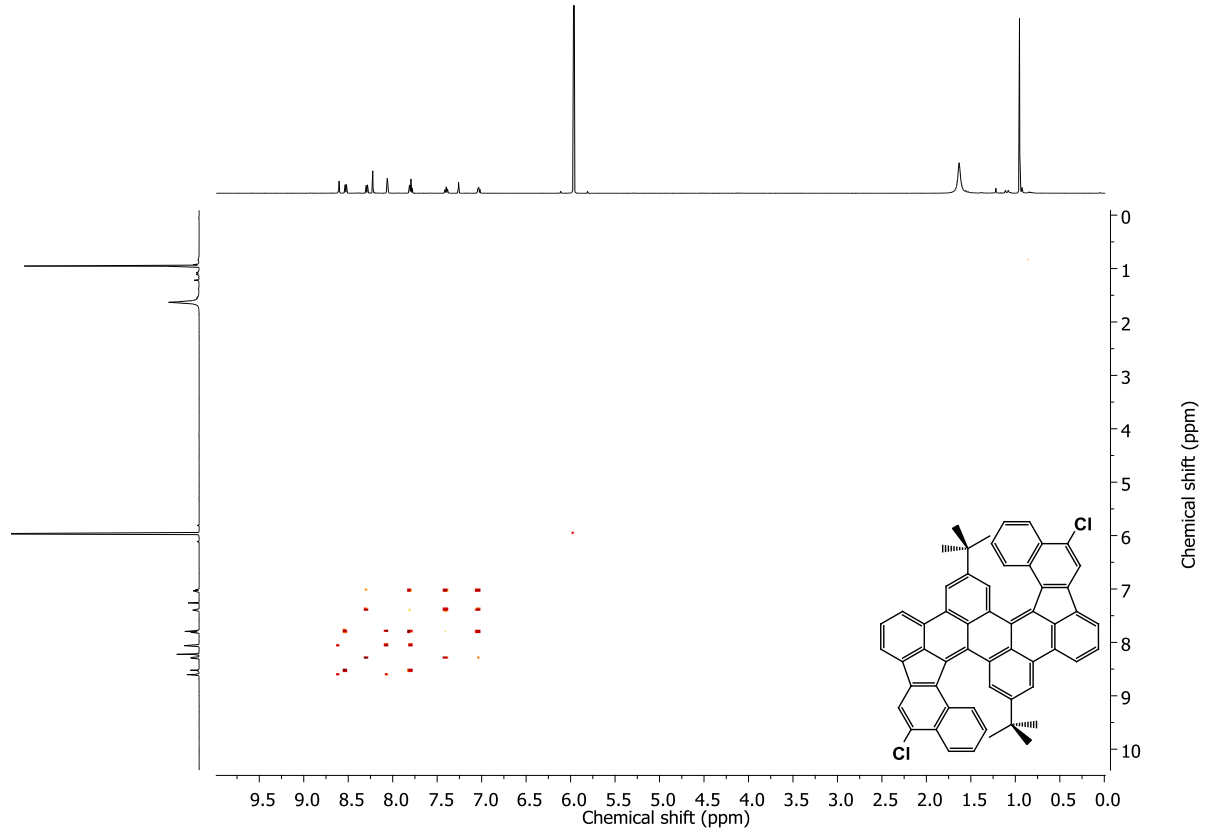

Figure S8. COSY NMR spectrum (600 MHz, $Cl_2CDCDCl_2$, 298 K) of **7**.

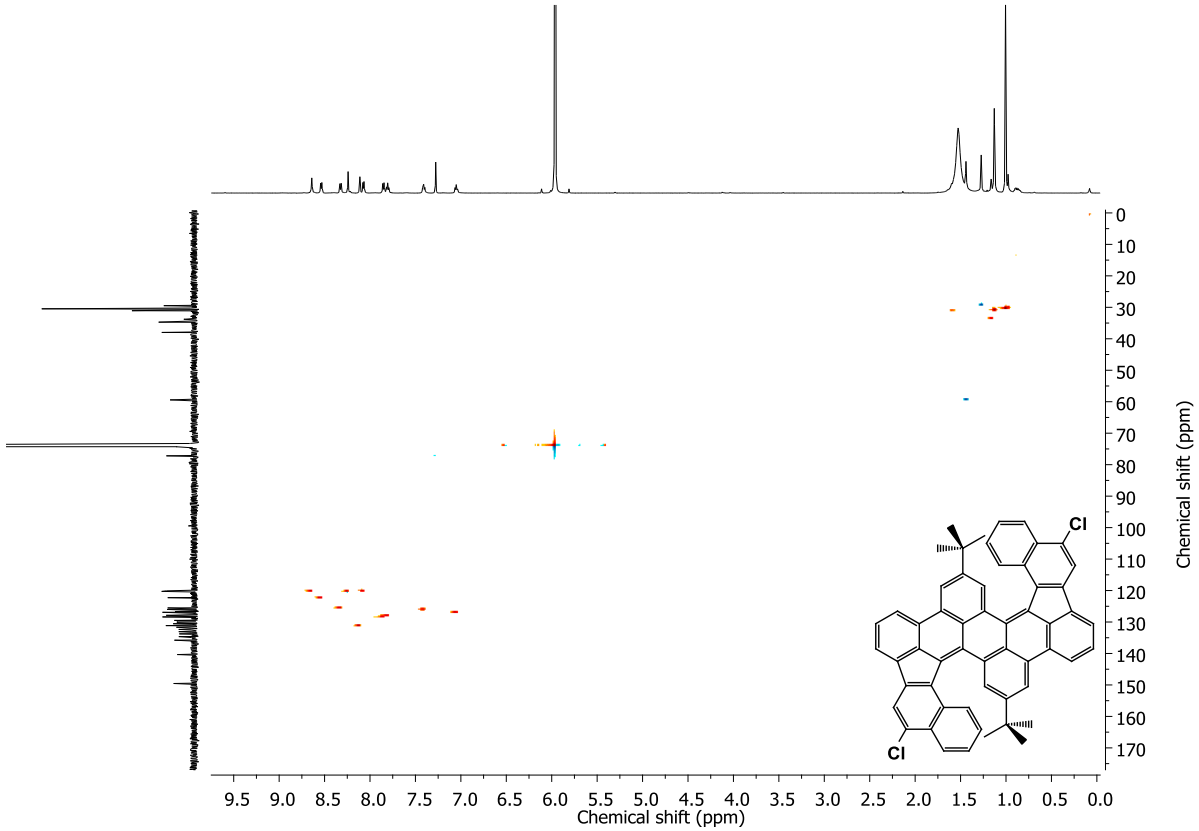

Figure S9. HSQC NMR spectrum (600 MHz, $Cl_2CDCDCl_2$, 343 K) of **7**.

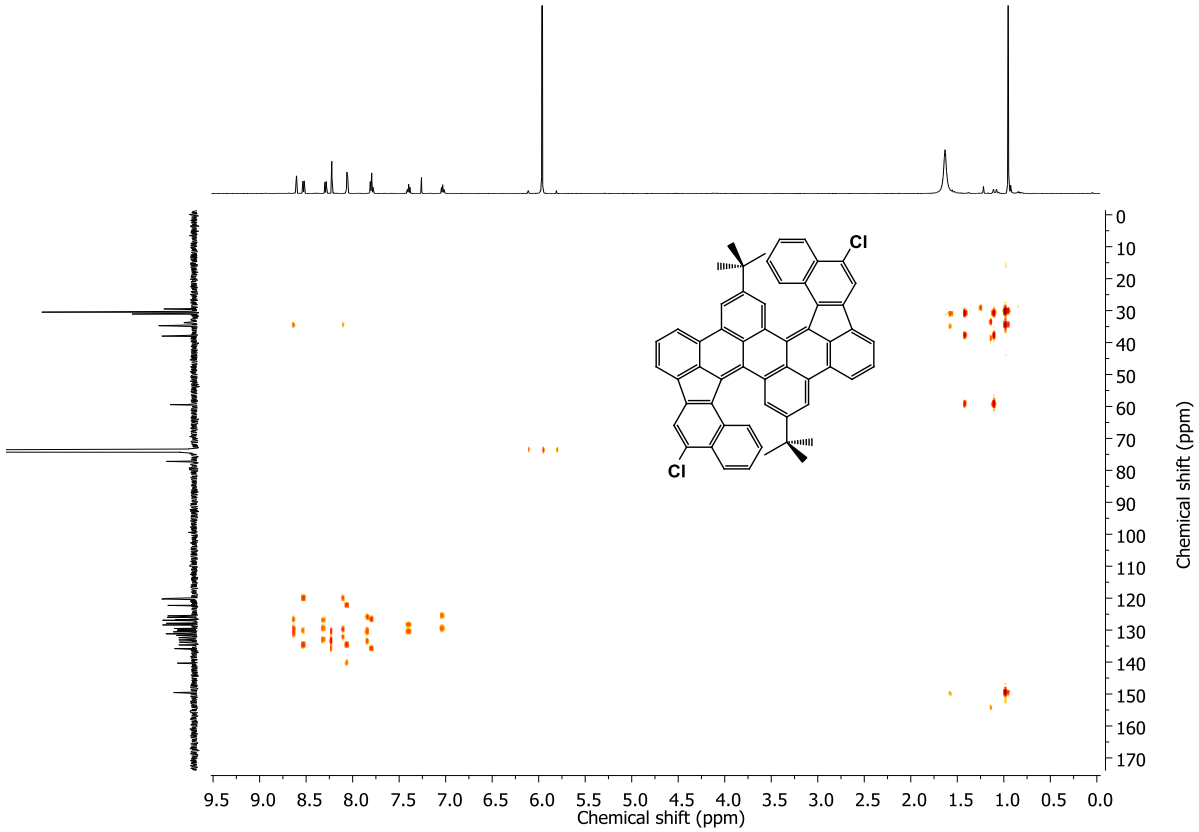

Figure S10. HMBC NMR spectrum (600 MHz, $Cl_2CDCDCl_2$, 343 K) of **7**.

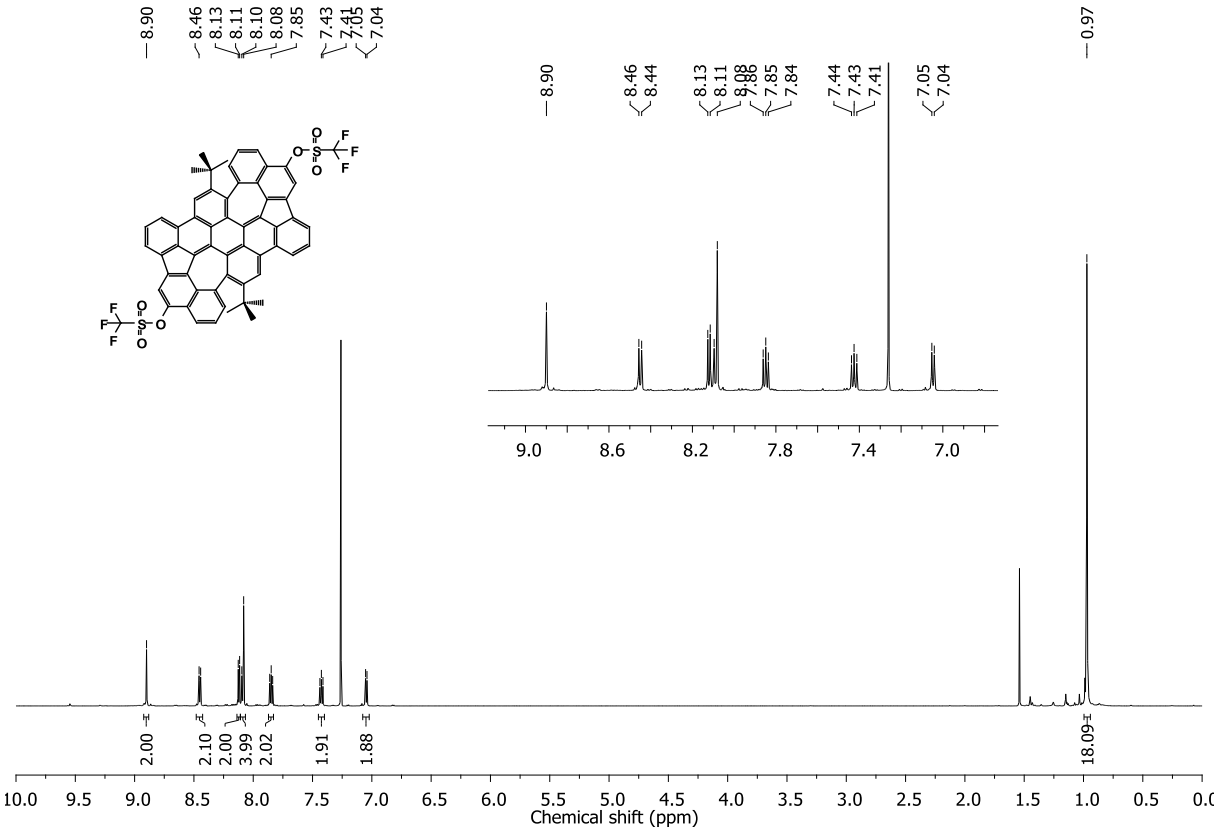

Figure S11. ^{1}H NMR spectrum (600 MHz, $CDCl_3$) of **8**.

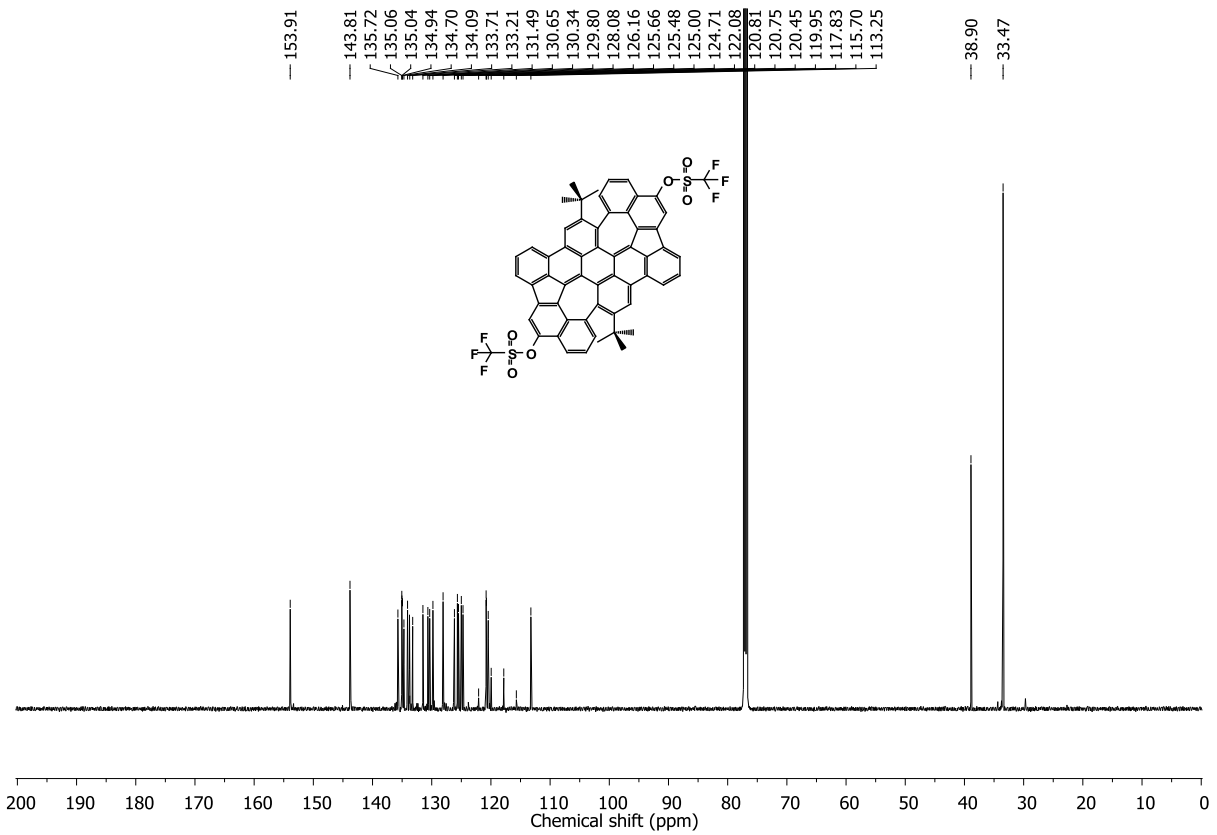

Figure S12. ^{13}C NMR spectrum (151 MHz, $CDCl_3$) of **8**.

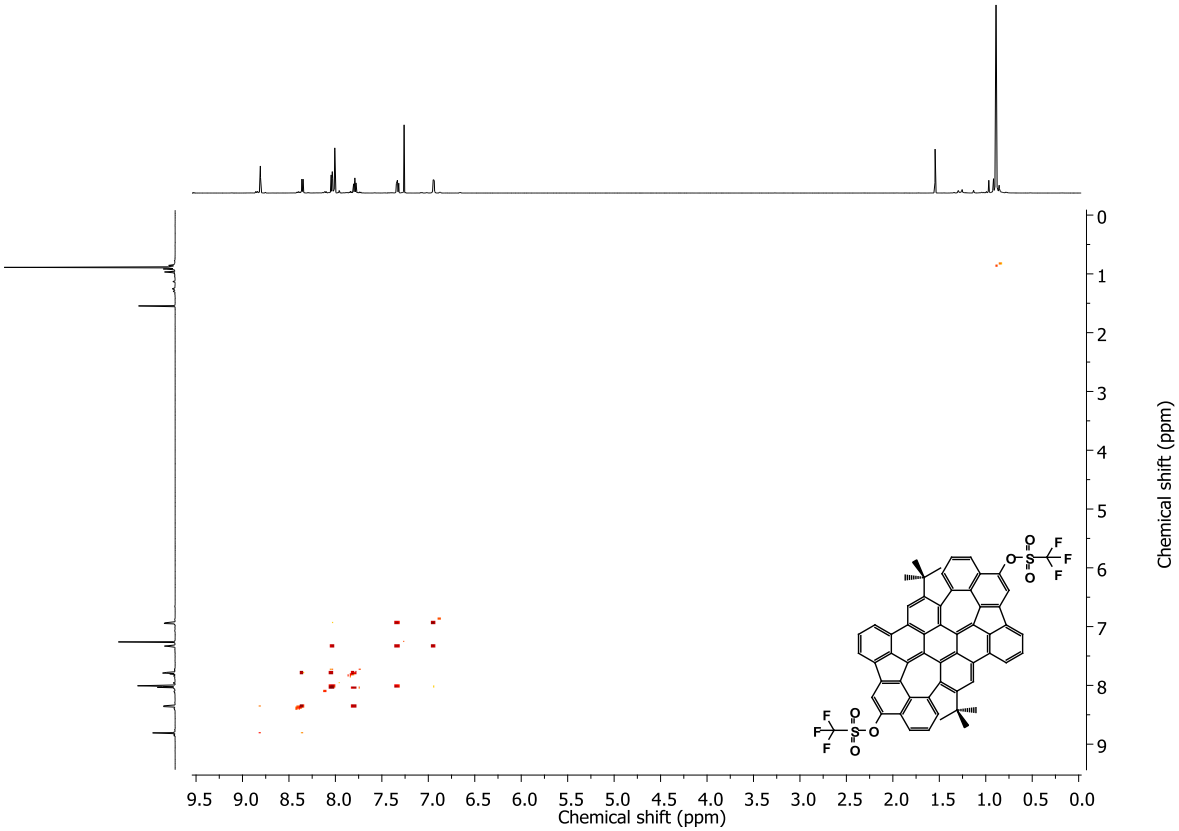

Figure S13. COSY NMR spectrum (600 MHz, $CDCl_3$) of **8**.

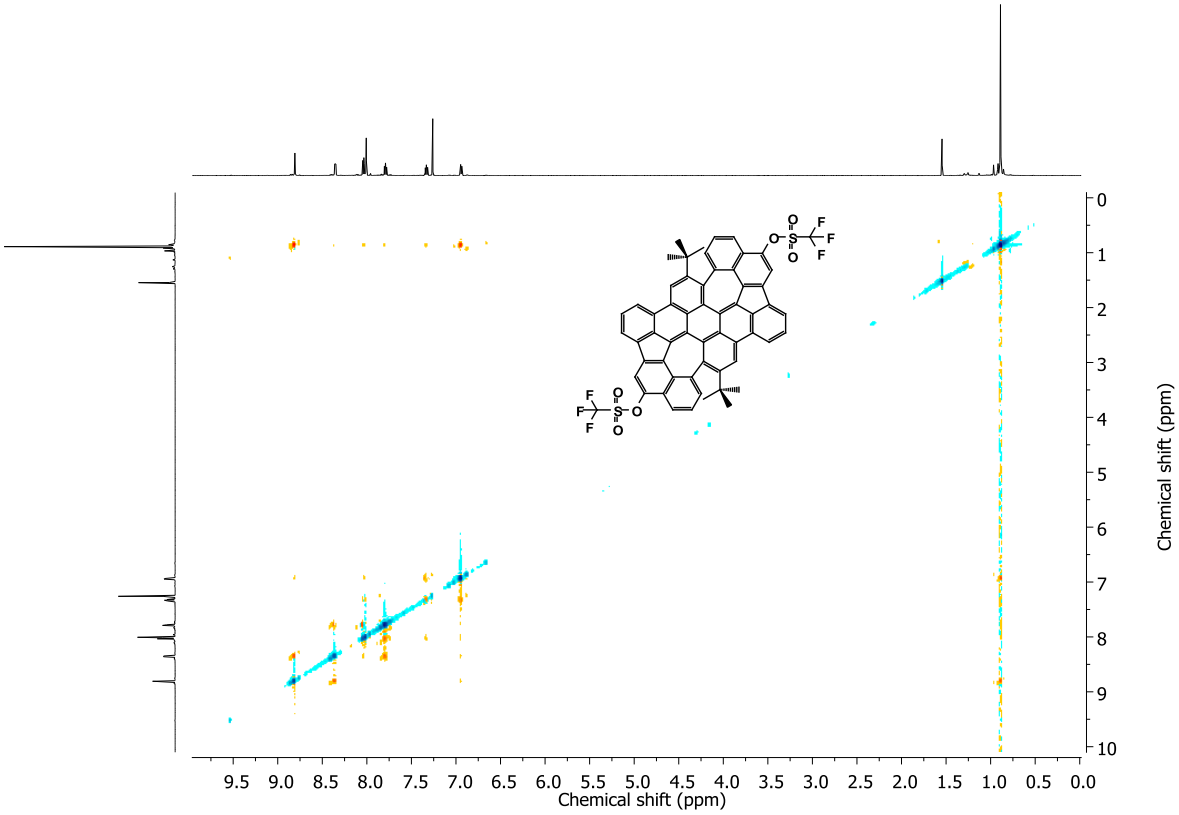

Figure S14. ROSEY NMR spectrum (600 MHz, $CDCl_3$) of **8**.

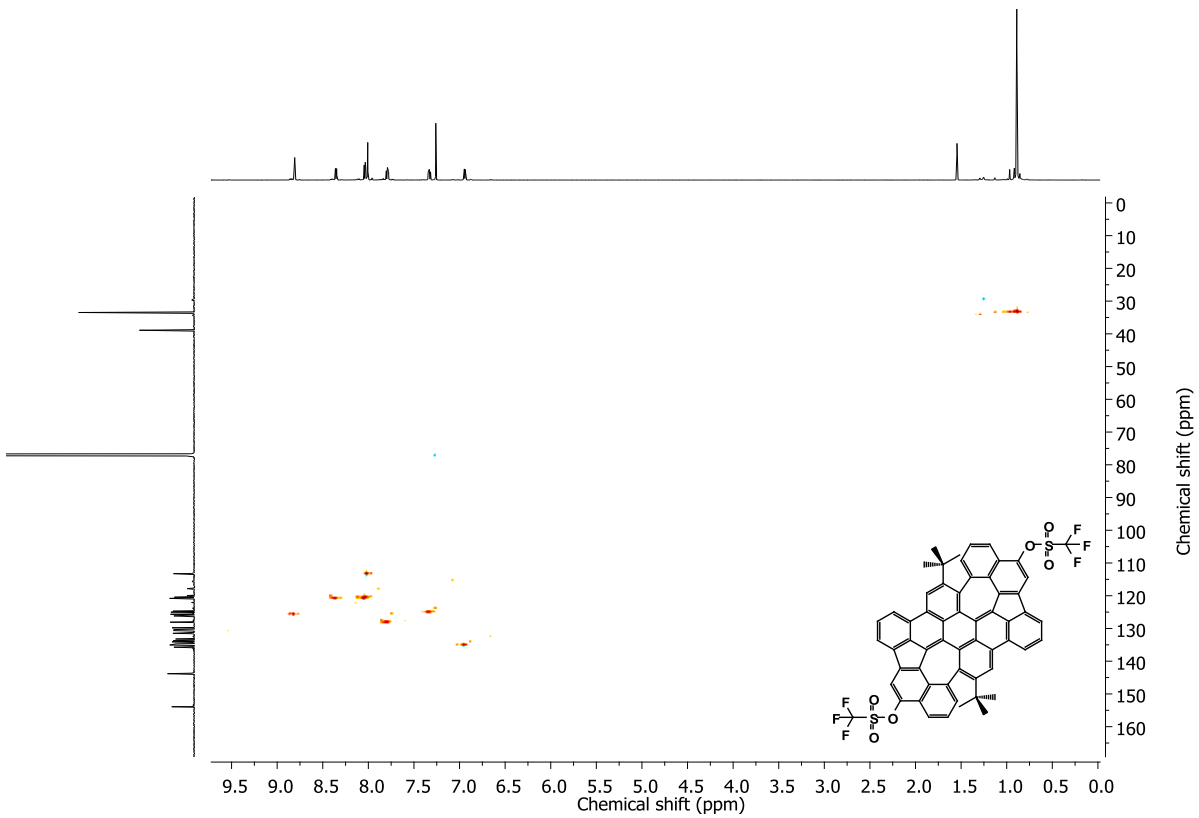

Figure S15. HSQC NMR spectrum (600 MHz, $CDCl_3$) of **8**.

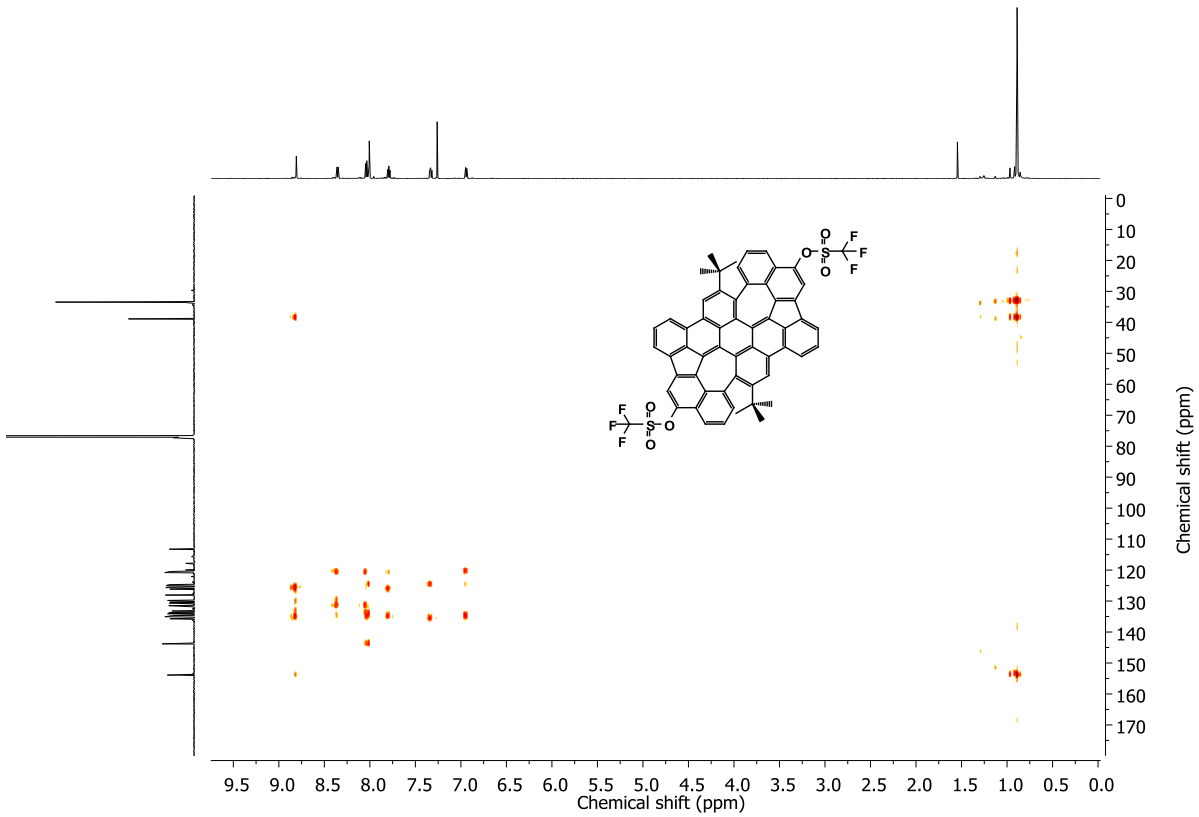

Figure S16. HMBC NMR spectrum (600 MHz, $CDCl_3$) of **8**.

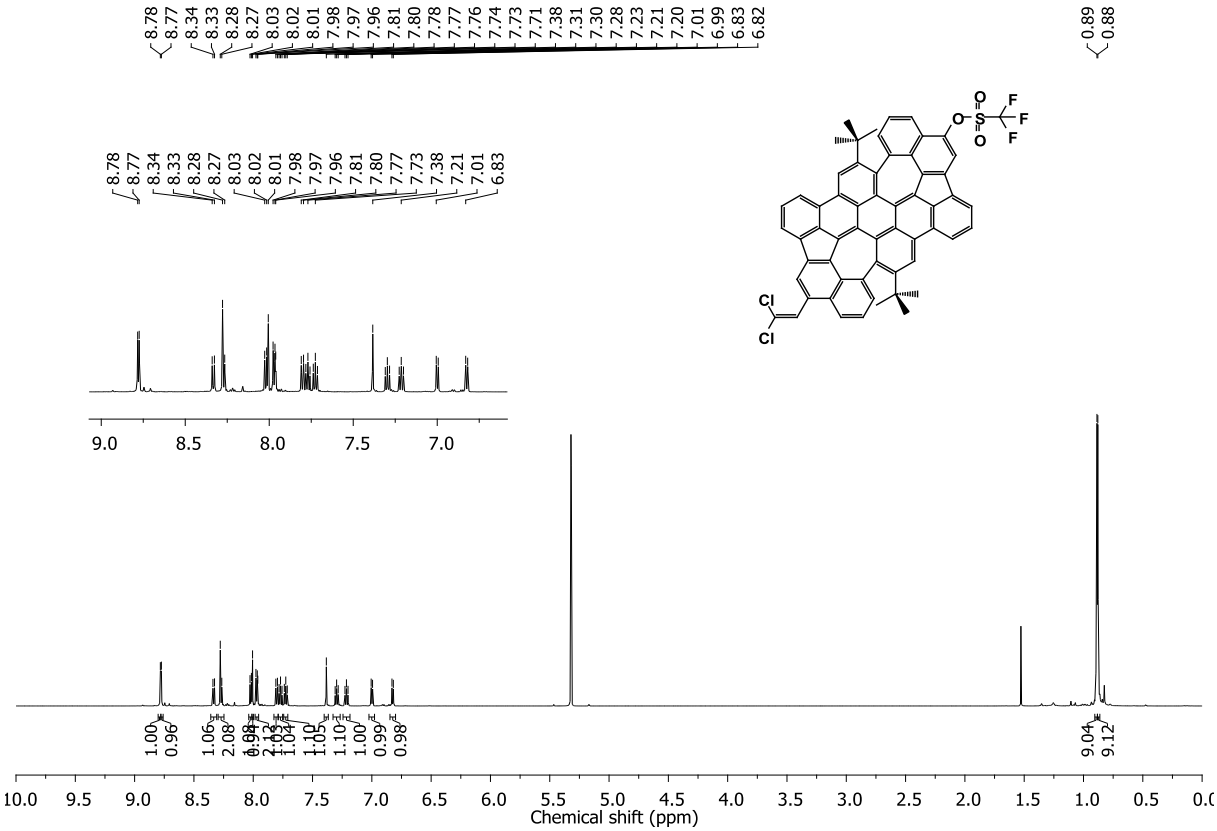

Figure S17. ^{1}H NMR spectrum (600 MHz, CD_2Cl_2) of **9**.

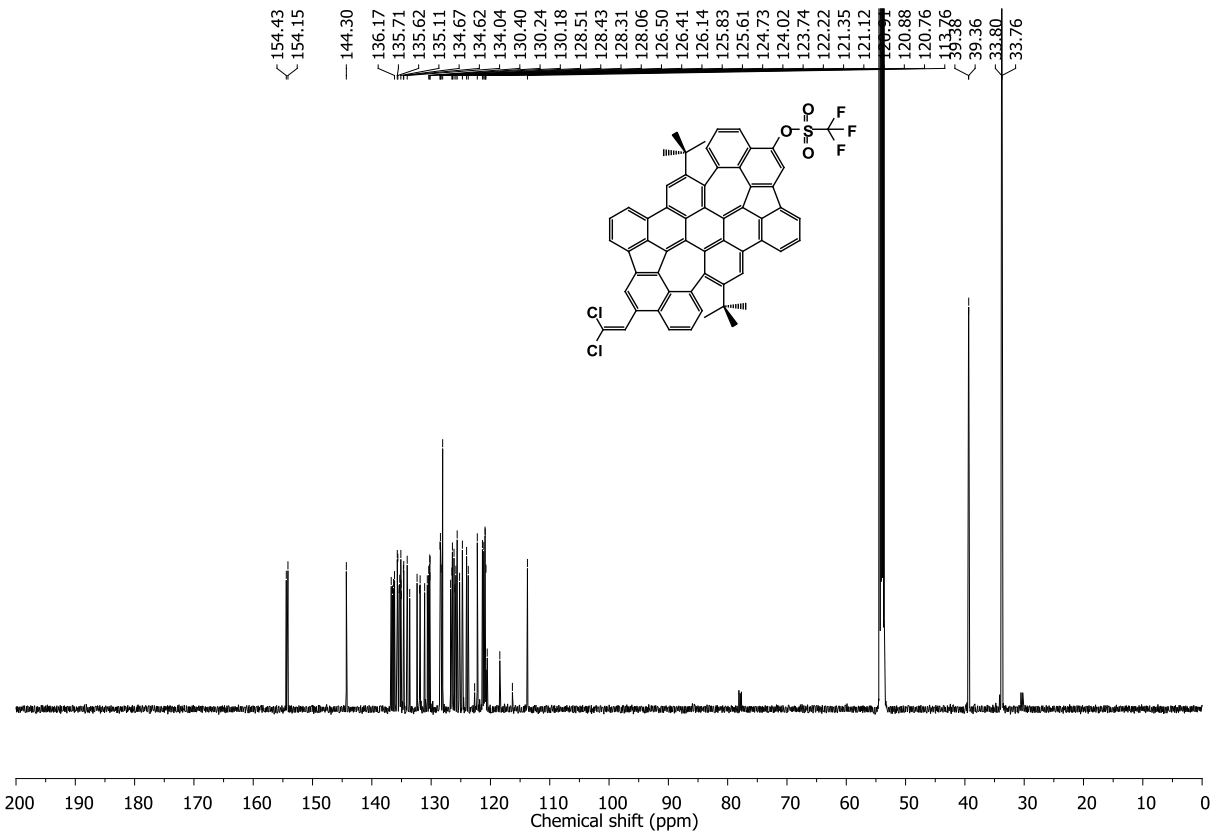

Figure S18. ^{13}C NMR spectrum (151 MHz, CD_2Cl_2) of **9**.

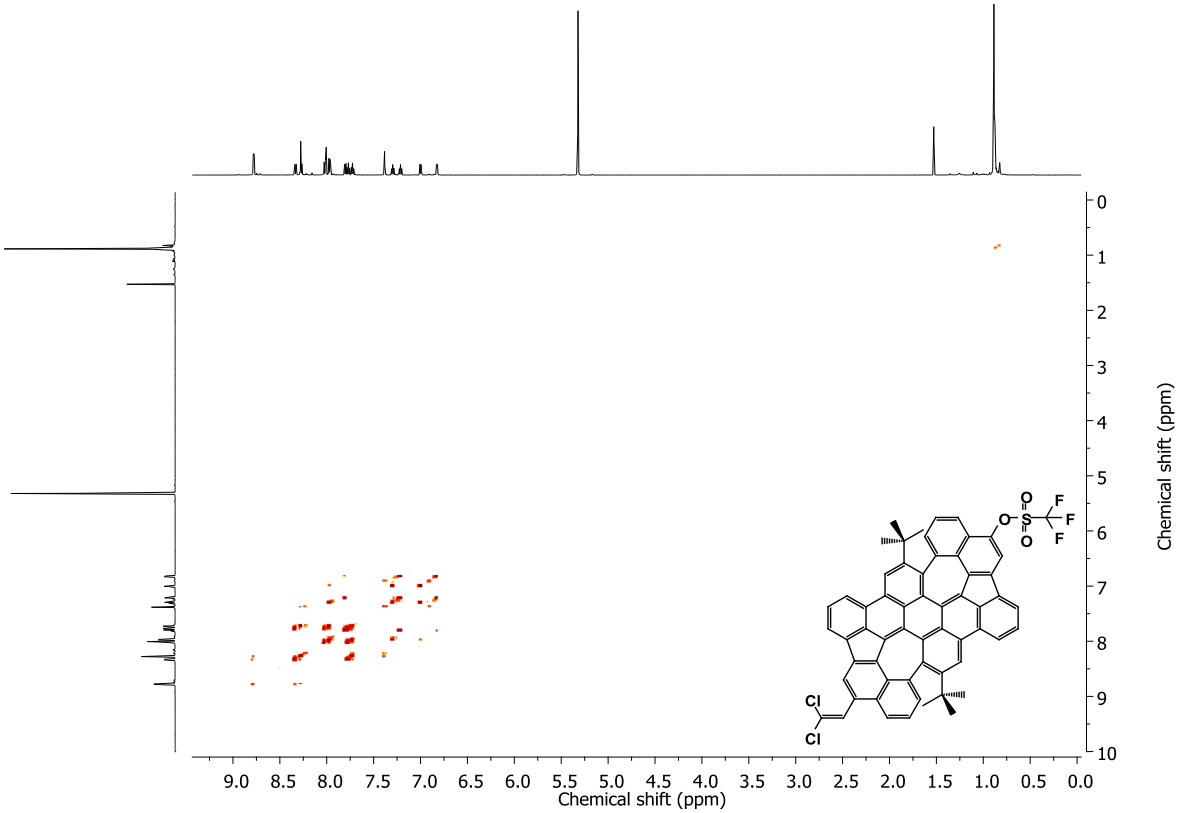

Figure S19. COSY NMR spectrum (600 MHz, CD_2Cl_2) of **9**.

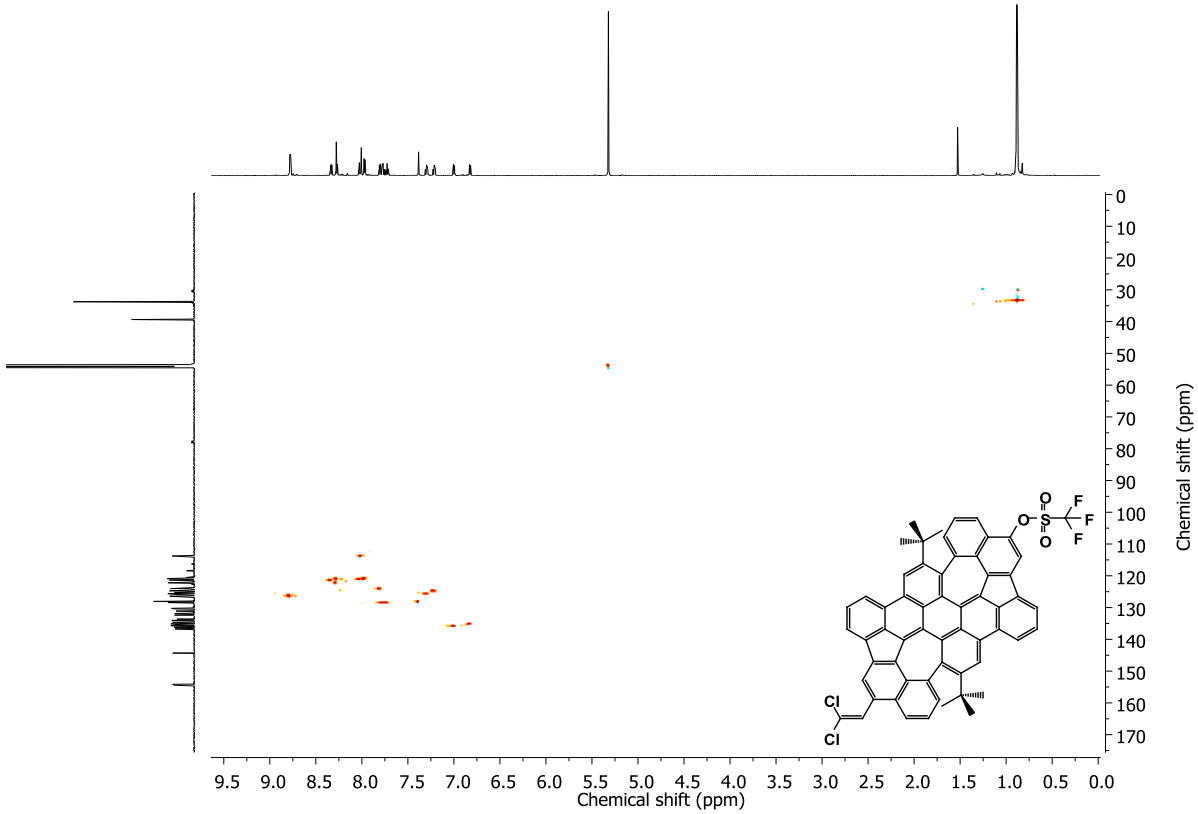

Figure S20. HSQC NMR spectrum (600 MHz, CD_2Cl_2) of **9**.

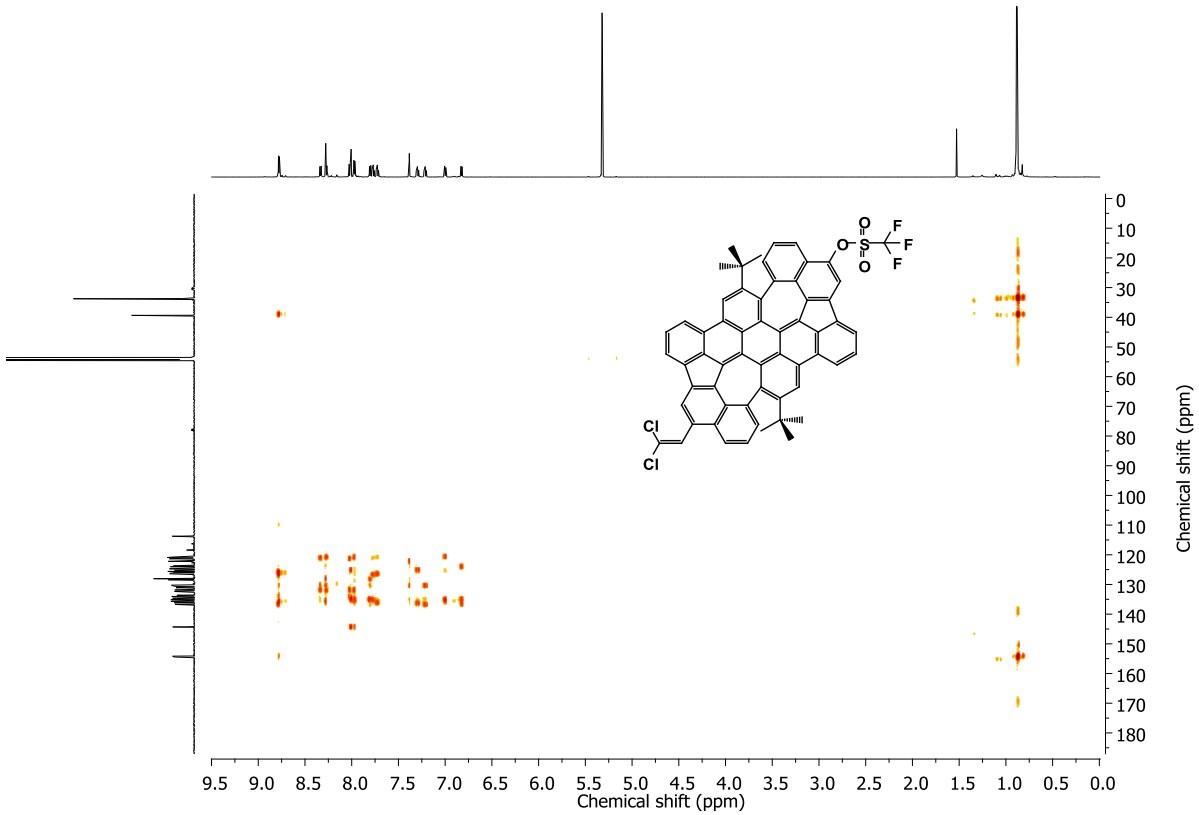

Figure S21. HMBC NMR spectrum (600 MHz, CD_2Cl_2) of **9**.

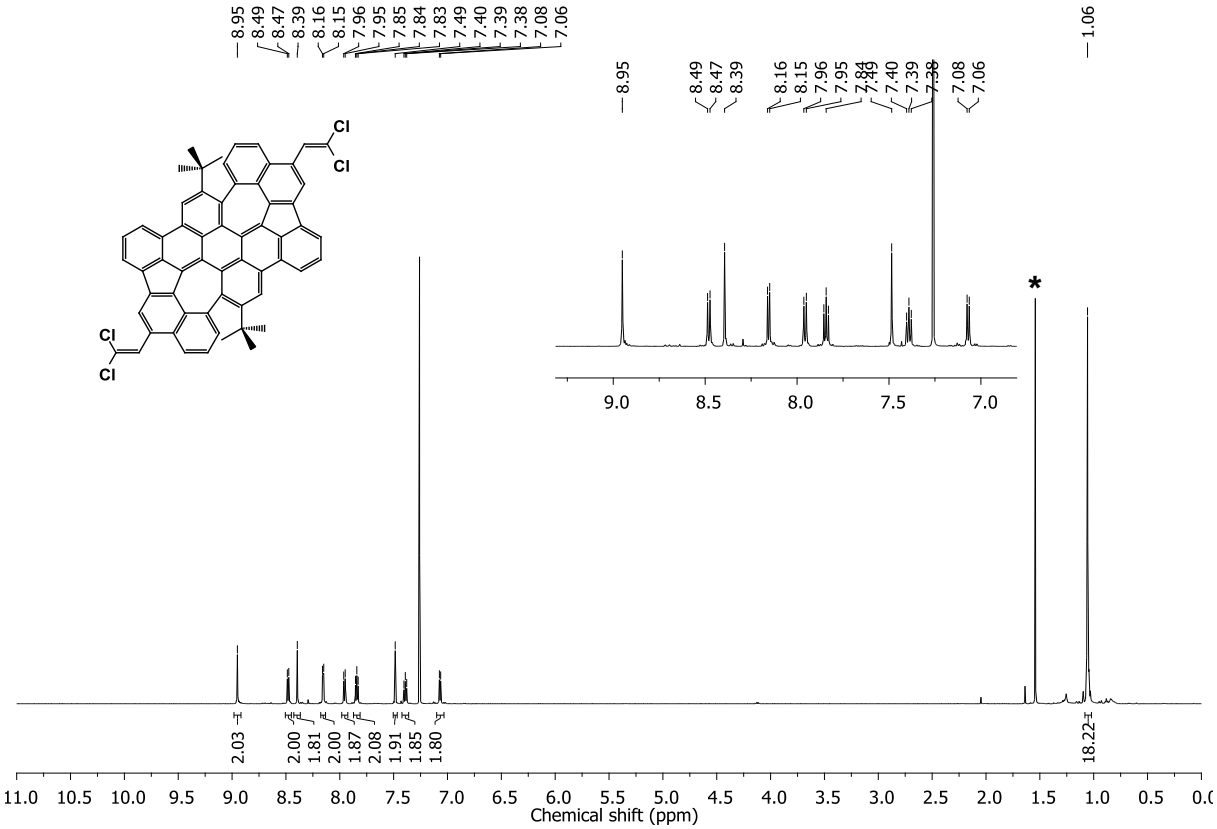

Figure S22. ^{1}H NMR spectrum (600 MHz, $CDCl_3$) of **10**. *H_2O.

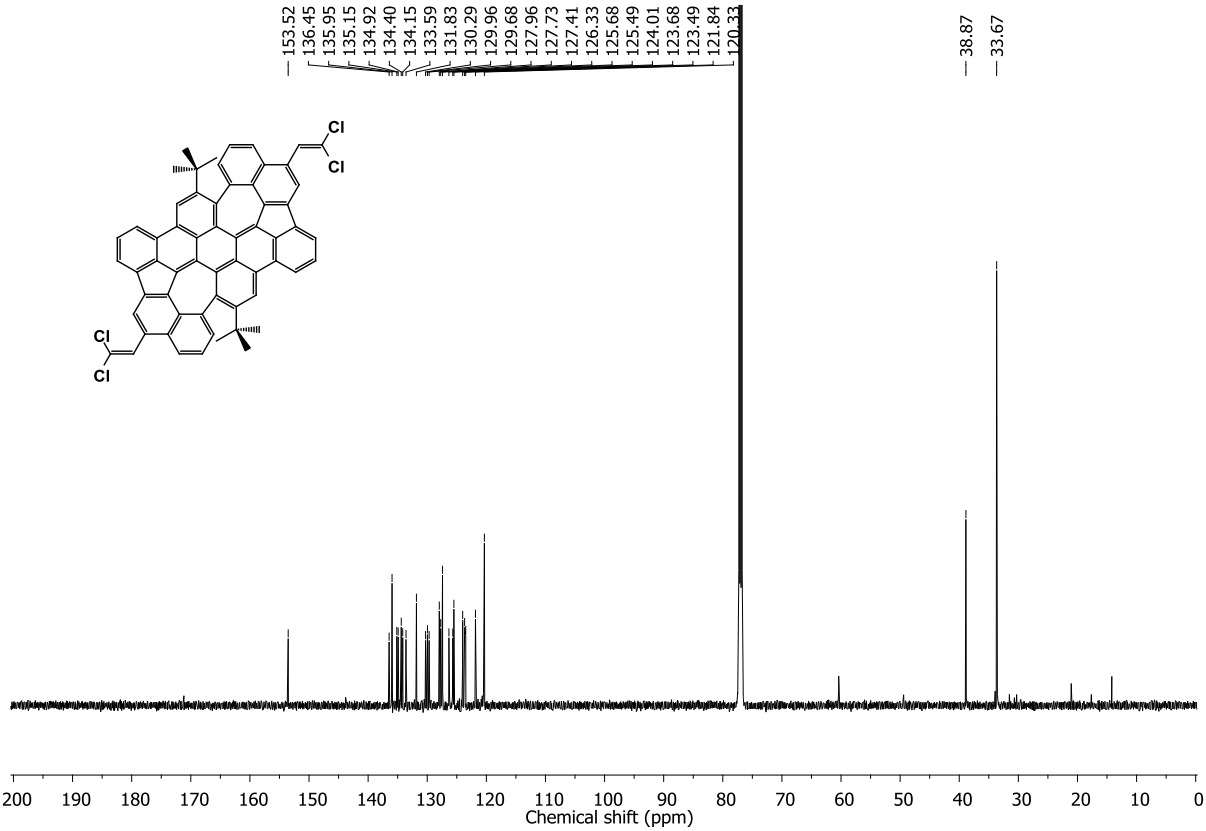

Figure S23. ^{13}C NMR spectrum (151 MHz, $CDCl_3$) of **10**.

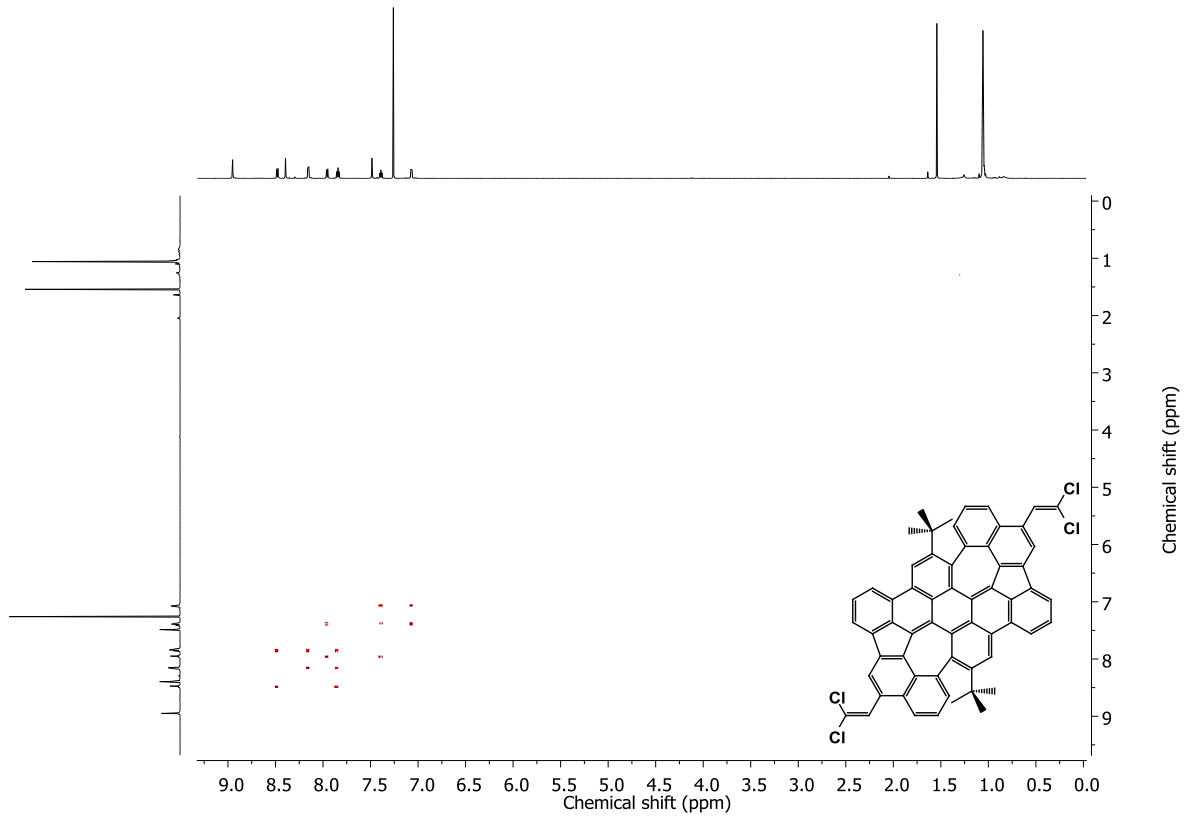

Figure S24. COSY NMR spectrum (600 MHz, $CDCl_3$) of **10**.

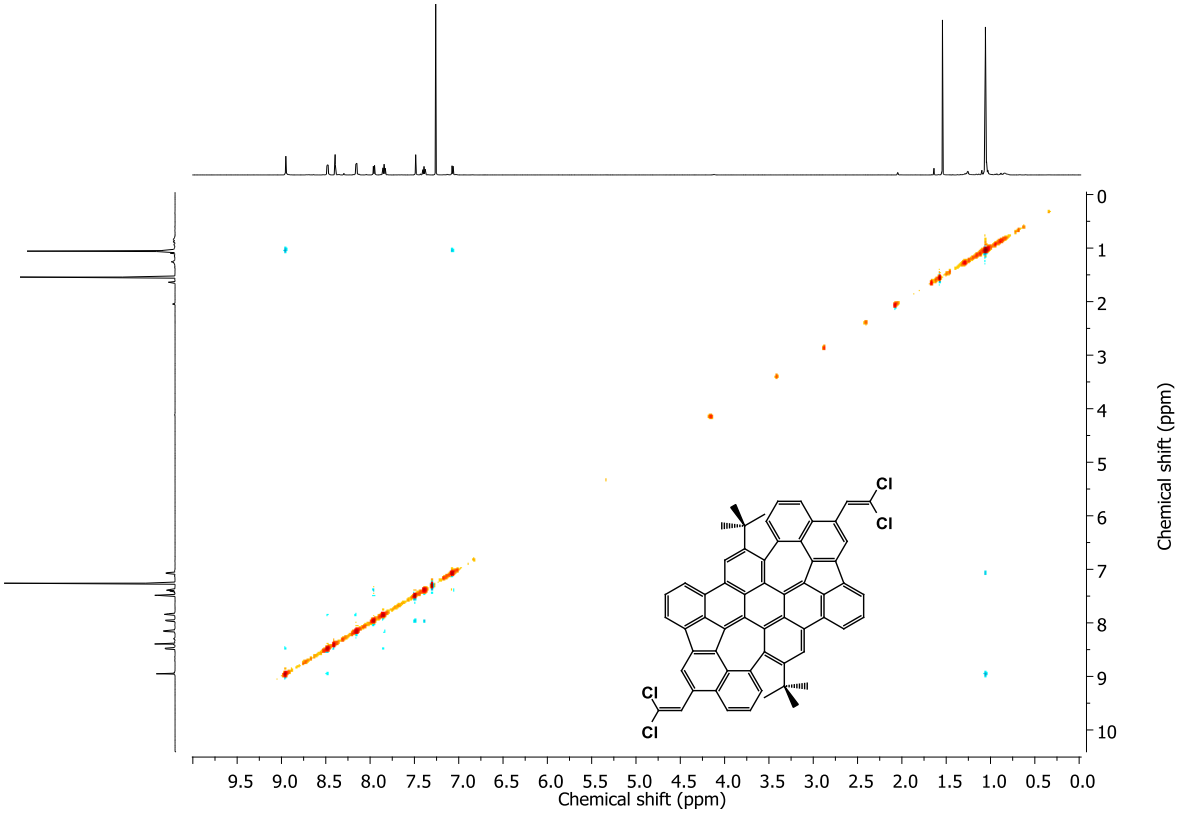

Figure S25. NOSEY NMR spectrum (600 MHz, $CDCl_3$) of **10**.

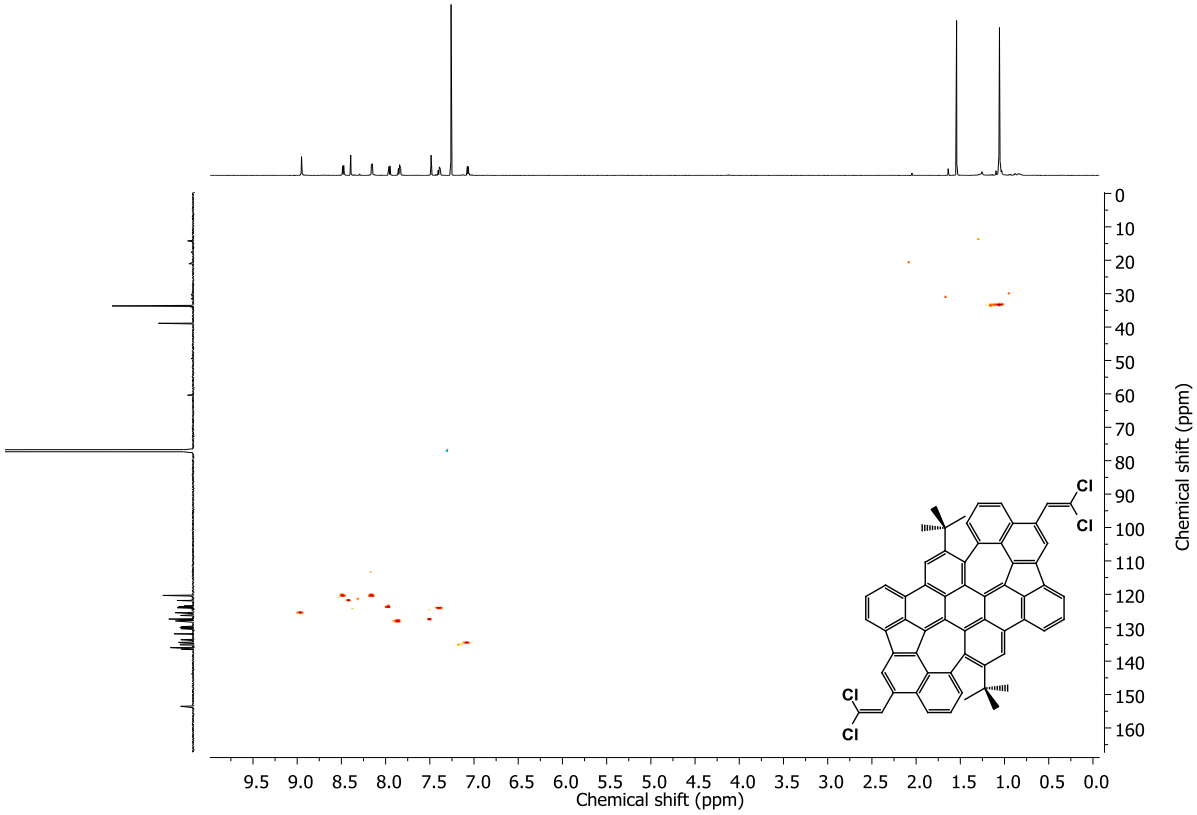

Figure S26. HSQC NMR spectrum (600 MHz, $CDCl_3$) of **10**.

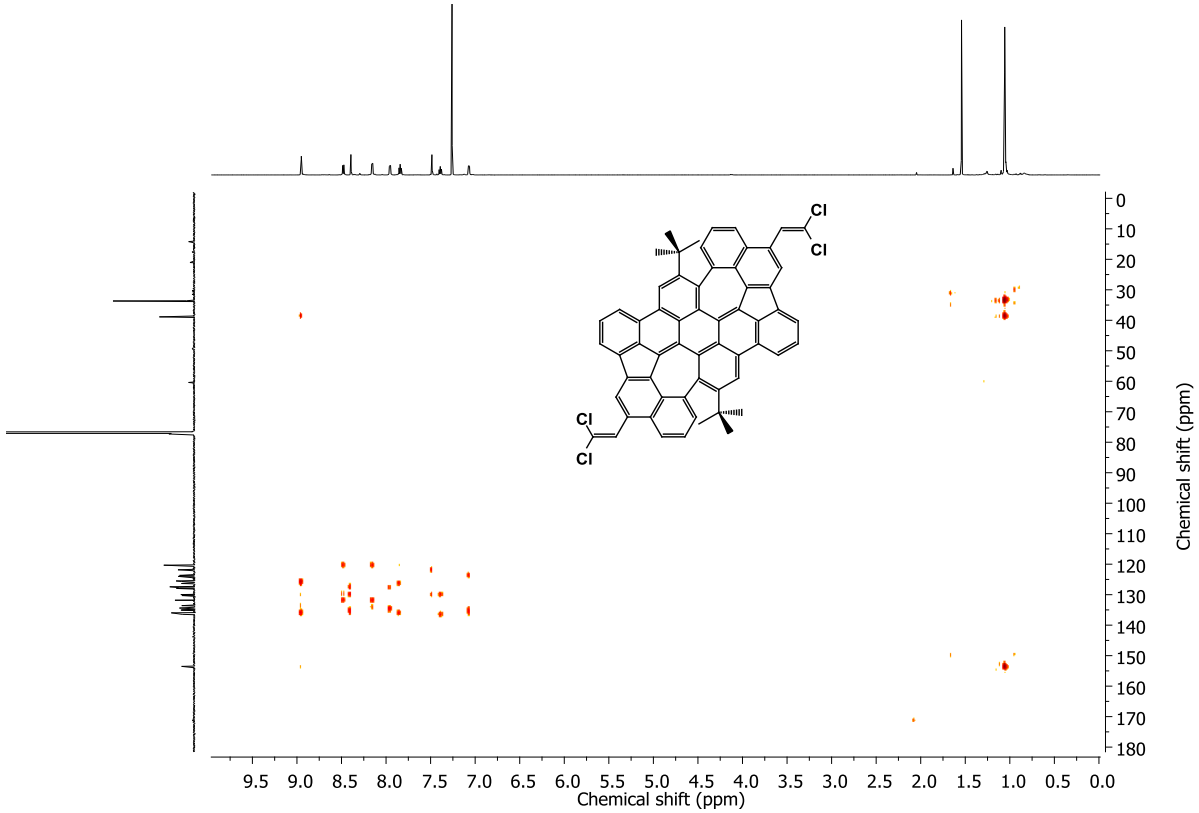

Figure S27. HMBC NMR spectrum (600 MHz, $CDCl_3$) of **10**.

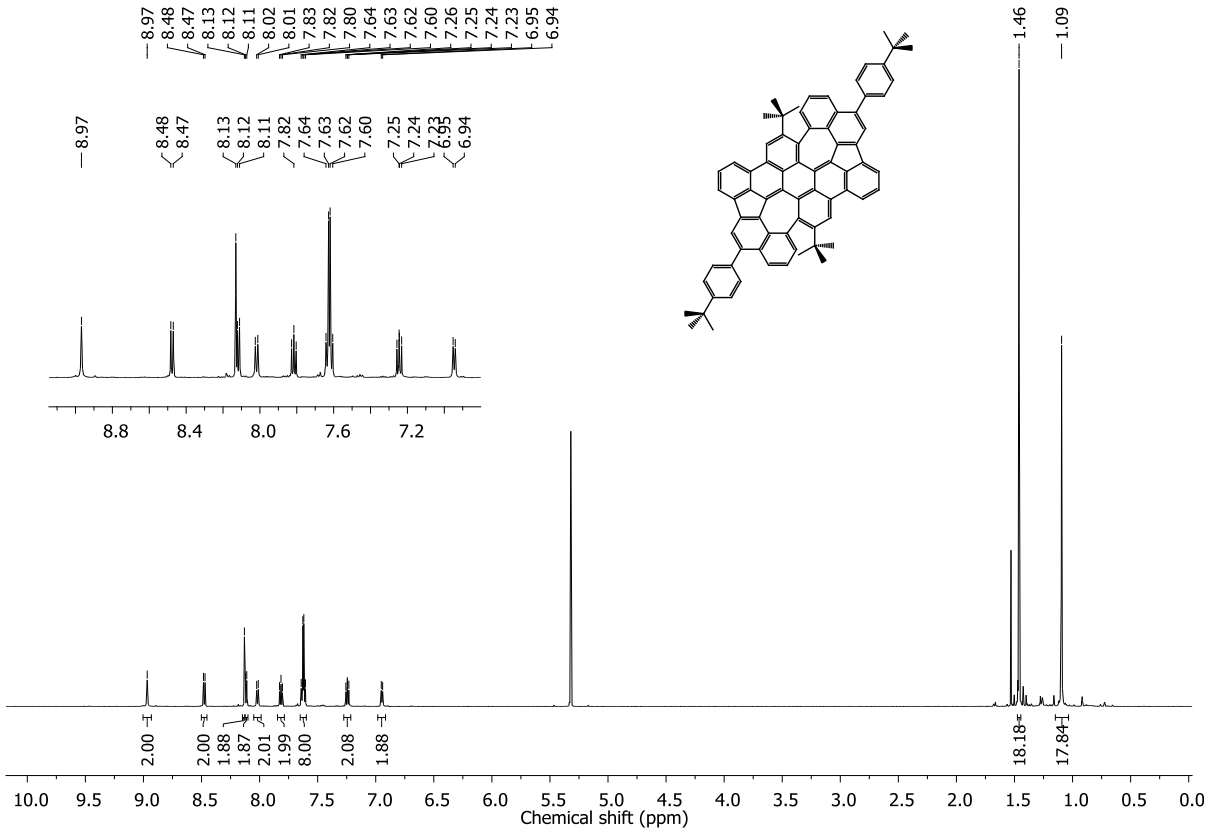

Figure S28. ^{1}H NMR spectrum (600 MHz, CD_2Cl_2) of **11**.

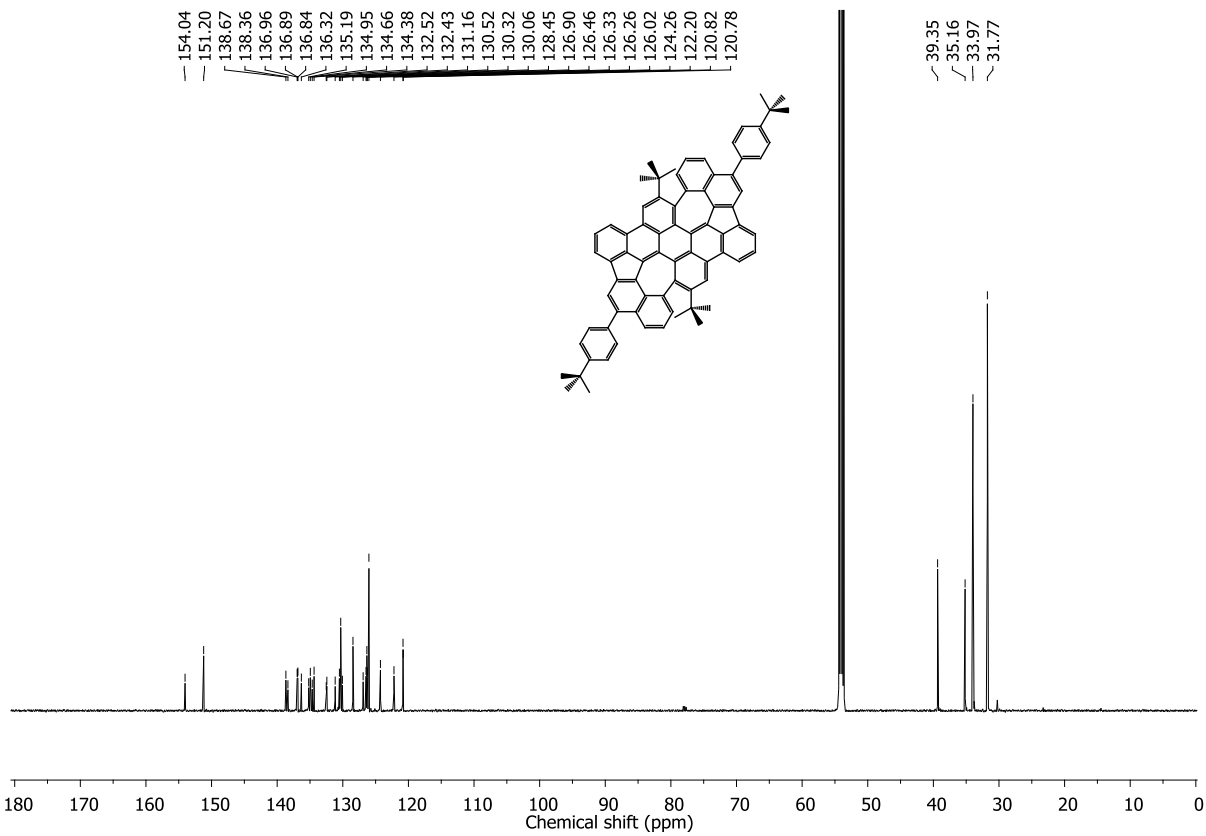

Figure S29. ^{13}C NMR spectrum (151 MHz, CD_2Cl_2) of **11**.

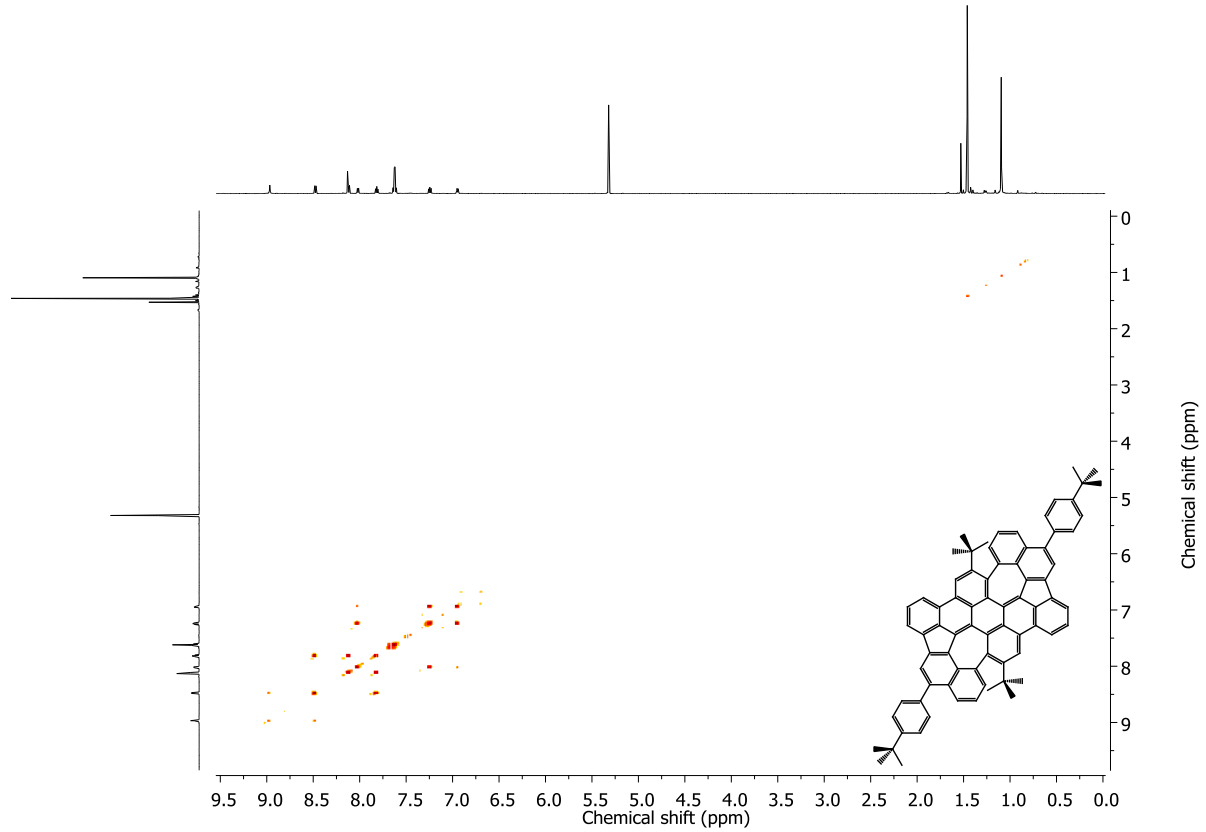

Figure S30. COSY NMR spectrum (600 MHz, CD_2Cl_2) of **11**.

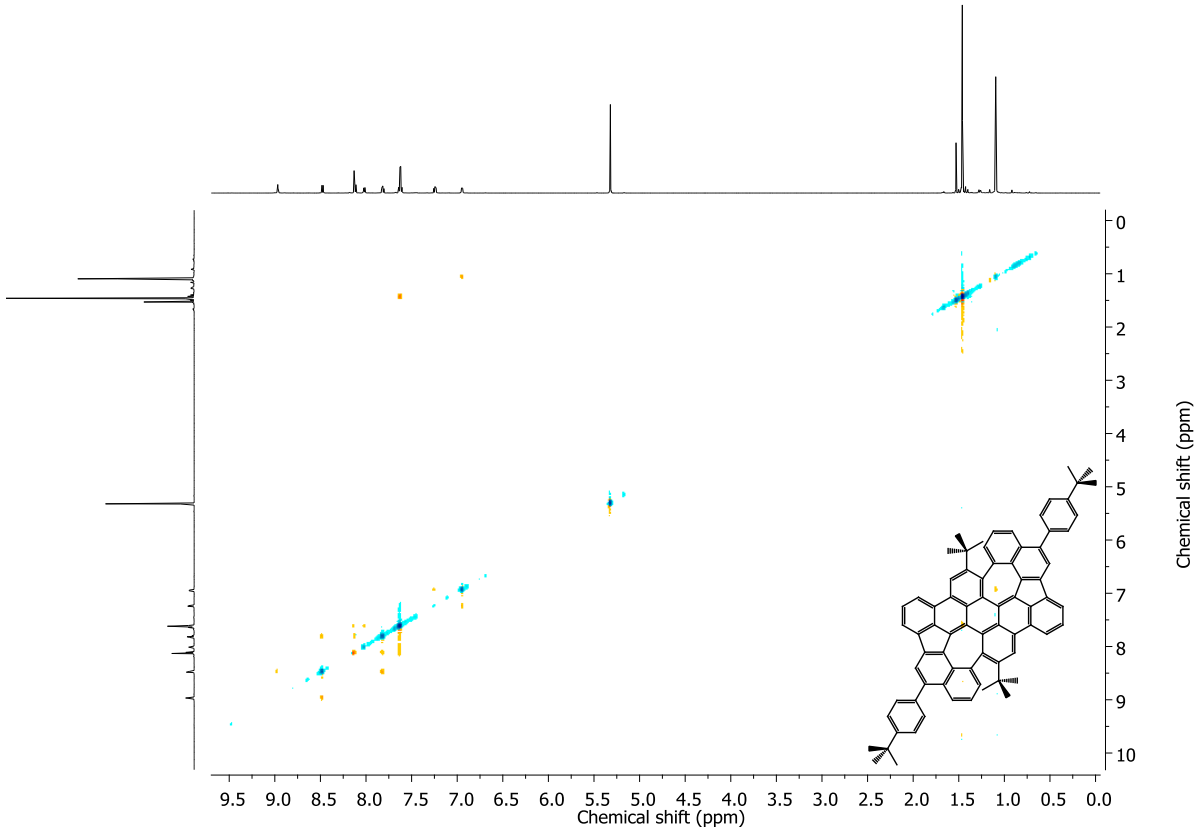

Figure S31. ROSEY NMR spectrum (600 MHz, CD_2Cl_2) of **11**.

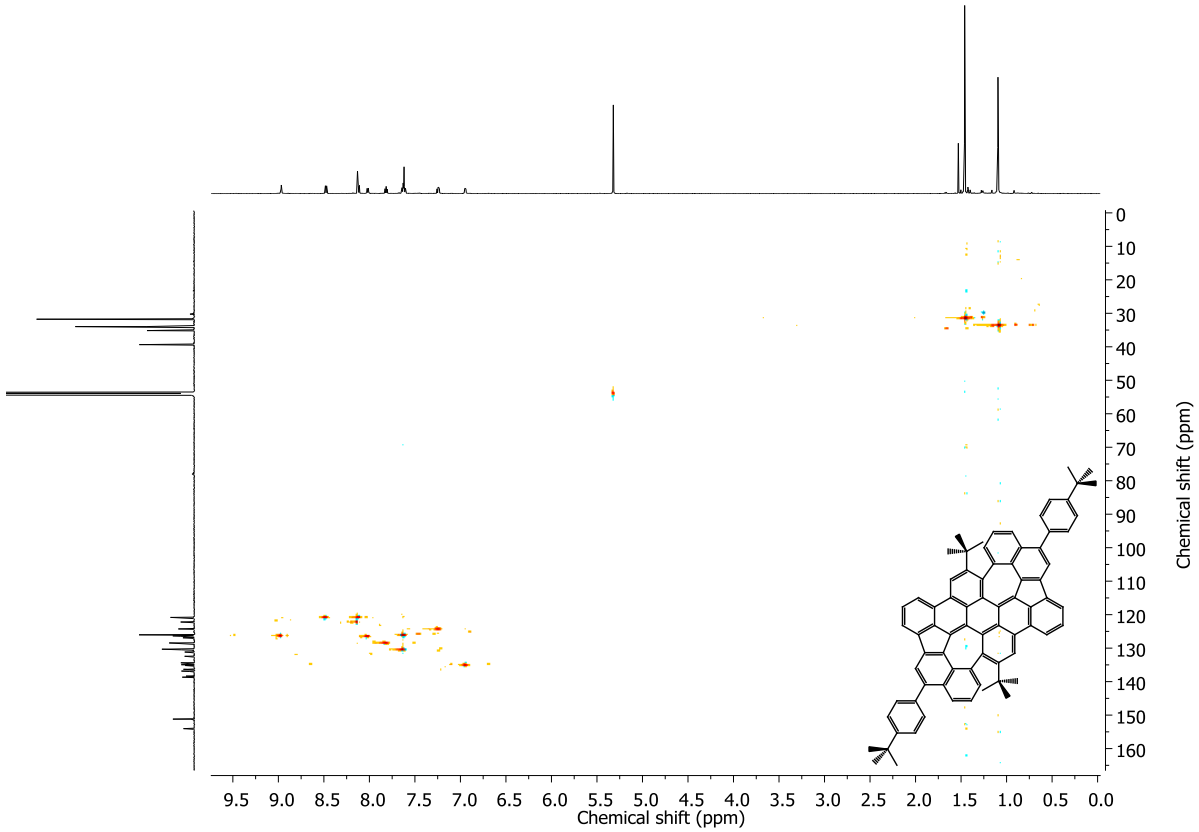

Figure S32. HSQC NMR spectrum (600 MHz, CD_2Cl_2) of **11**.

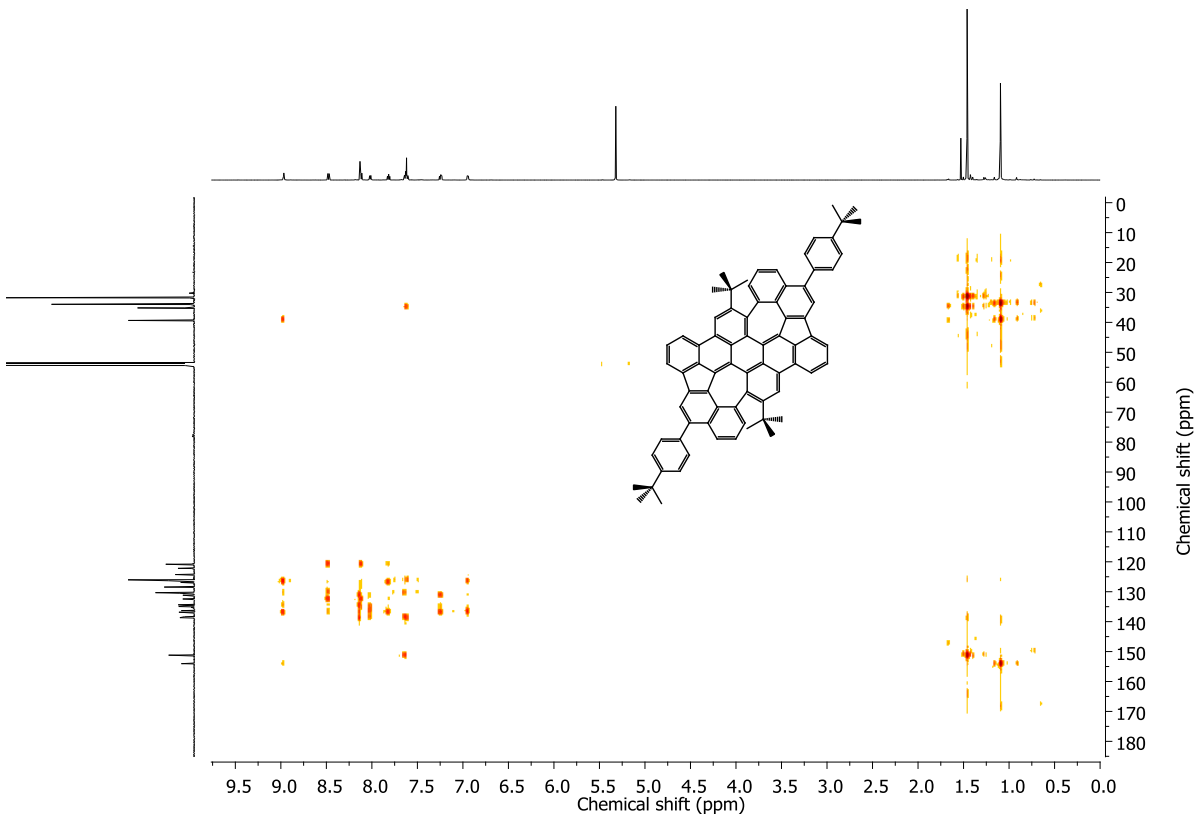

Figure S33. HMBC NMR spectrum (600 MHz, CD_2Cl_2) of **11**.

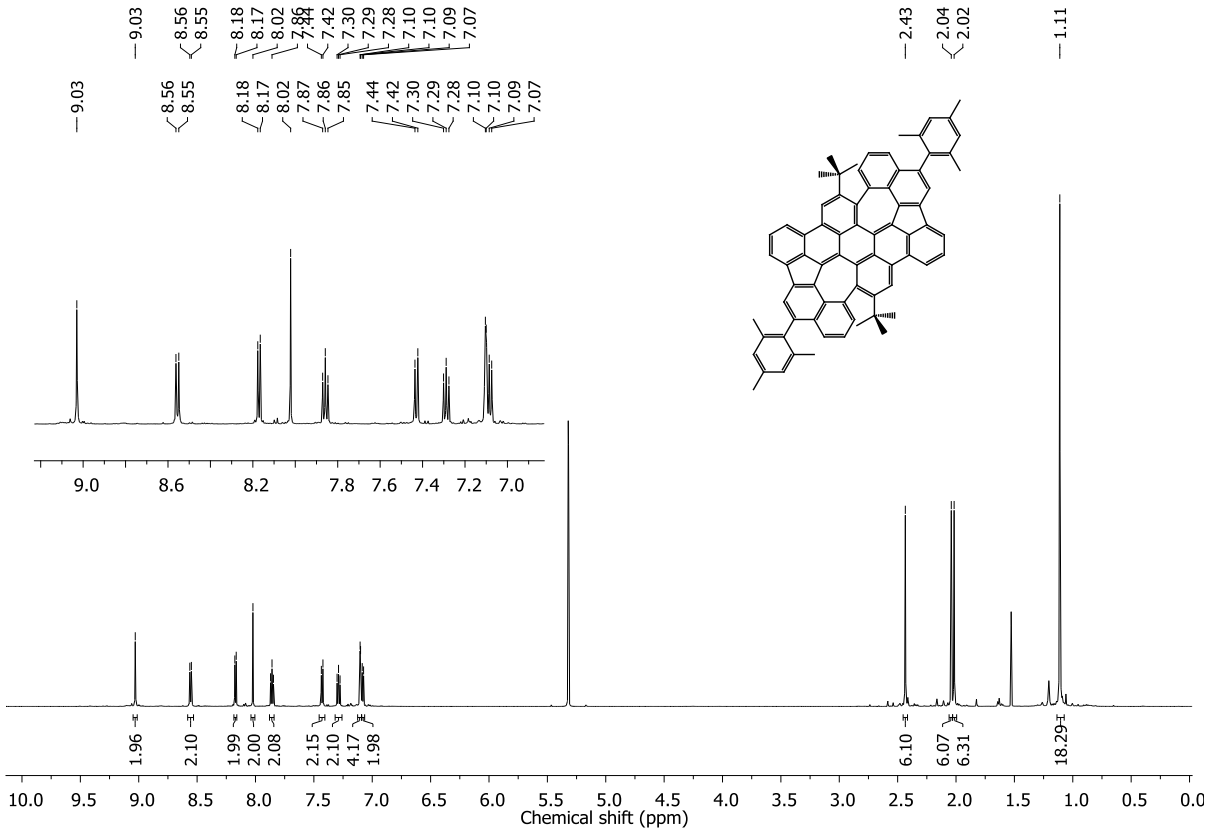

Figure S34. ^{1}H NMR spectrum (600 MHz, CD_2Cl_2) of **12**.

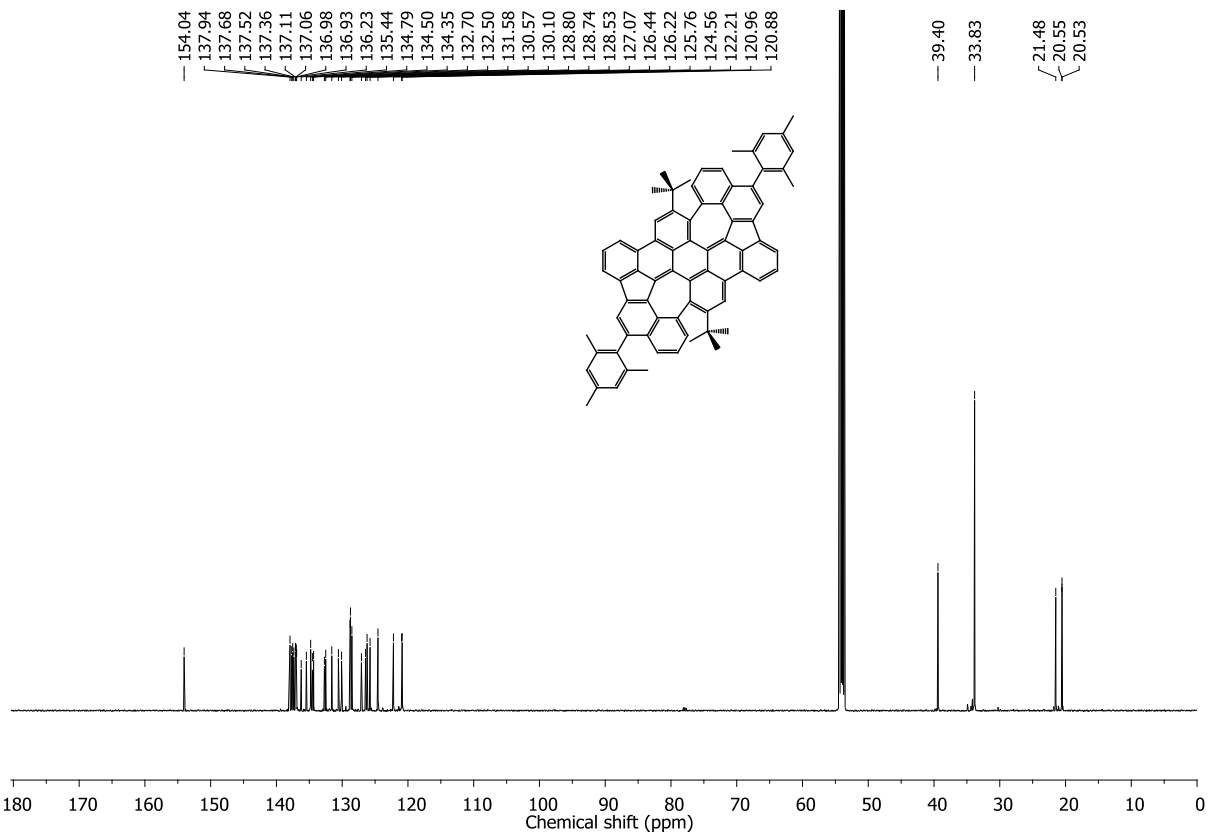

Figure S35. ^{13}C NMR spectrum (151 MHz, CD_2Cl_2) of **12**.

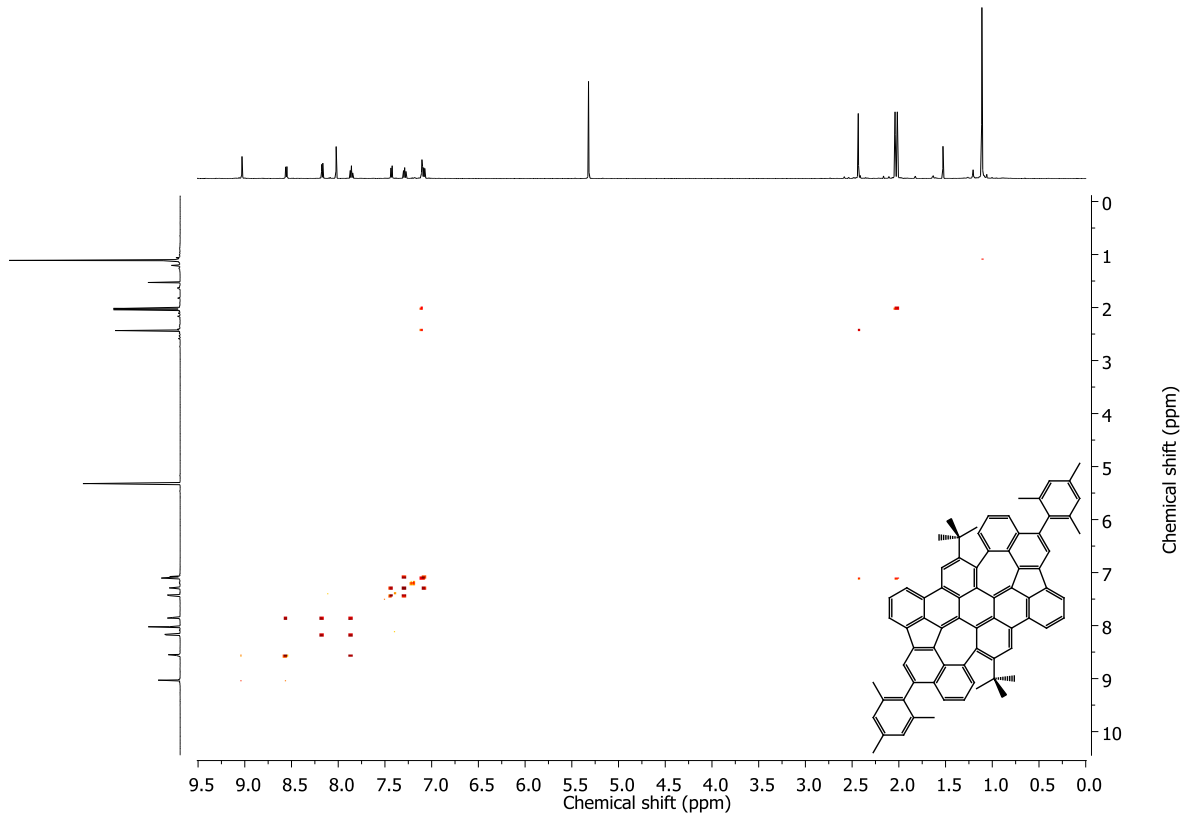

Figure S36. COSY NMR spectrum (600 MHz, CD_2Cl_2) of **12**.

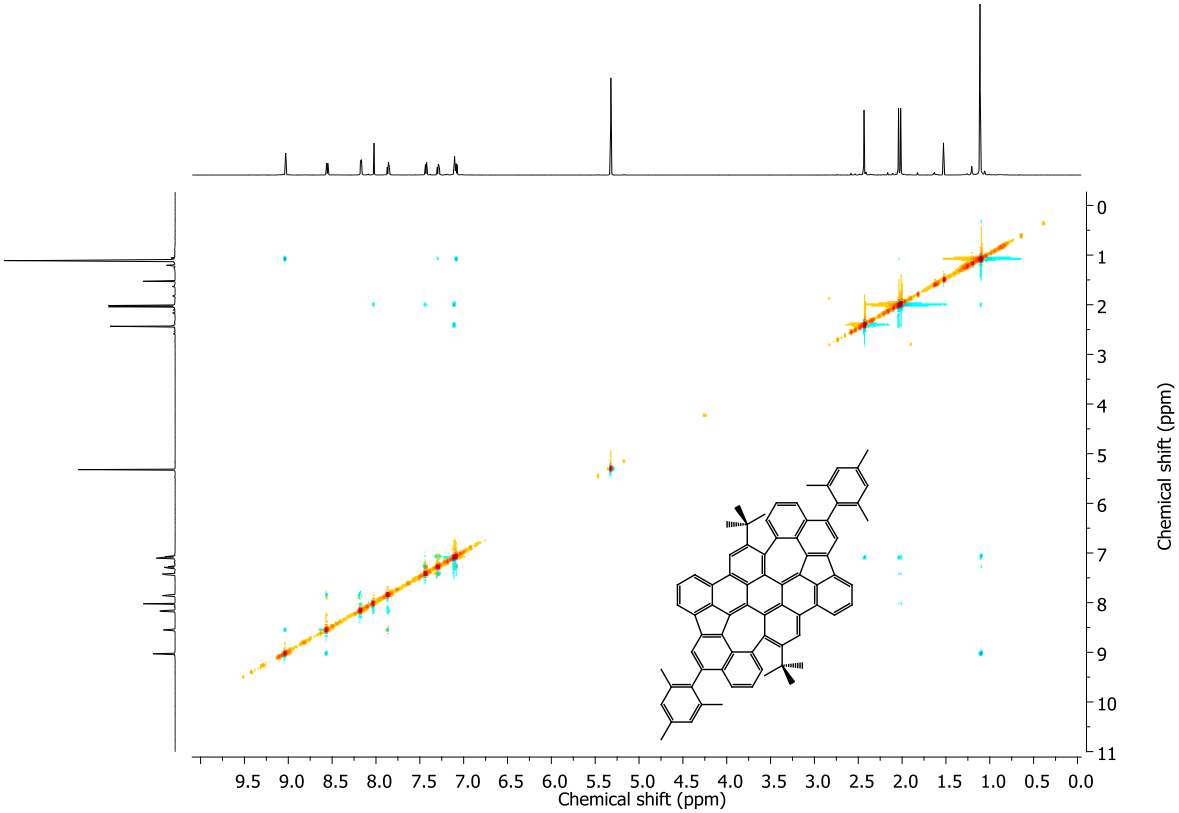

Figure S37. NOSEY NMR spectrum (600 MHz, CD_2Cl_2) of **12**.

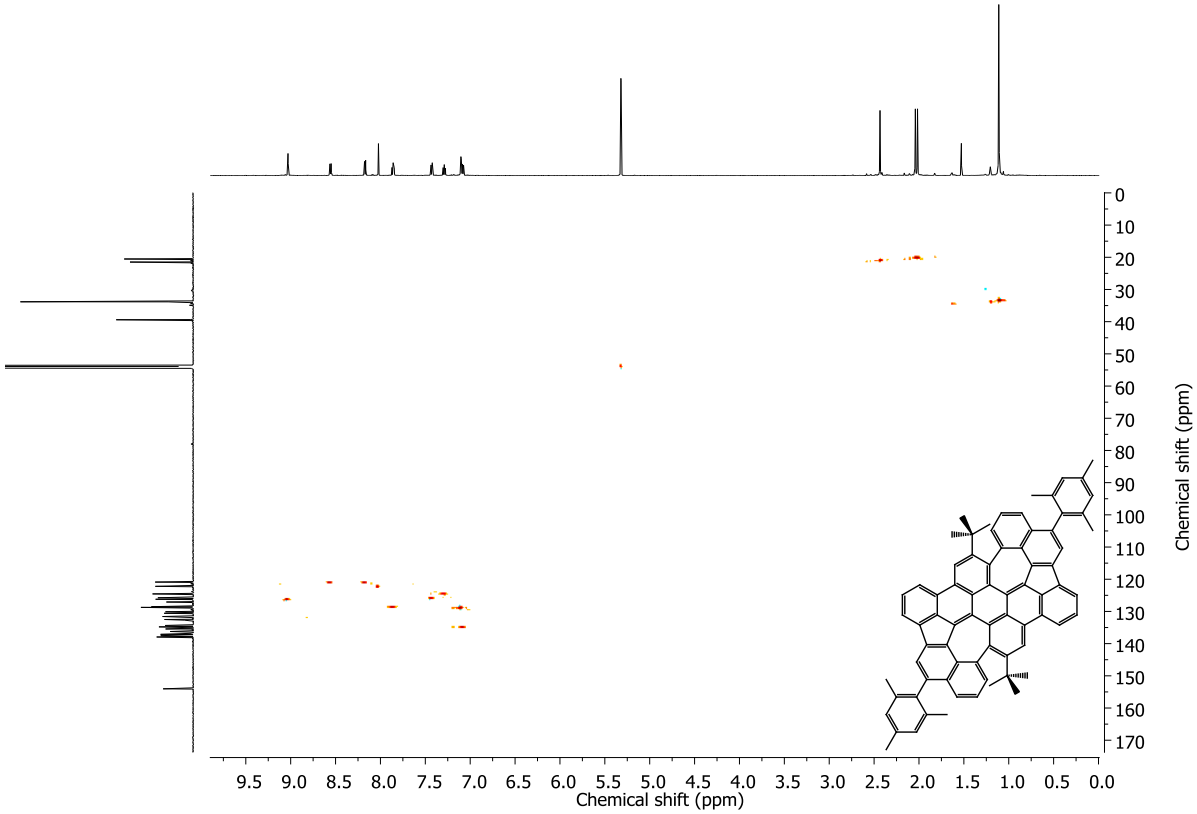

Figure S38. HSQC NMR spectrum (600 MHz, CD_2Cl_2) of **12**.

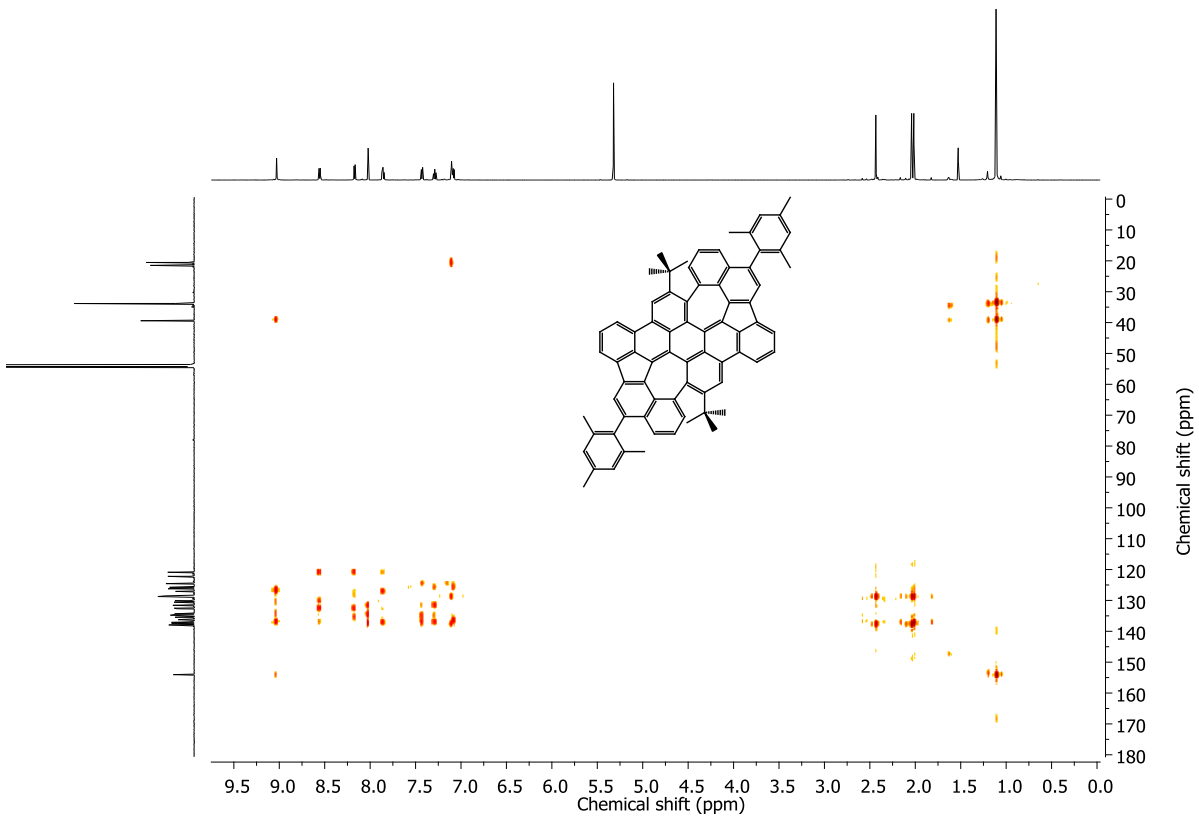

Figure S39. HMBC NMR spectrum (600 MHz, CD_2Cl_2) of **12**.

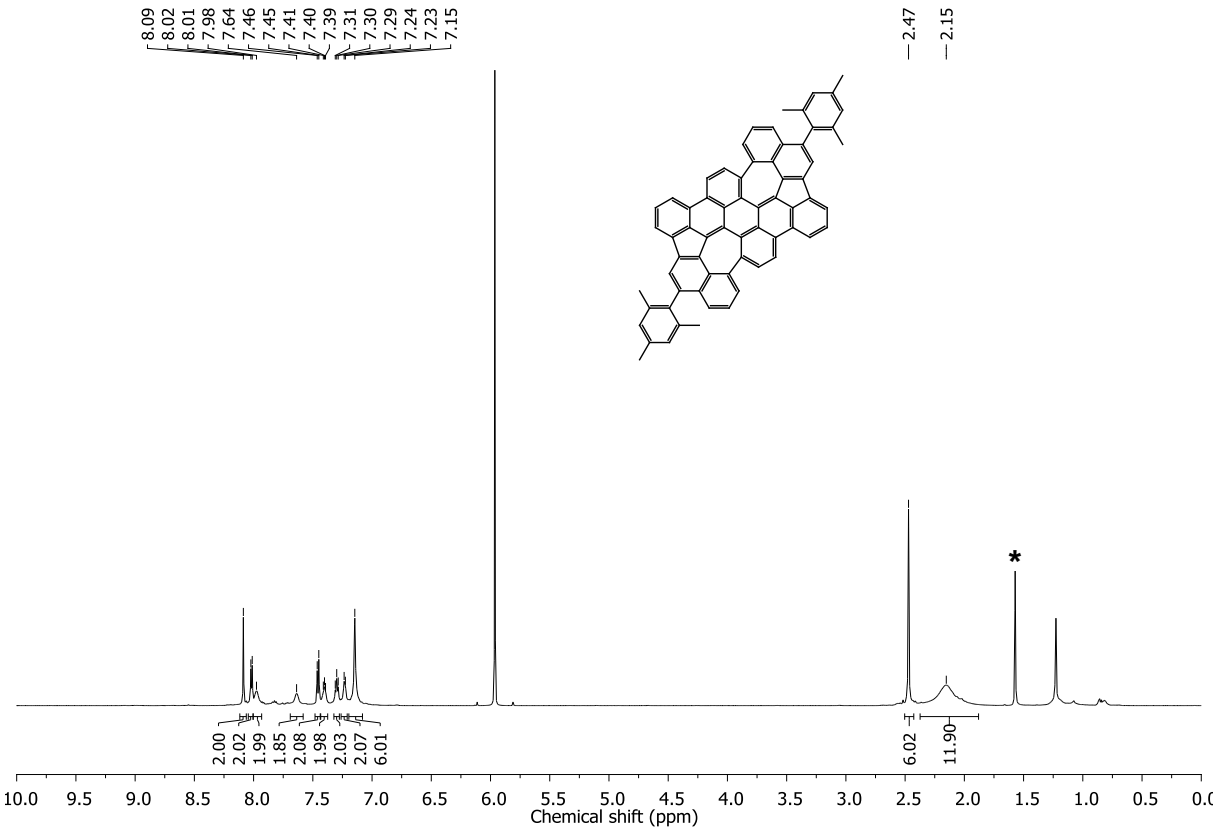

Figure S40. ^{1}H NMR spectrum (600 MHz, $Cl_2CDCDCl_2$, 298 K, c= 14.4 mmol·L^{-1}) of **13**. *H_2O.

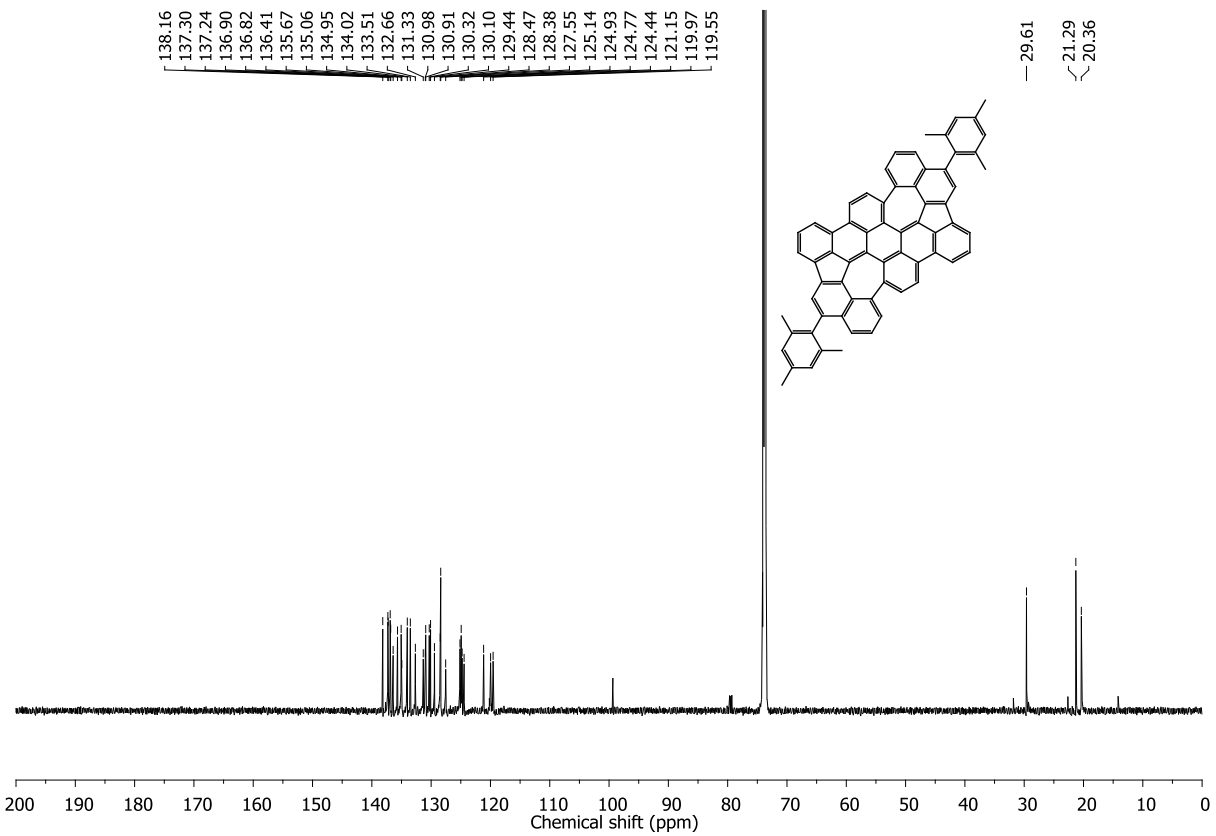

Figure S41. ^{13}C NMR spectrum (151 MHz, $Cl_2CDCDCl_2$, 298 K) of **13**.

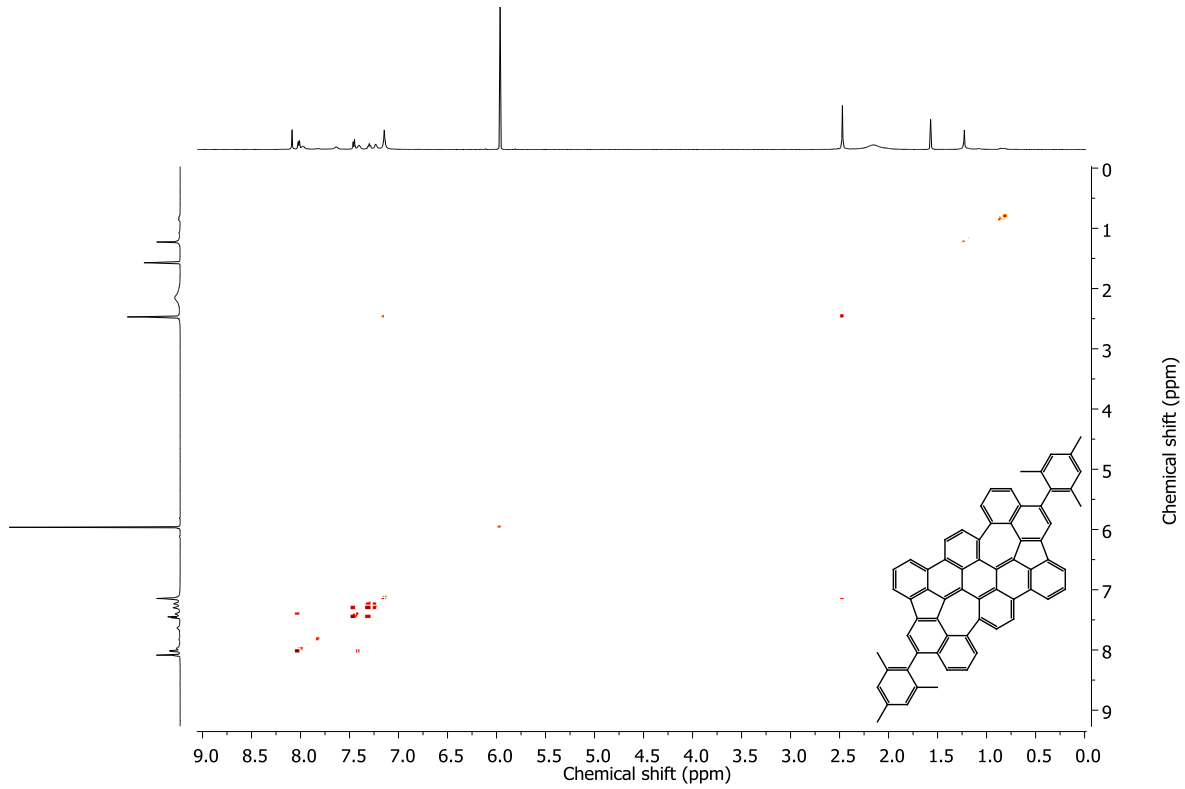

Figure S42. COSY NMR spectrum (600 MHz, $Cl_2CDCDCl_2$, 298 K) of **13**.

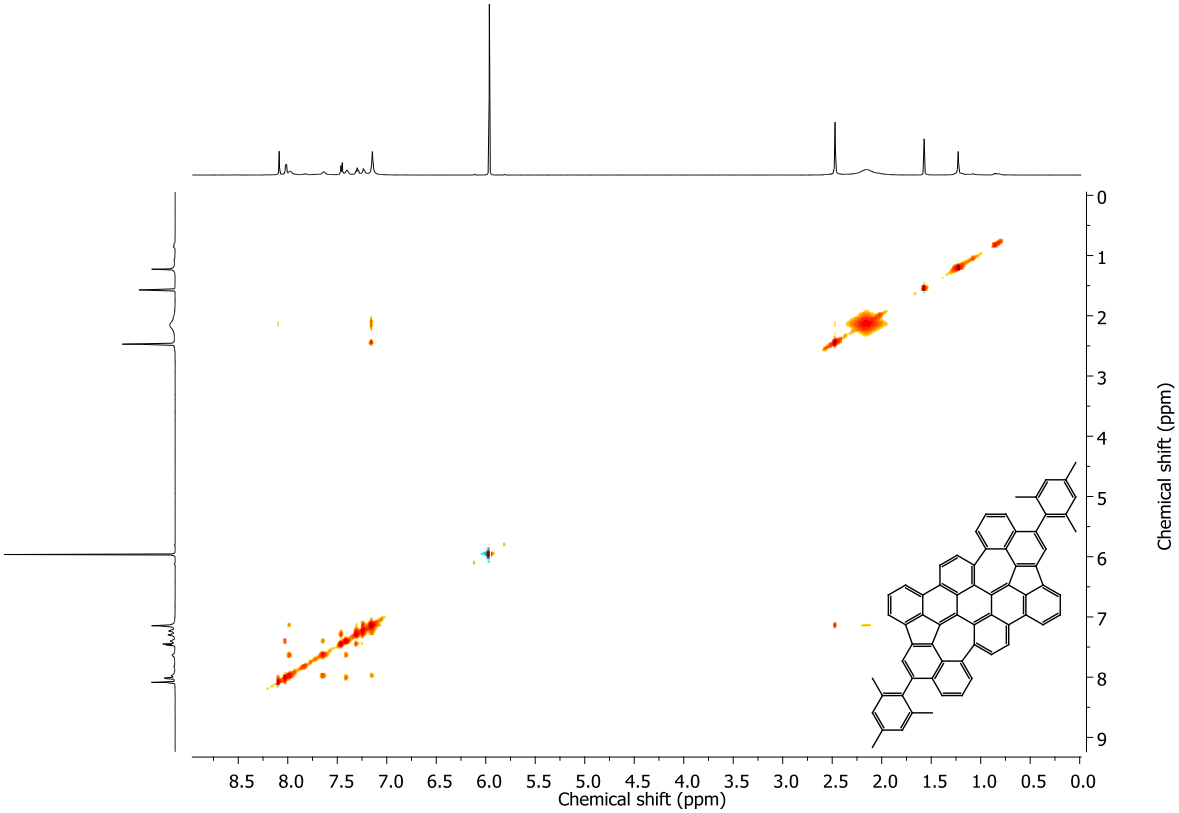

Figure S43. NOESY NMR spectrum (600 MHz, $Cl_2CDCDCl_2$, 298 K) of **13**.

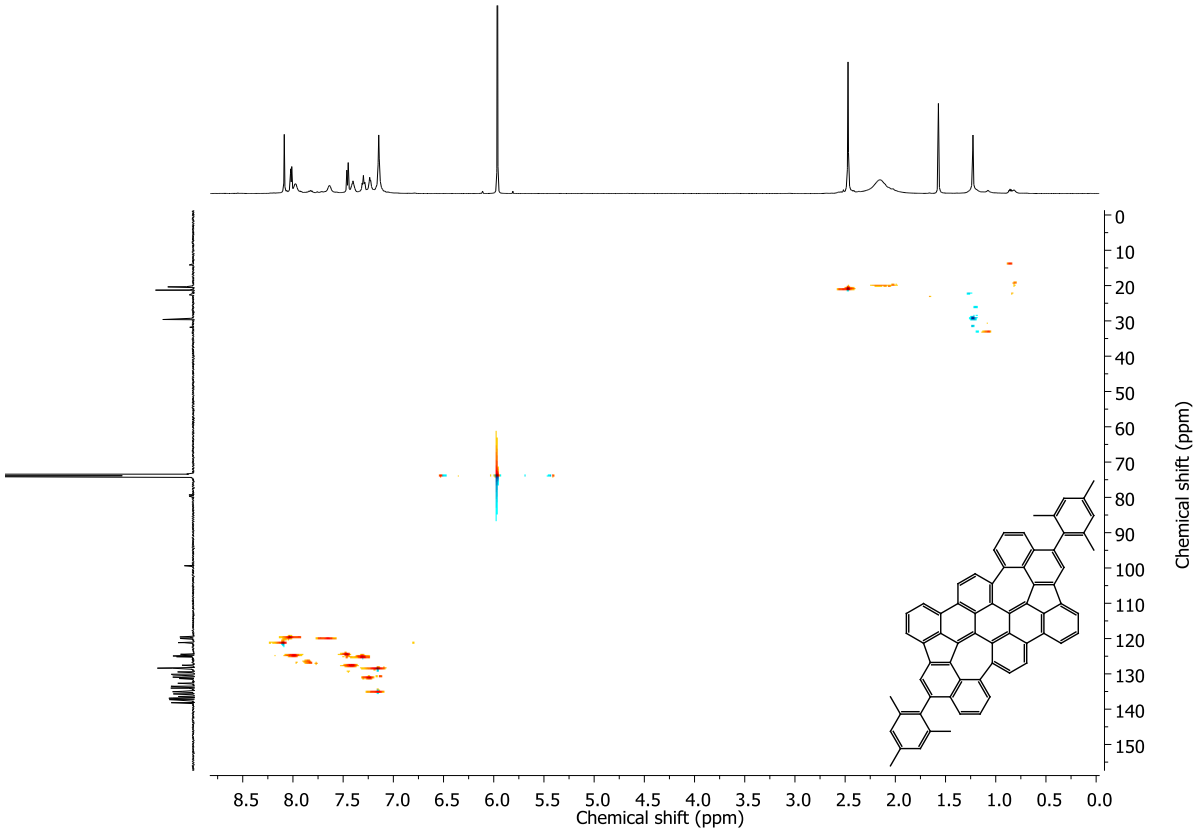

Figure S44. HSQC NMR spectrum (600 MHz, $Cl_2CDCDCl_2$, 298 K) of **13**.

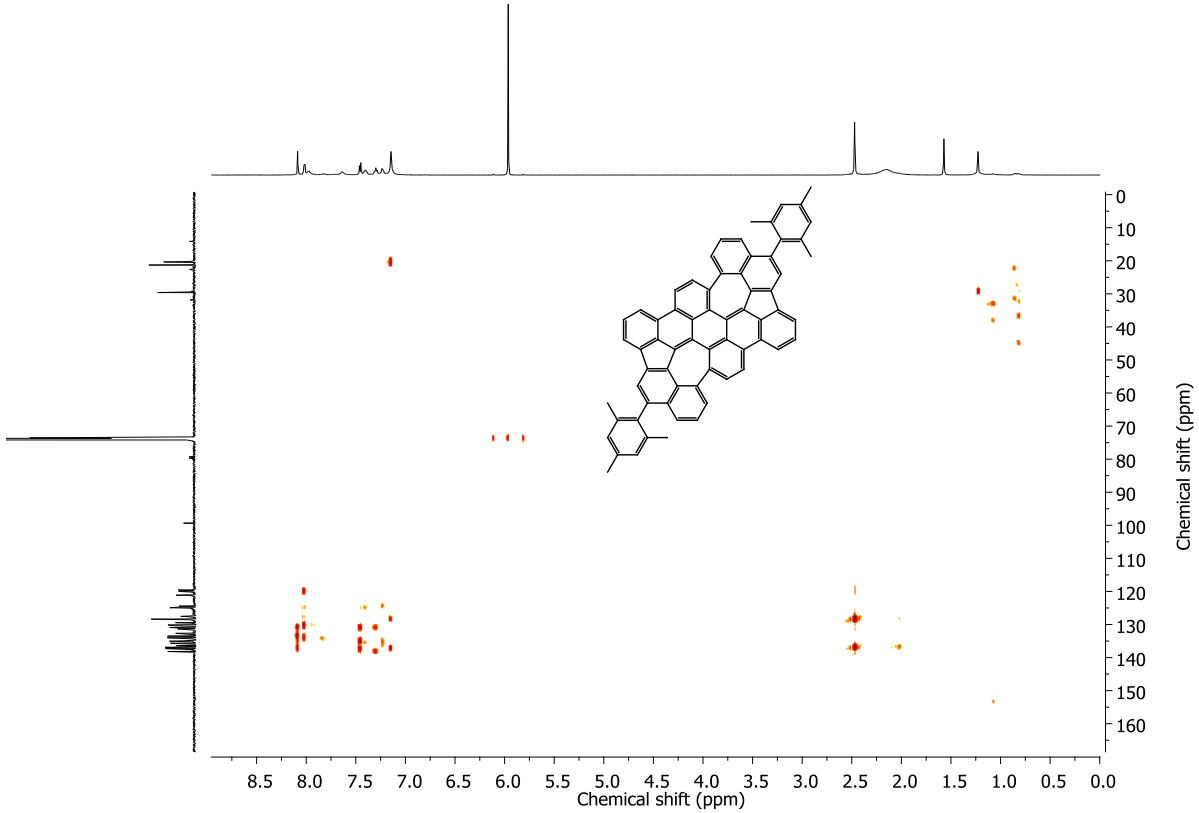

Figure S45. HMBC NMR spectrum (600 MHz, $Cl_2CDCDCl_2$, 298 K) of **13**.

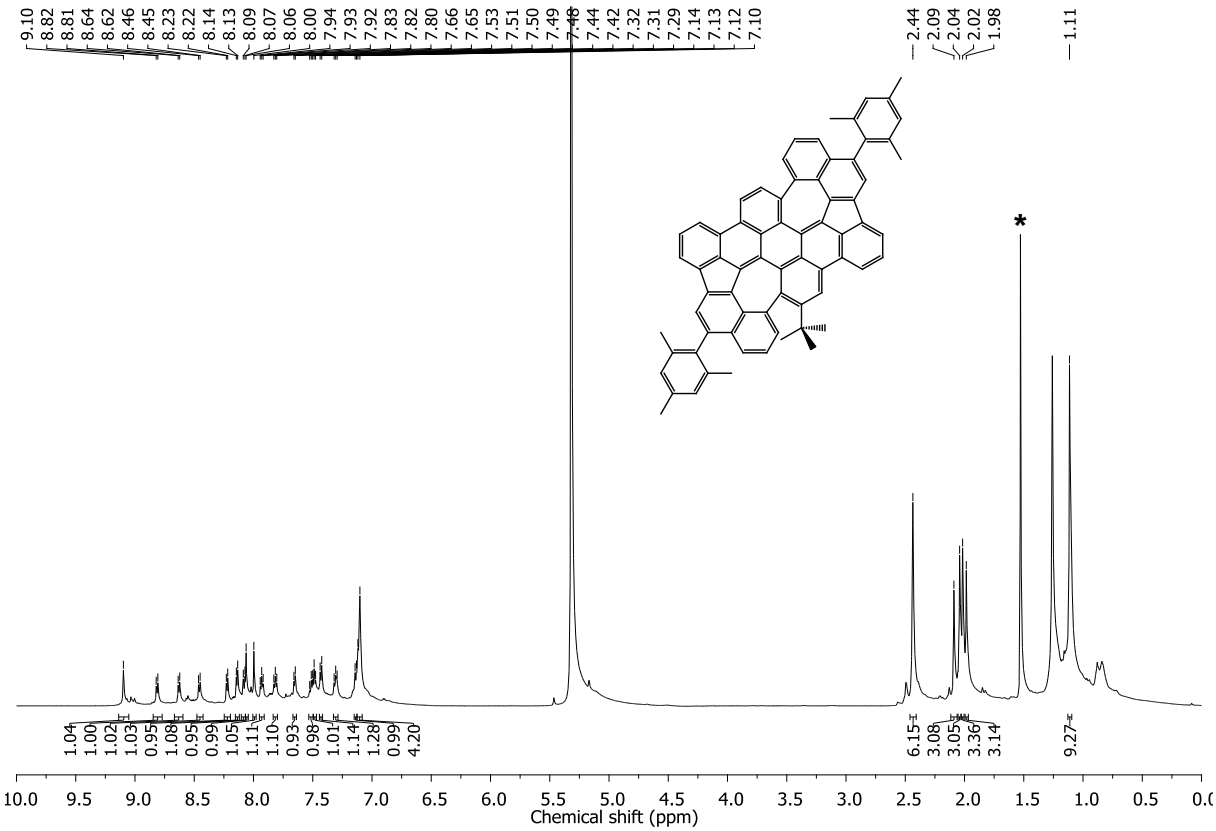

Figure S46. ^{1}H NMR spectrum (600 MHz, CD_2Cl_2) of **14**. *H_2O.

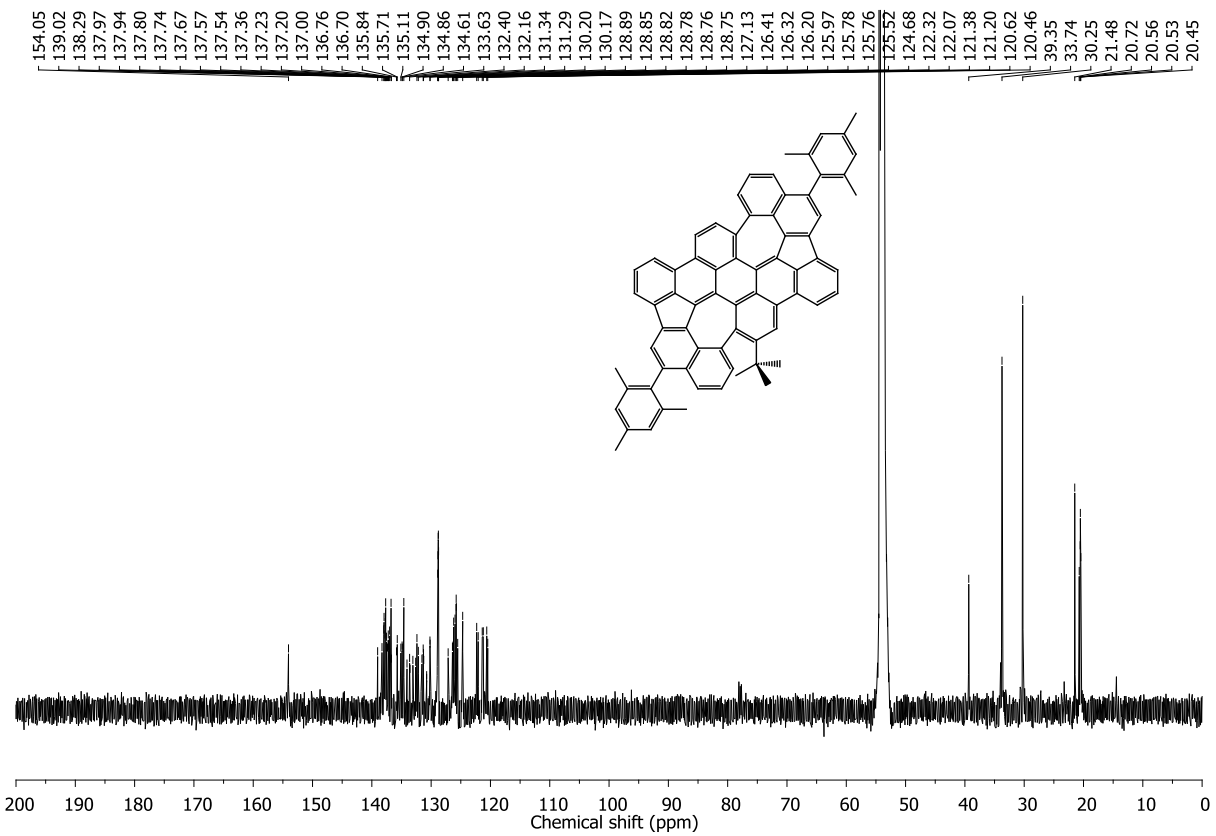

Figure S47. ^{13}C NMR spectrum (151 MHz, CD_2Cl_2) of **14**.

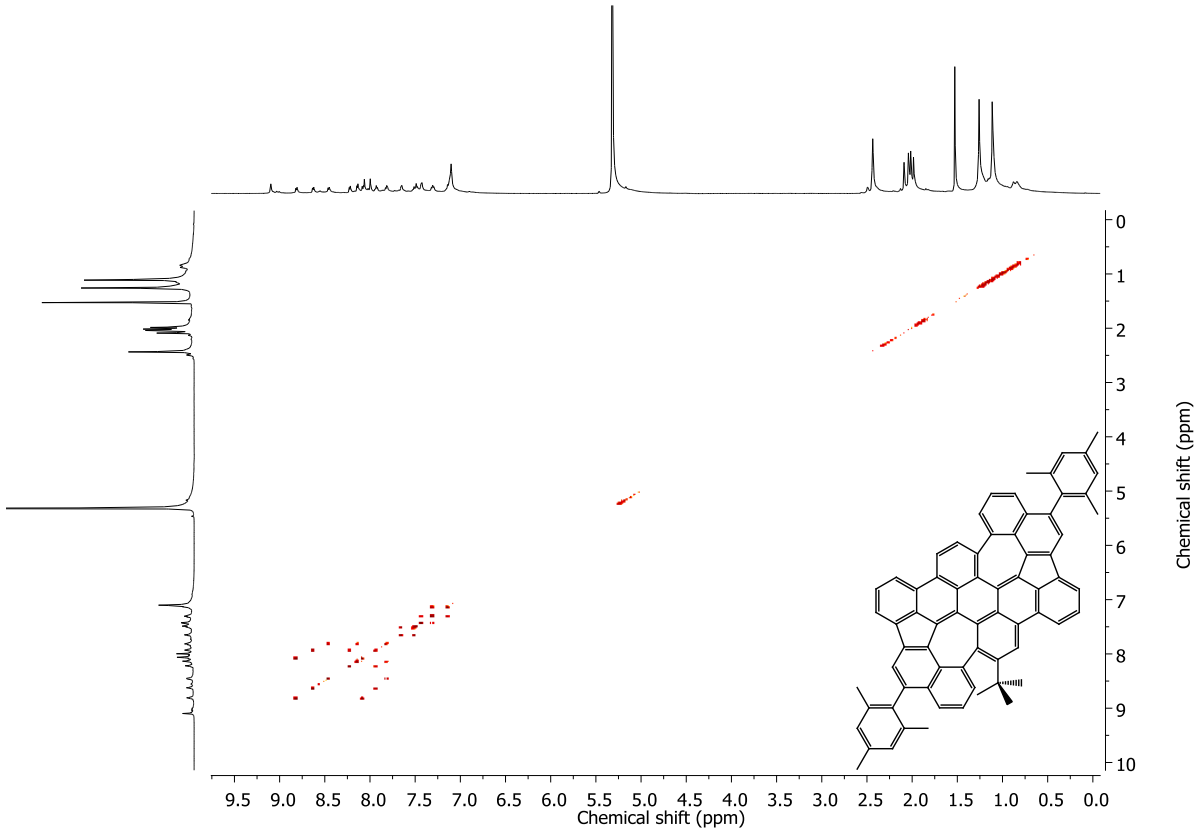

Figure S48. COSY NMR spectrum (600 MHz, CD_2Cl_2) of **14**.

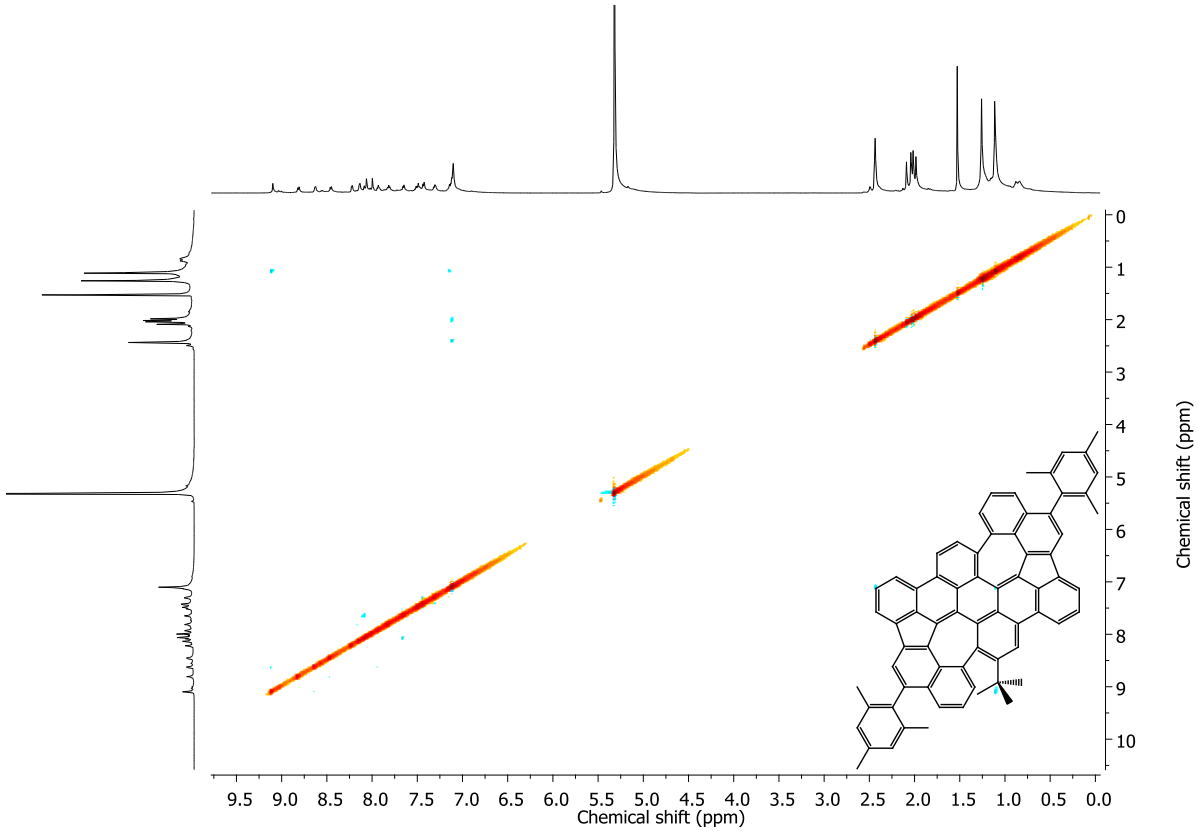

Figure S49. NOESY NMR spectrum (600 MHz, CD_2Cl_2) of **14**.

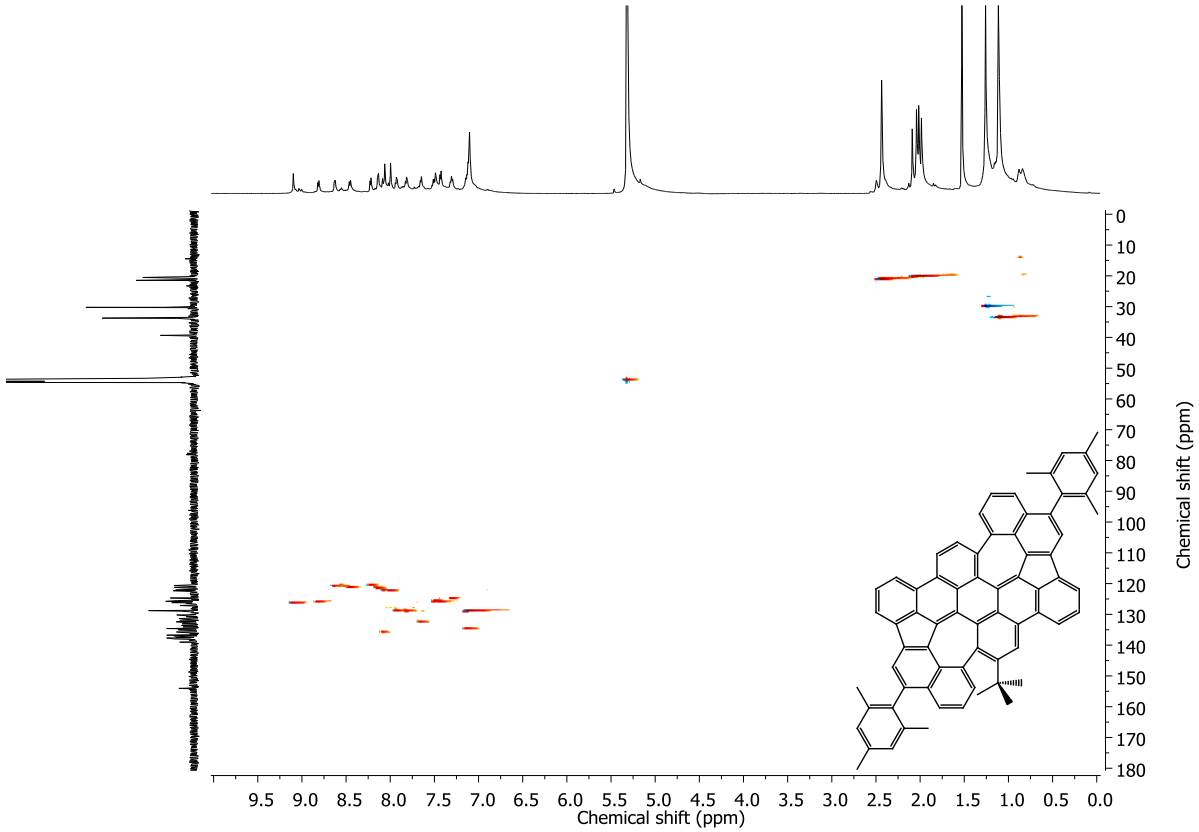

Figure S50. HSQC NMR spectrum (600 MHz, CD_2Cl_2) of **14**.

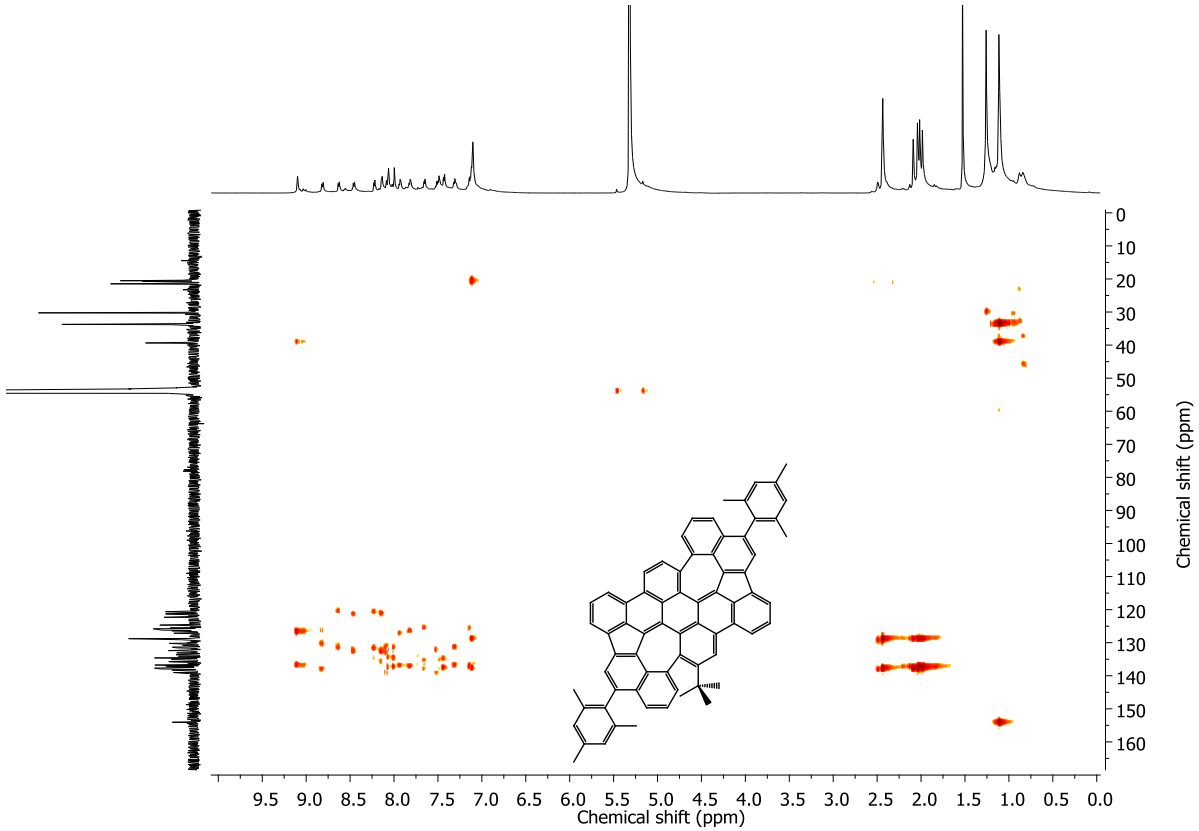

Figure S51. HMBC NMR spectrum (600 MHz, CD_2Cl_2) of **14**.

4. Mass spectra

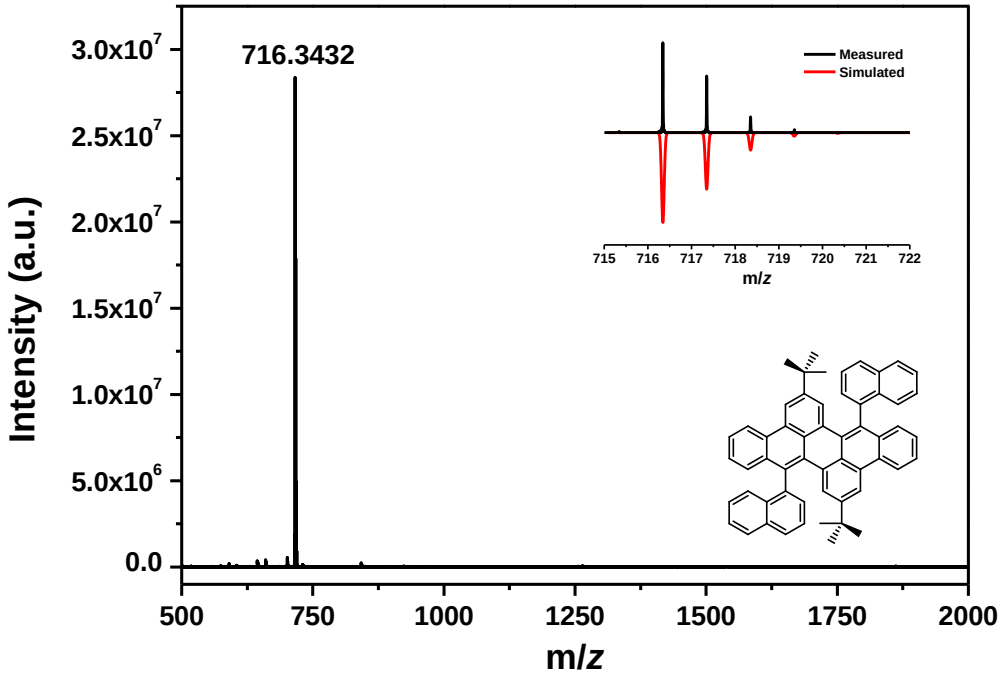

Figure S52. HRMS-MALDI (DCTB) of compound **3**.

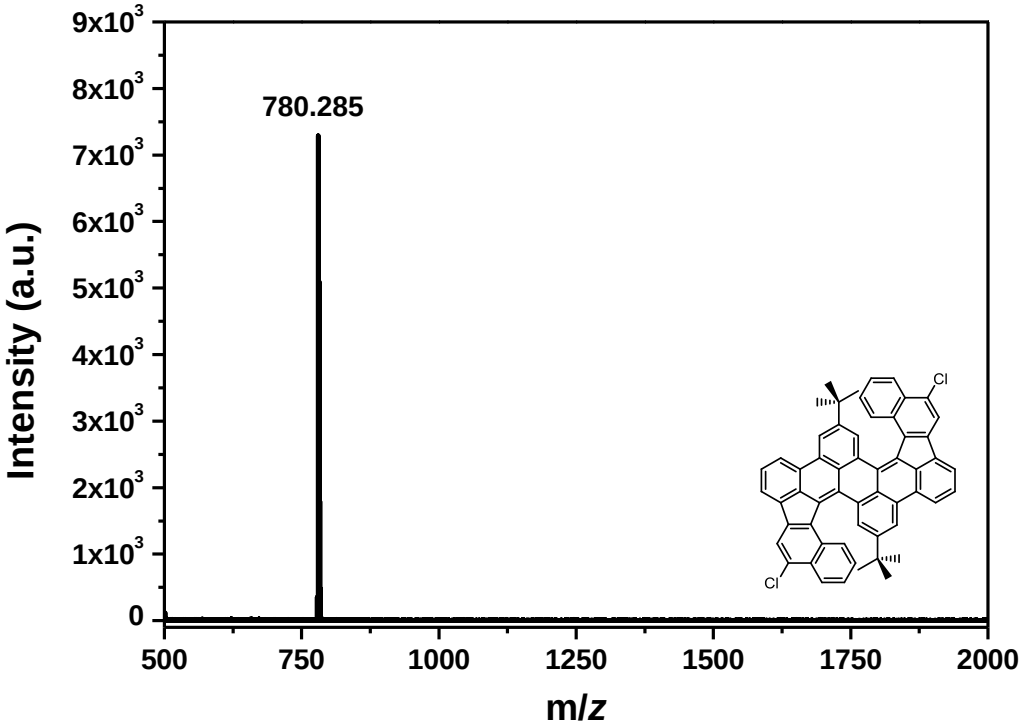

Figure S53. MS MALDI-TOF (DCTB) of compound **7**.

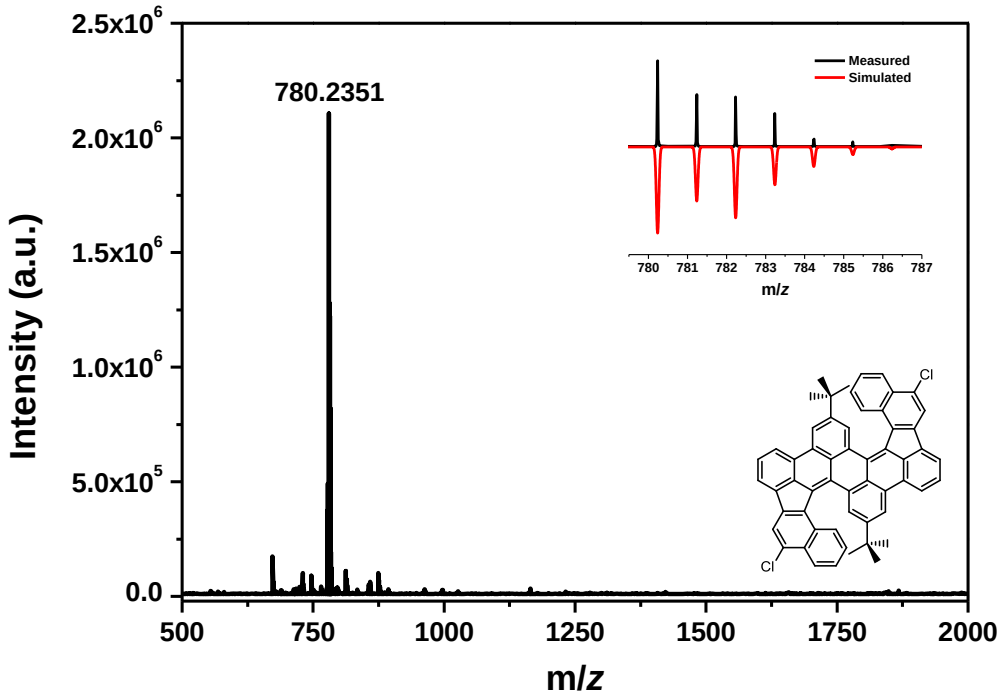

Figure S54. HRMS-MALDI (DCTB) of compound **7**.

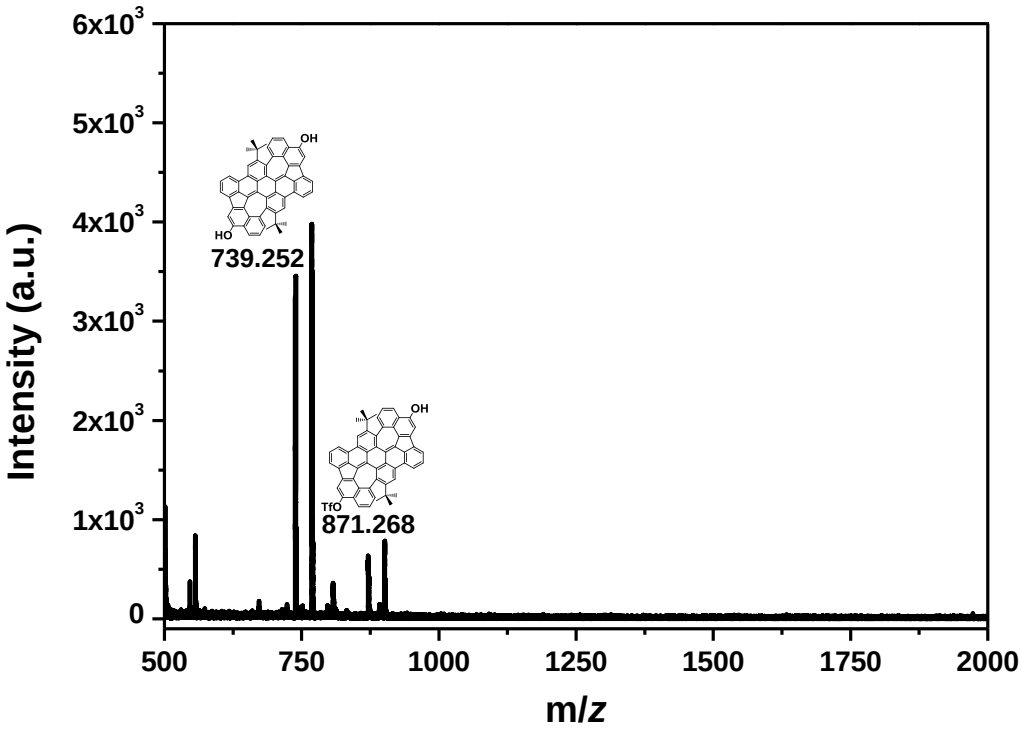

Figure S55. MS MALDI-TOF (DCTB) of compound **8**.

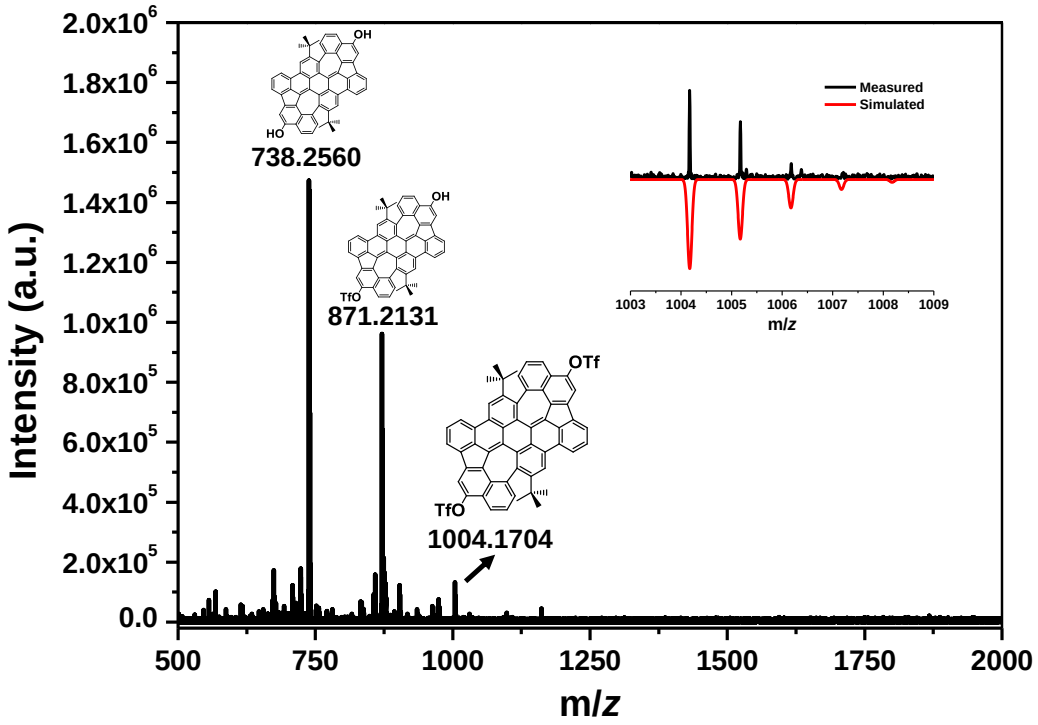

Figure S56. HRMS-MALDI (DCTB) of compound **8**.

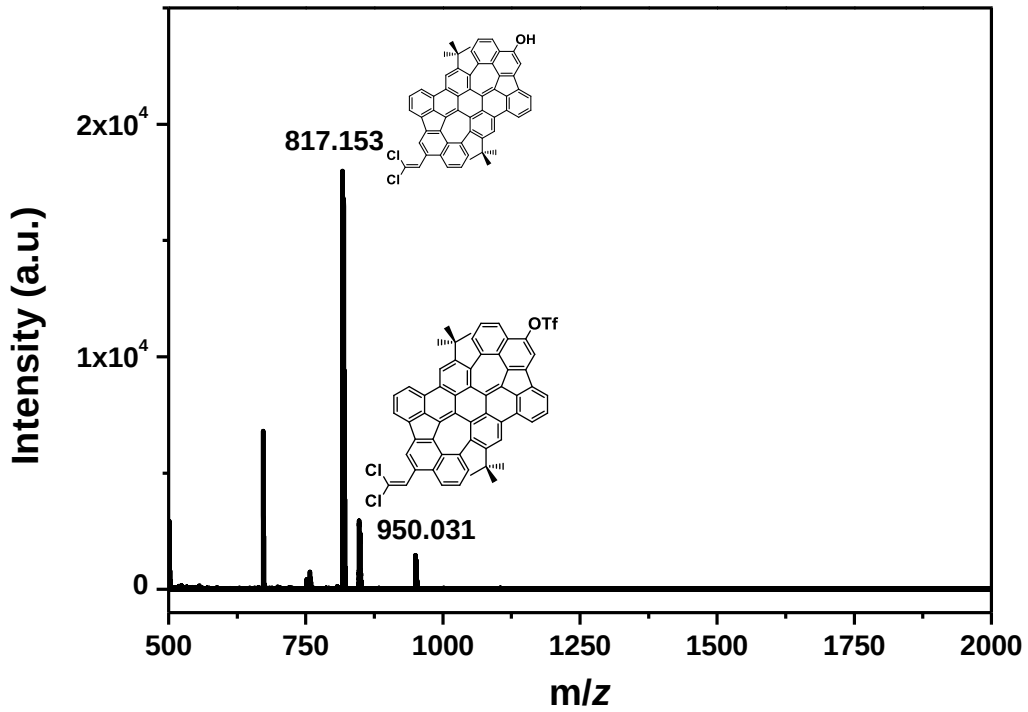

Figure S57. MS MALDI-TOF (DCTB) of compound **9**.

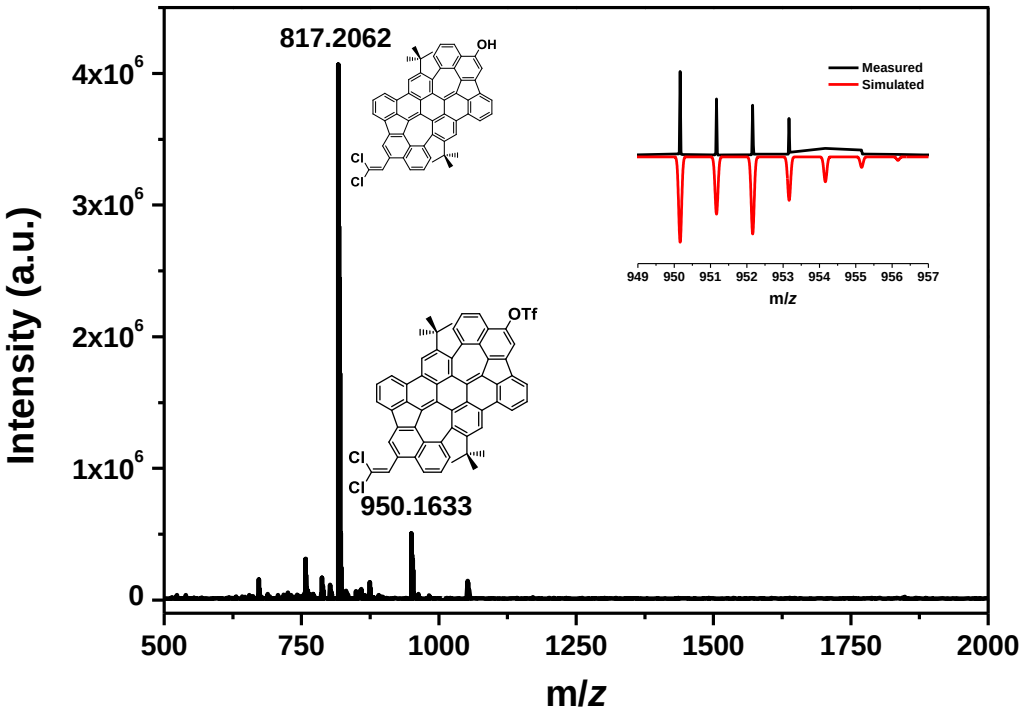

Figure S58. HRMS-MALDI (DCTB) of compound **9**.

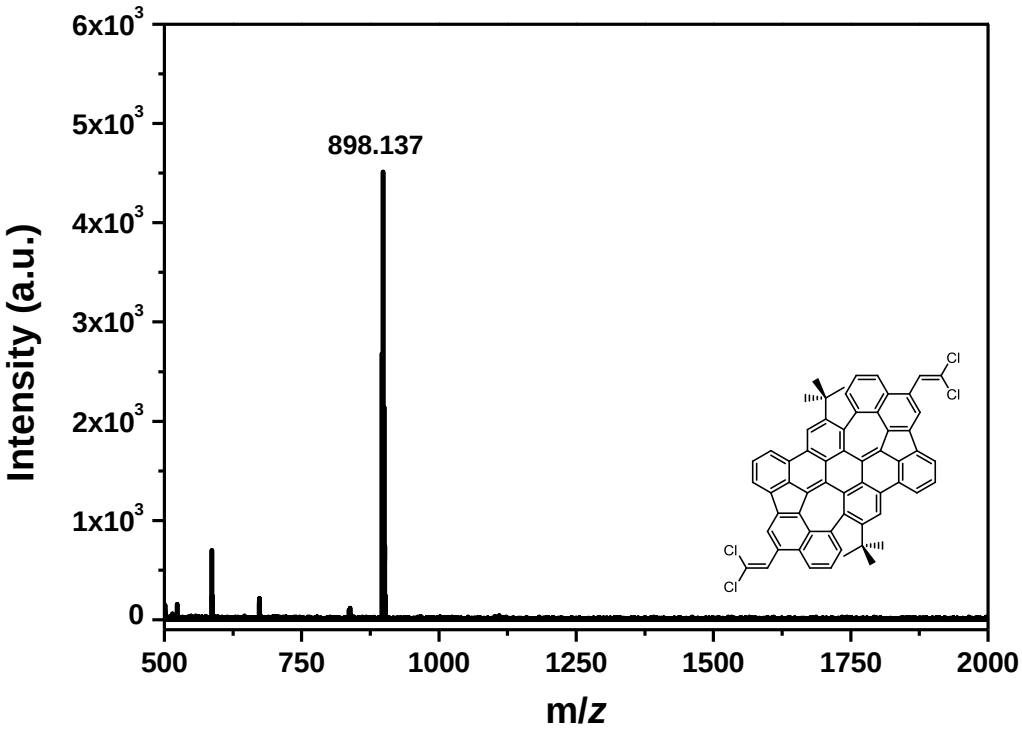

Figure S59. MS MALDI-TOF (DCTB) of compound **10**.

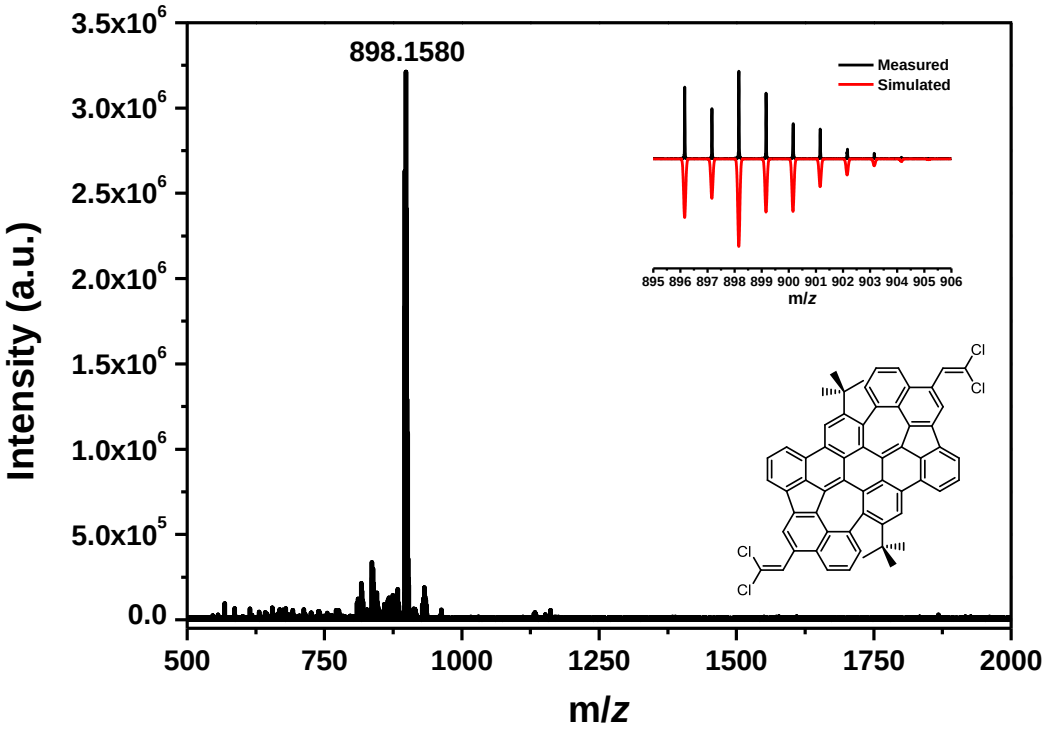

Figure S60. HRMS-MALDI (DCTB) of compound **10**.

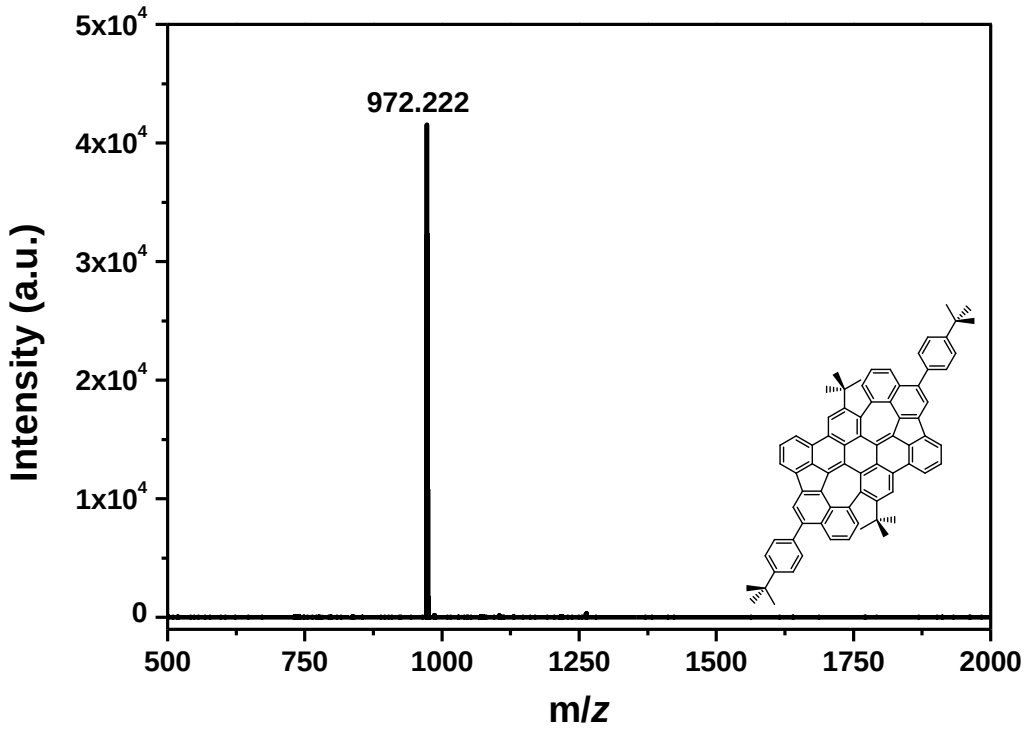

Figure S61. MS MALDI-TOF (DCTB) of compound **11**.

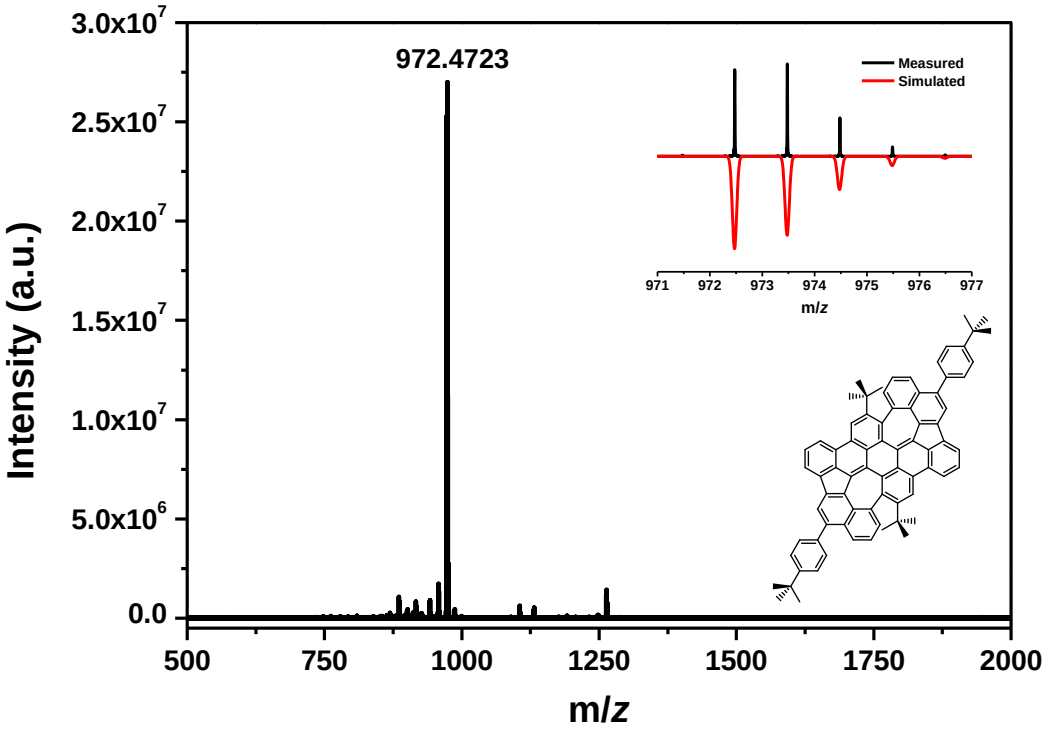

Figure S62. HRMS-MALDI (DCTB) of compound **11**.

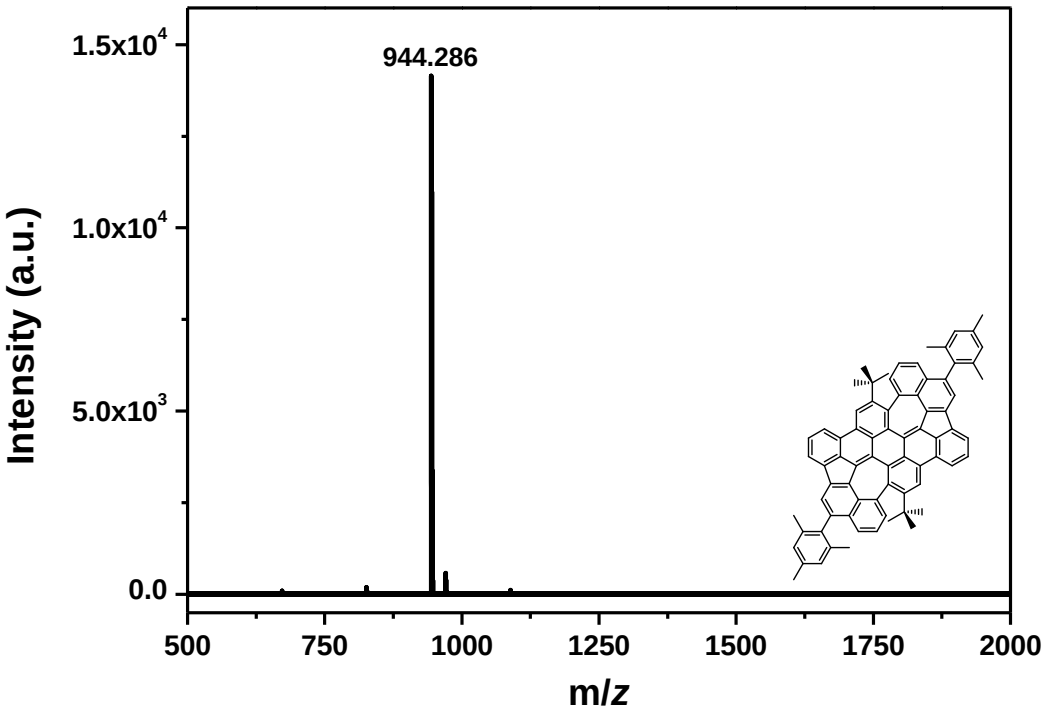

Figure S63. MS MALDI-TOF (DCTB) of compound **12**.

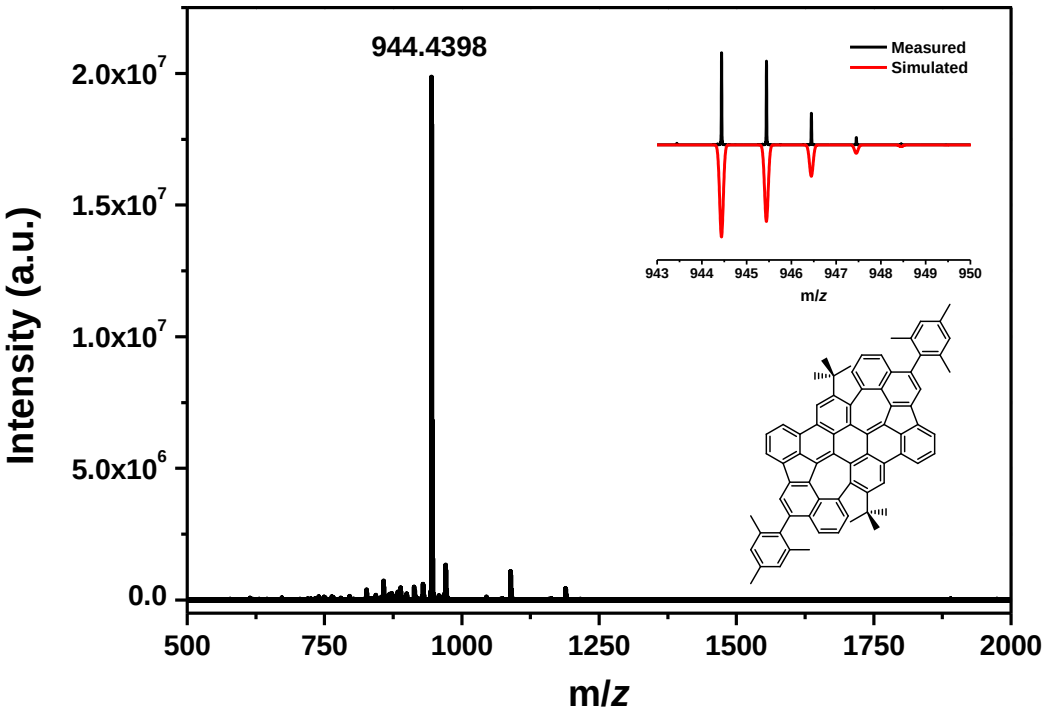

Figure S64. HRMS-MALDI (DCTB) of compound **12**.

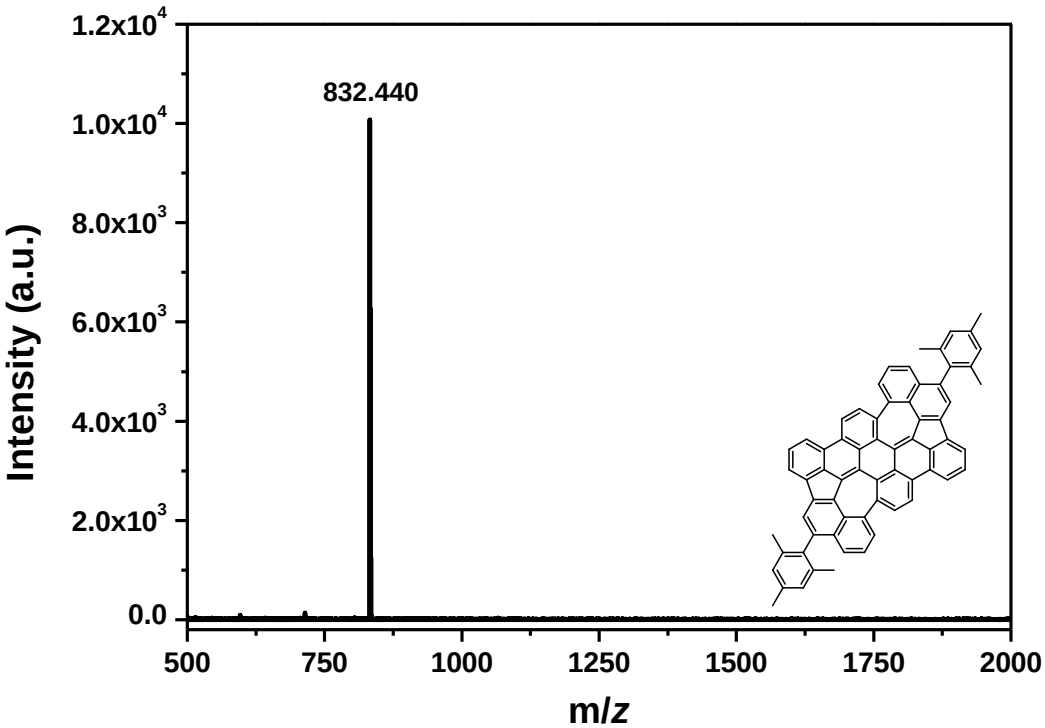

Figure S65. MS MALDI-TOF (DCTB) of compound **13**.

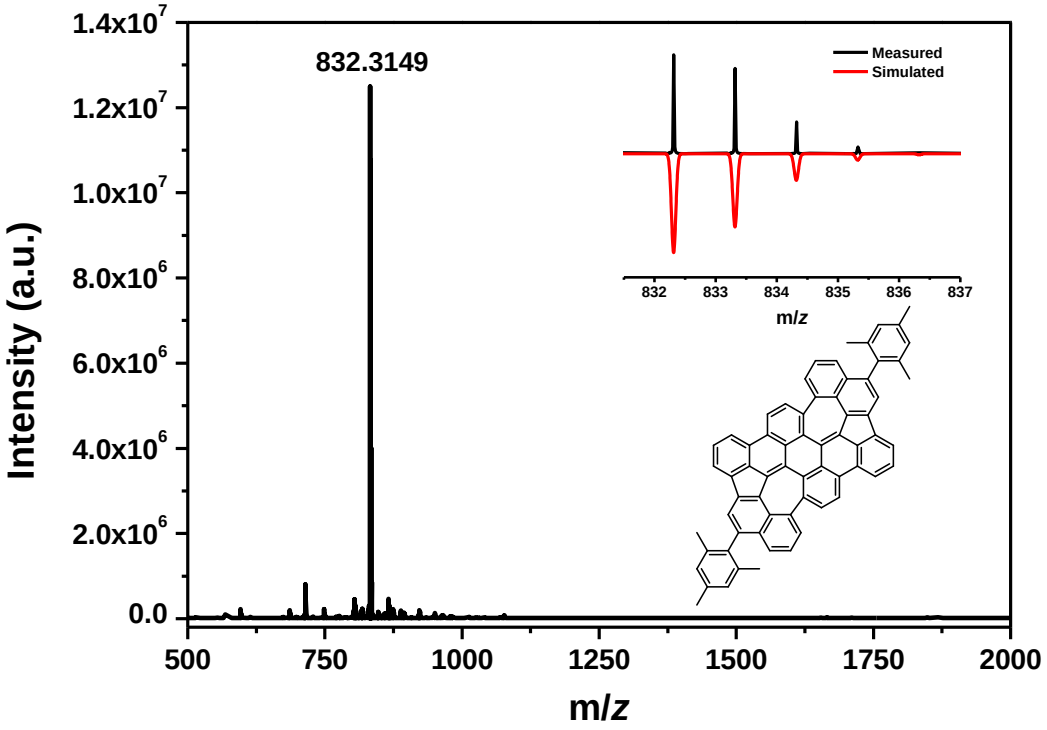

Figure S66. HRMS-MALDI (DCTB) of compound **13**.

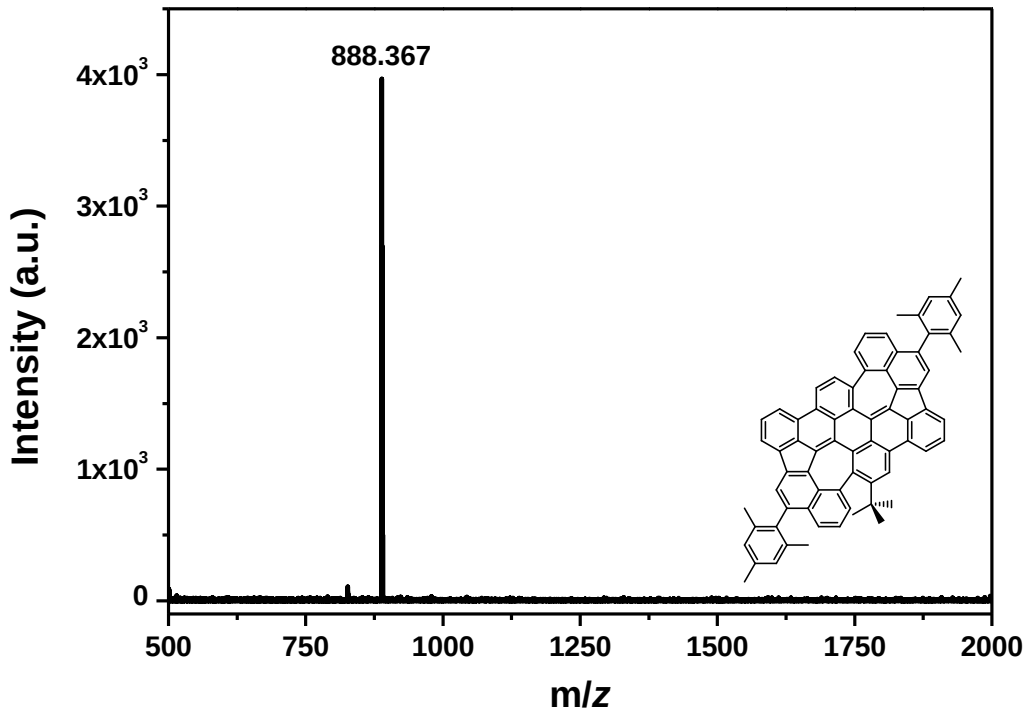

Figure S67. MS MALDI-TOF (DCTB) of compound **14**.

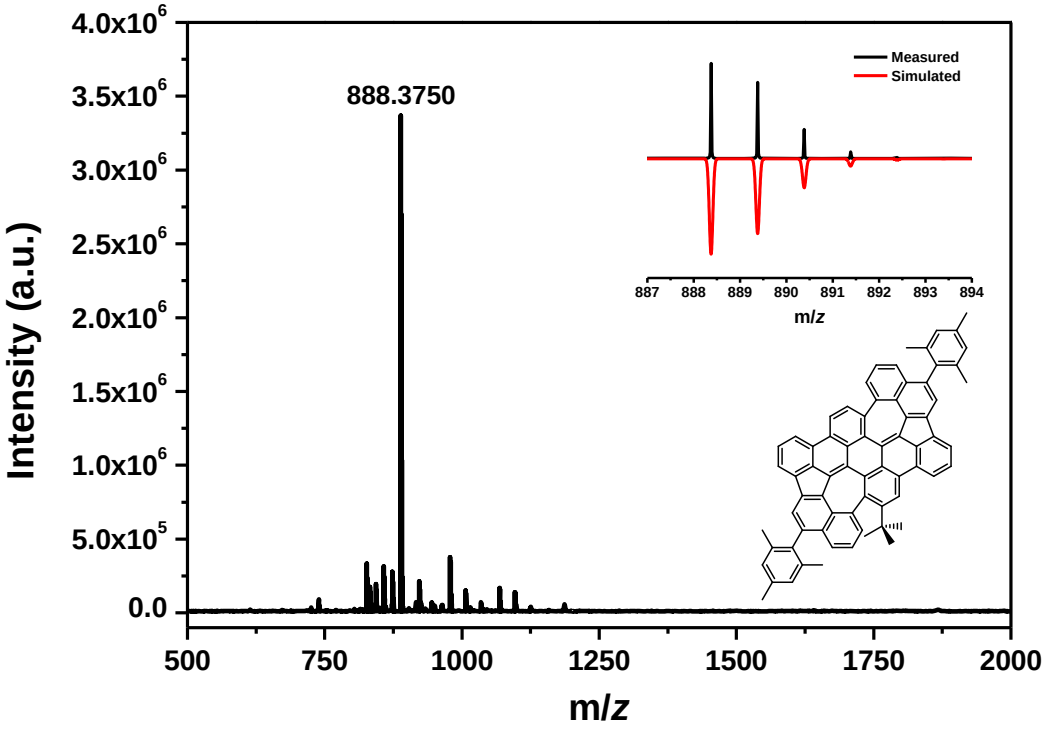

Figure S68. HRMS-MALDI (DCTB) of compound **14**.

5. FT-IR spectra

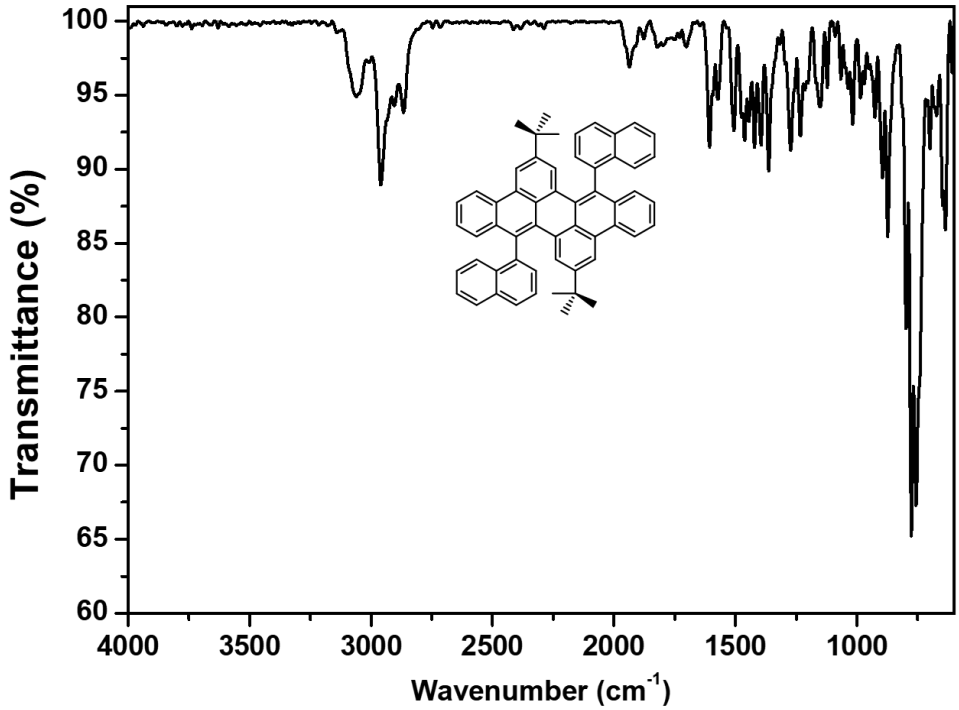

Figure S69. FT-IR spectrum (ATR) of **3**.

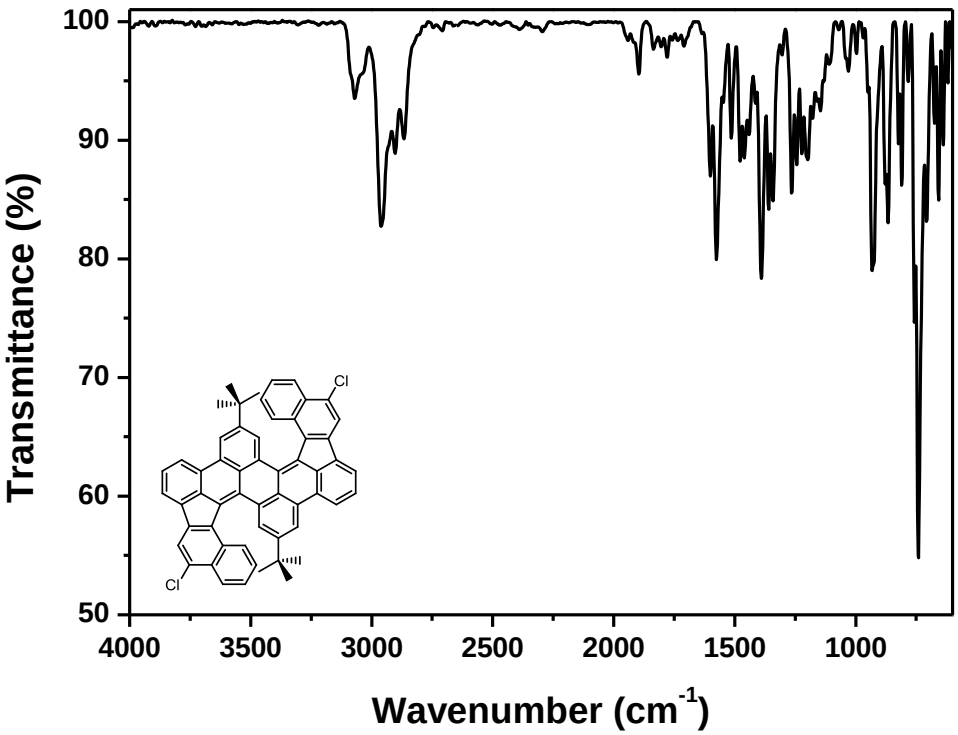

Figure S70. FT-IR spectrum (ATR) of **7**.

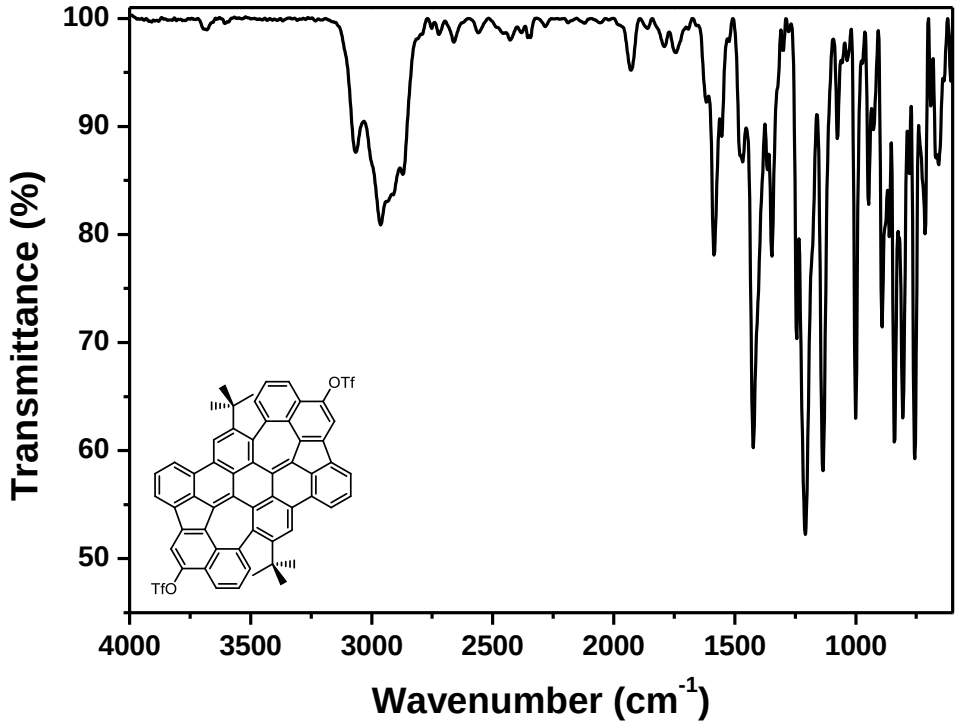

Figure S71. FT-IR spectrum (ATR) of **8**.

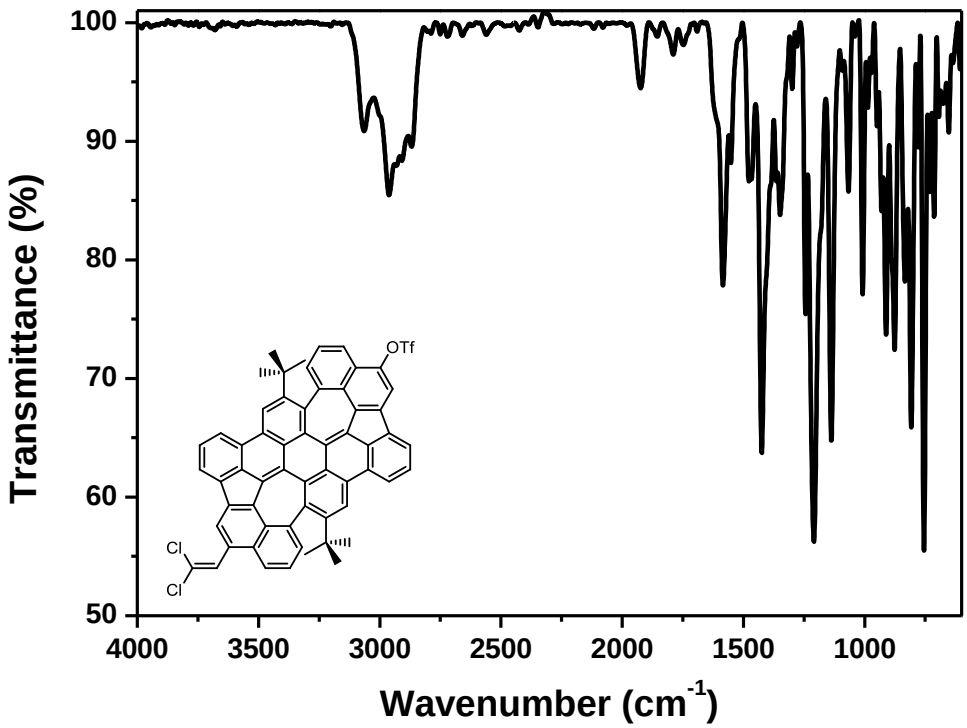

Figure S72. FT-IR spectrum (ATR) of **9**.

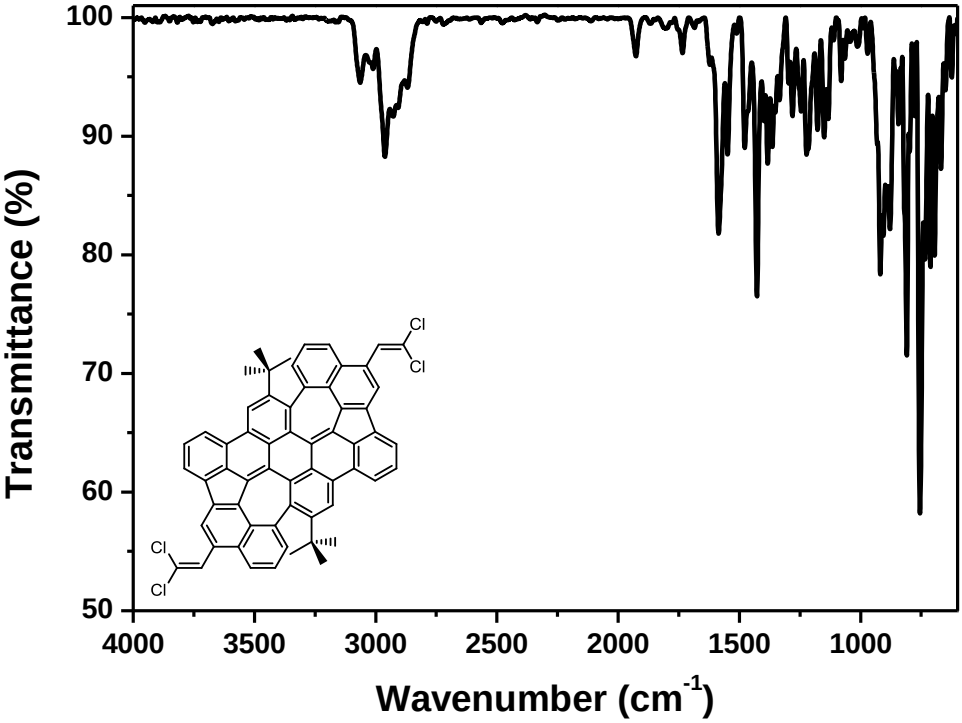

Figure S73. FT-IR spectrum (ATR) of **10**.

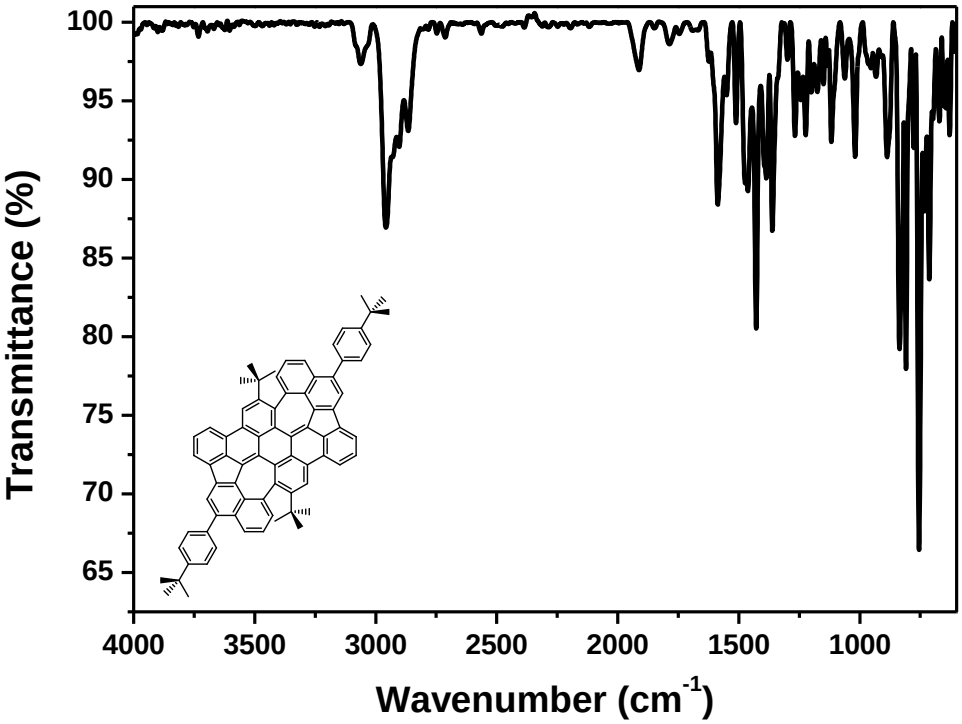

Figure S74. FT-IR spectrum (ATR) of **11**.

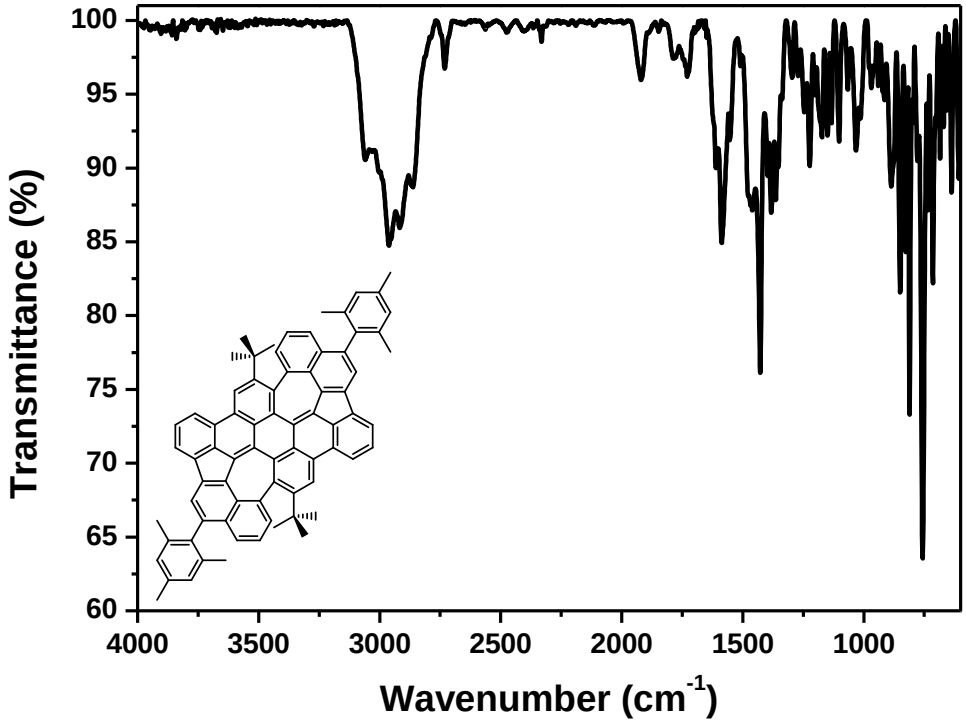

Figure S75. FT-IR spectrum (ATR) of **12**.

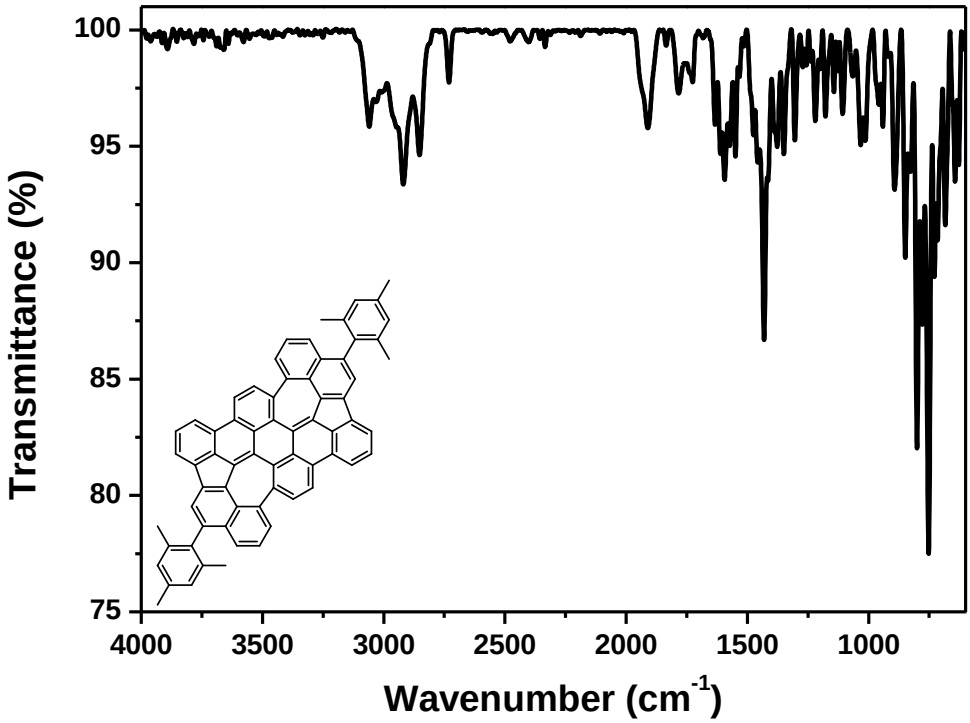

Figure S76. FT-IR spectrum (ATR) of **13**.

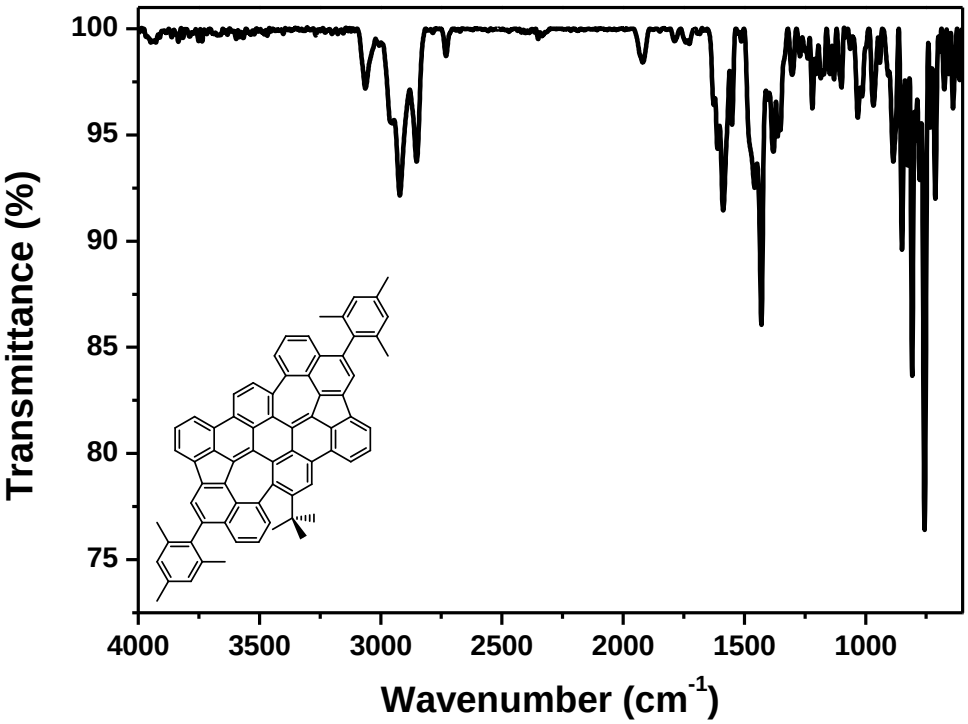

Figure S77. FT-IR spectrum (ATR) of **14**.

6. UV/vis and fluorescence spectra

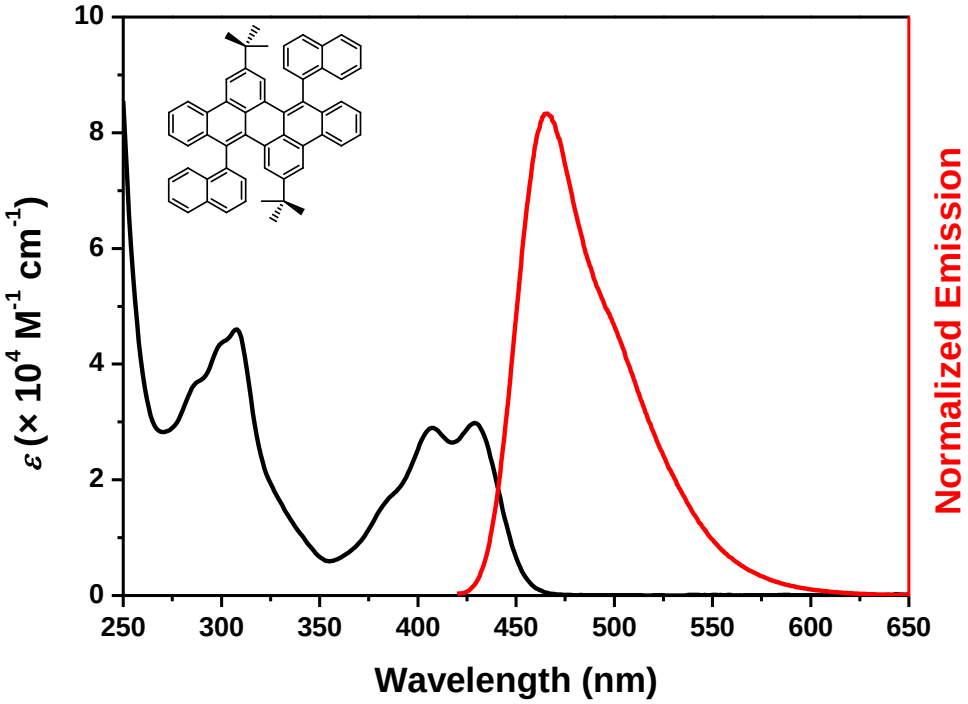

Figure S78. UV/Vis (black, *c* = 18.6 μM) and emission (Ex 407 nm) (red) spectra of compound **3** measured in $CHCl_3$ at room temperature.

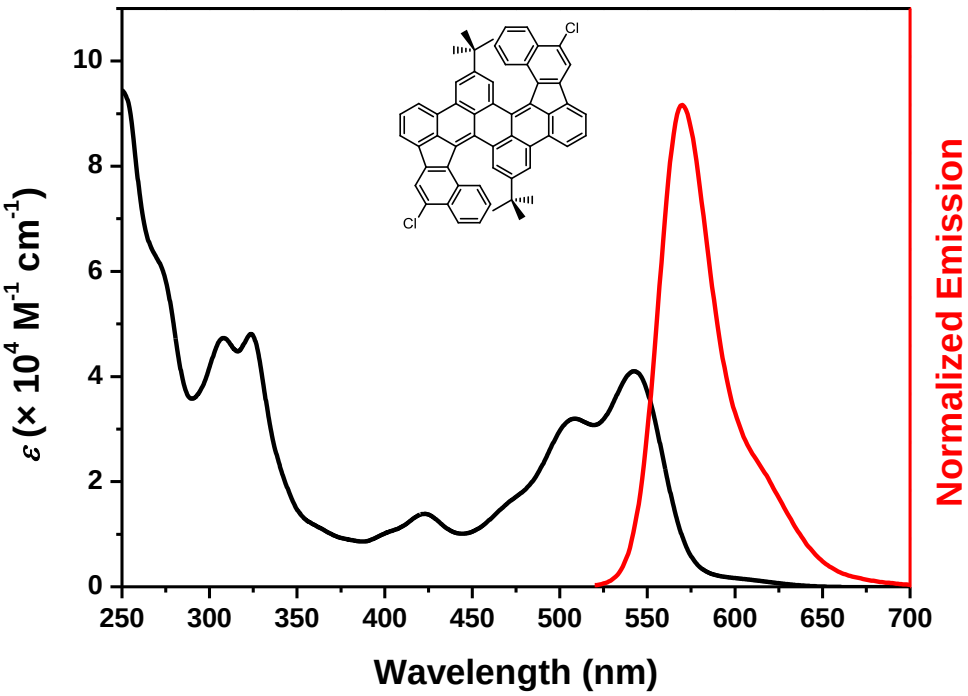

Figure S79. UV/Vis (black, *c* = 14.5 μM) and emission (Ex 509 nm) (red) spectra of compound **7** measured in $CHCl_3$ at room temperature.

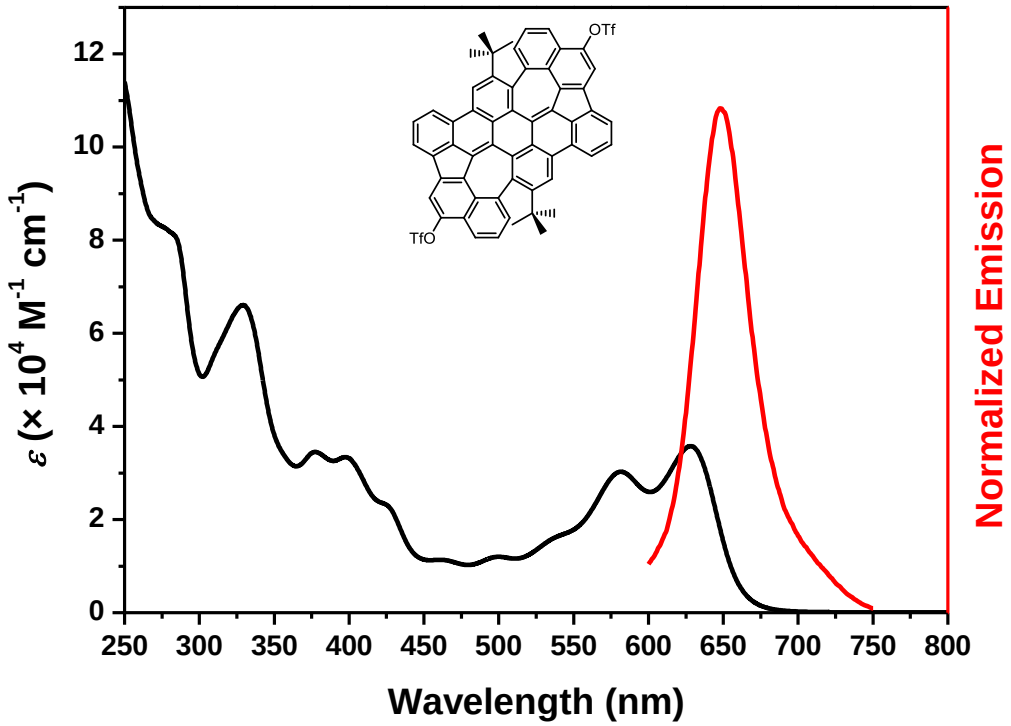

Figure S80. UV/Vis (black, c = 11.9 μM) and emission (Ex 280 nm) (red) spectra of compound **8** measured in $CHCl_3$ at room temperature.

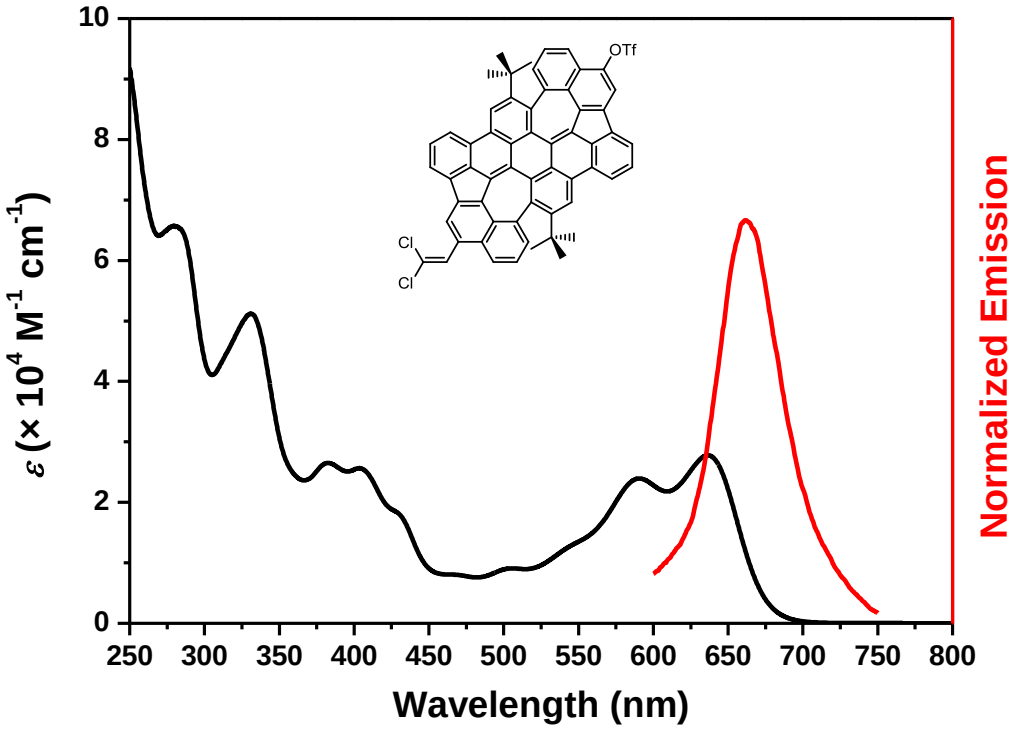

Figure S81. UV/Vis (black, c = 25.2 μM) and emission (Ex 280 nm) (red) spectra of compound **9** measured in $CHCl_3$ at room temperature.

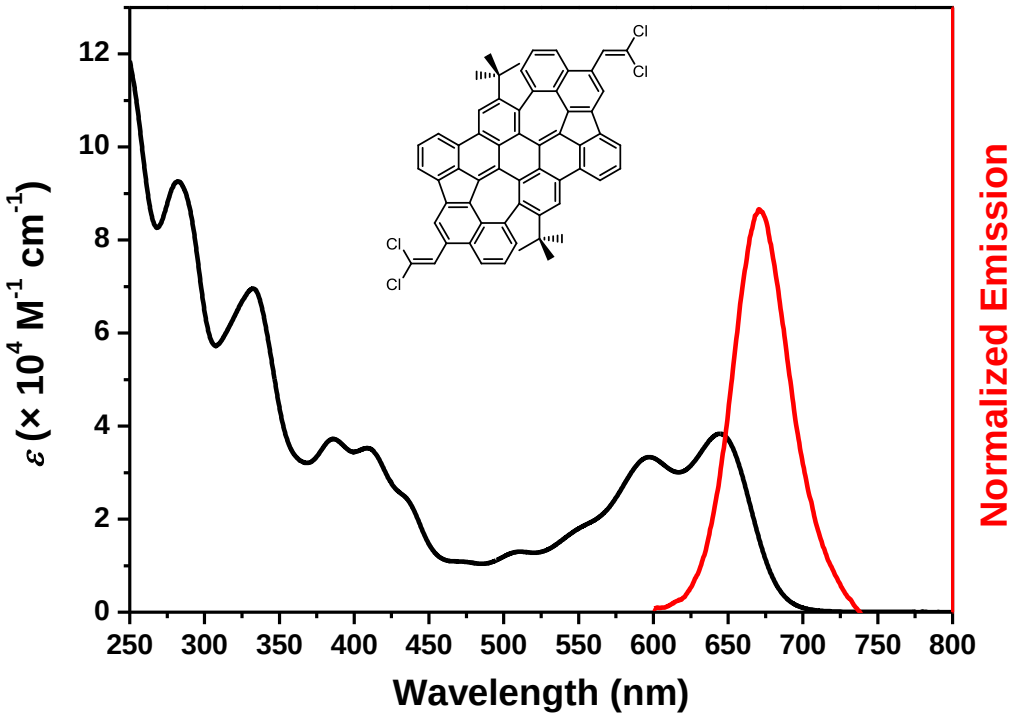

Figure S82. UV/Vis (black, *c* = 11.1 μM) and emission (Ex 282 nm) (red) spectra of compound **10** measured in $CHCl_3$ at room temperature.

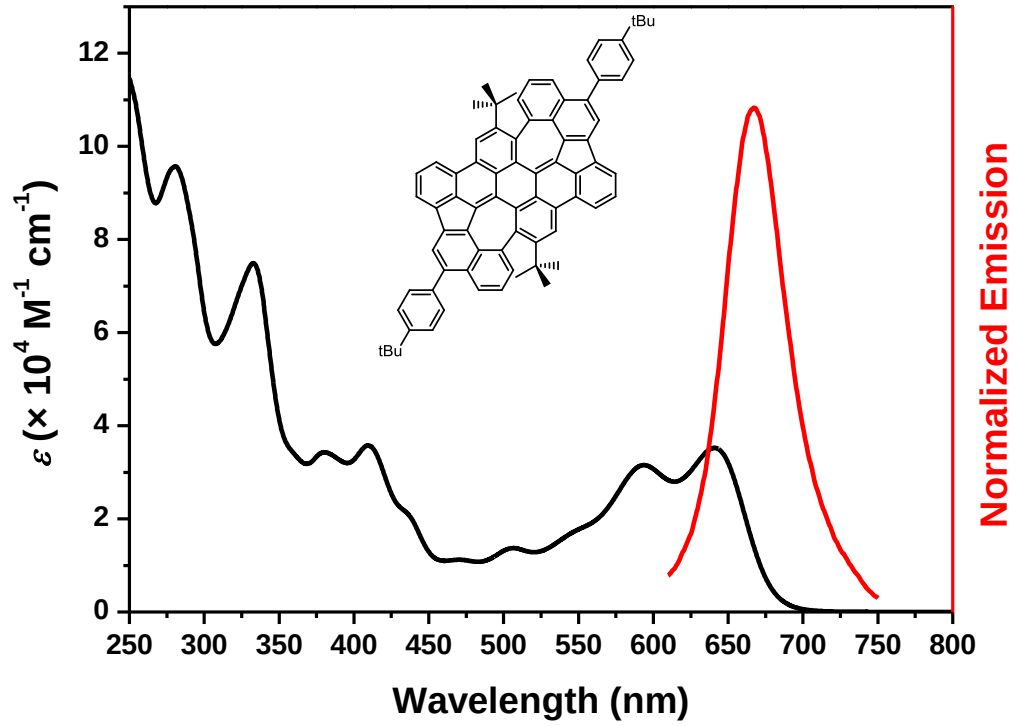

Figure S83. UV/Vis (black, *c* = 11.5 μM) and emission (Ex 594 nm) (red) spectra of compound **11** measured in $CHCl_3$ at room temperature.

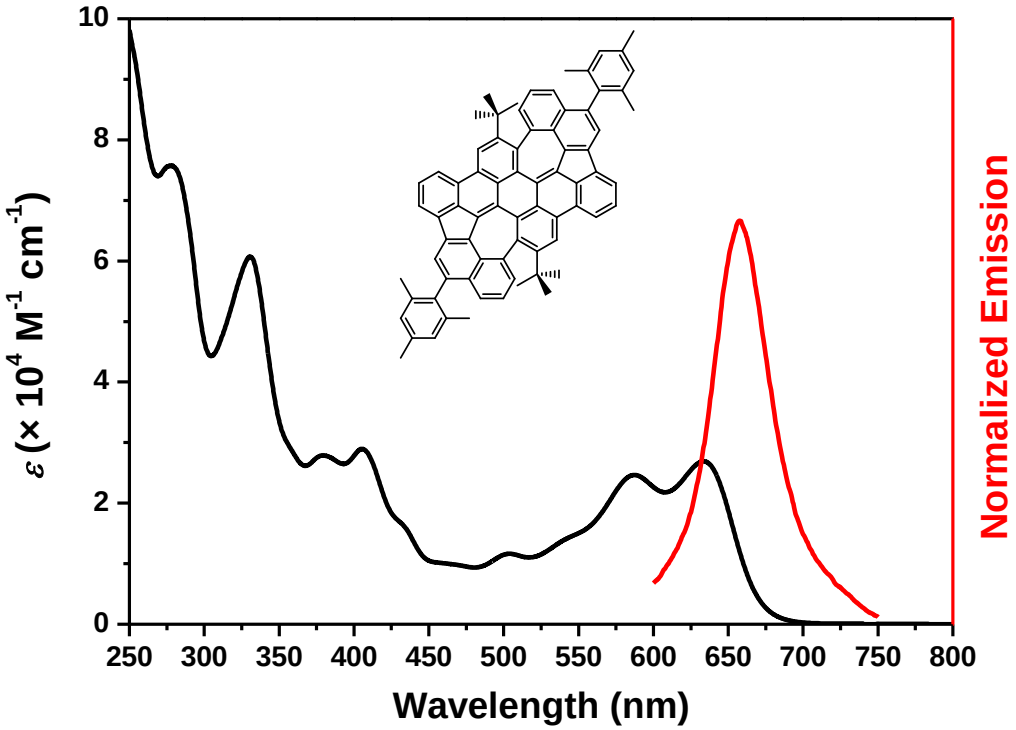

Figure S84. UV/Vis (black, c = 17.6 µM) and emission (Ex 277 nm) (red) spectra of compound **12** measured in $CHCl_3$ at room temperature.

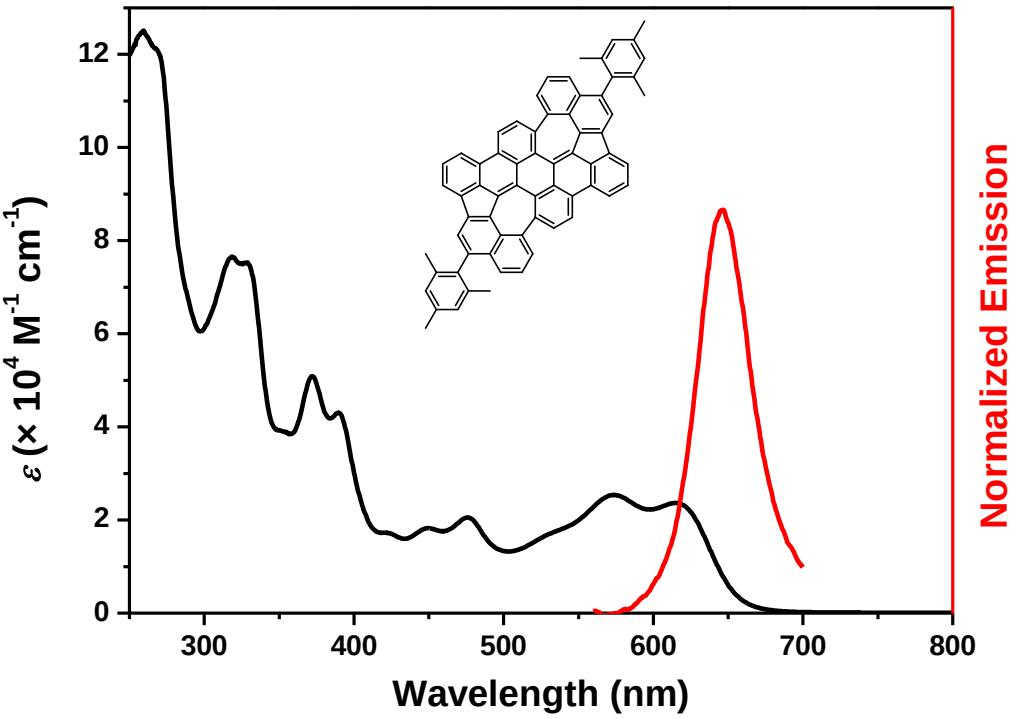

Figure S85. UV/Vis (black, c = 15.0 µM) and emission (Ex 260 nm) (red) spectra of compound **13** measured in $CHCl_3$ at room temperature.

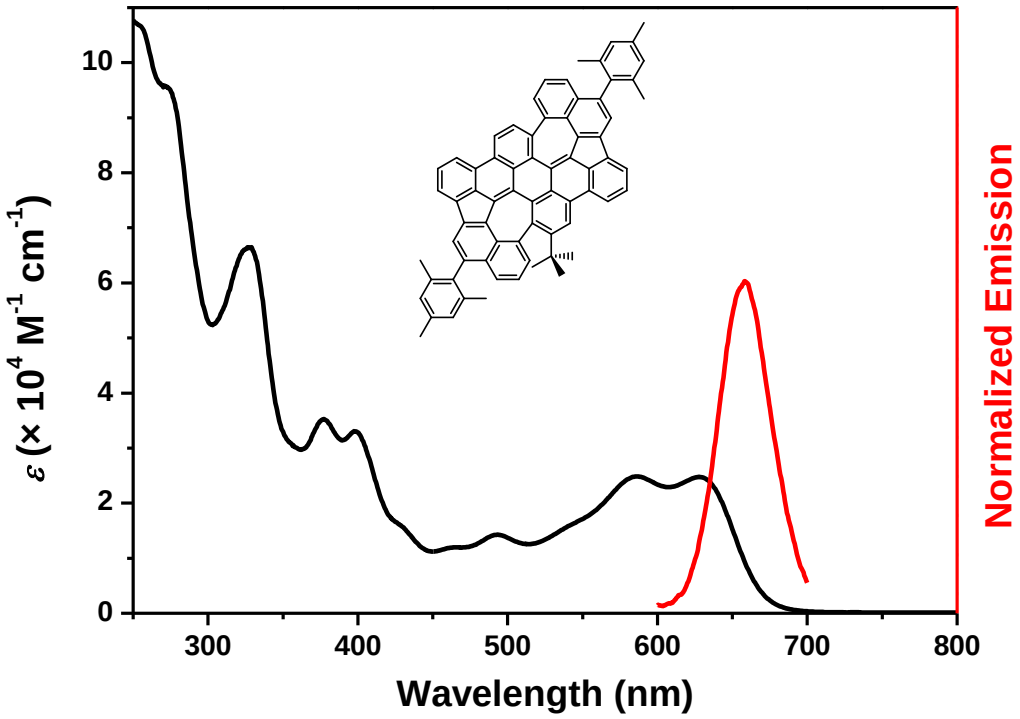

Figure S86. UV/Vis (black, *c* = 15.0 μM) and emission (Ex 272 nm) (red) spectra of compound **14** measured in $CHCl_3$ at room temperature.

7. Cyclovoltammograms

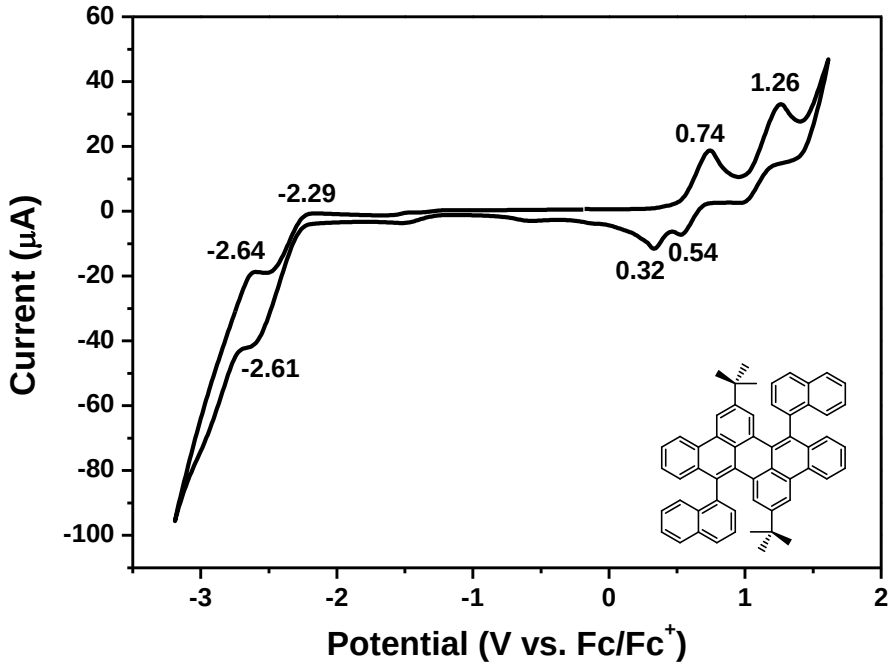

Figure S87. Cyclic voltammogram of compound **3** measured in 0.1 M nBu$_4$NClO$_4$ in CH_2Cl_2 at room temperature. The scan speed was 100 mV/s, and ferrocene/ferrocenium (Fc/Fc$^+$) was used as internal reference.

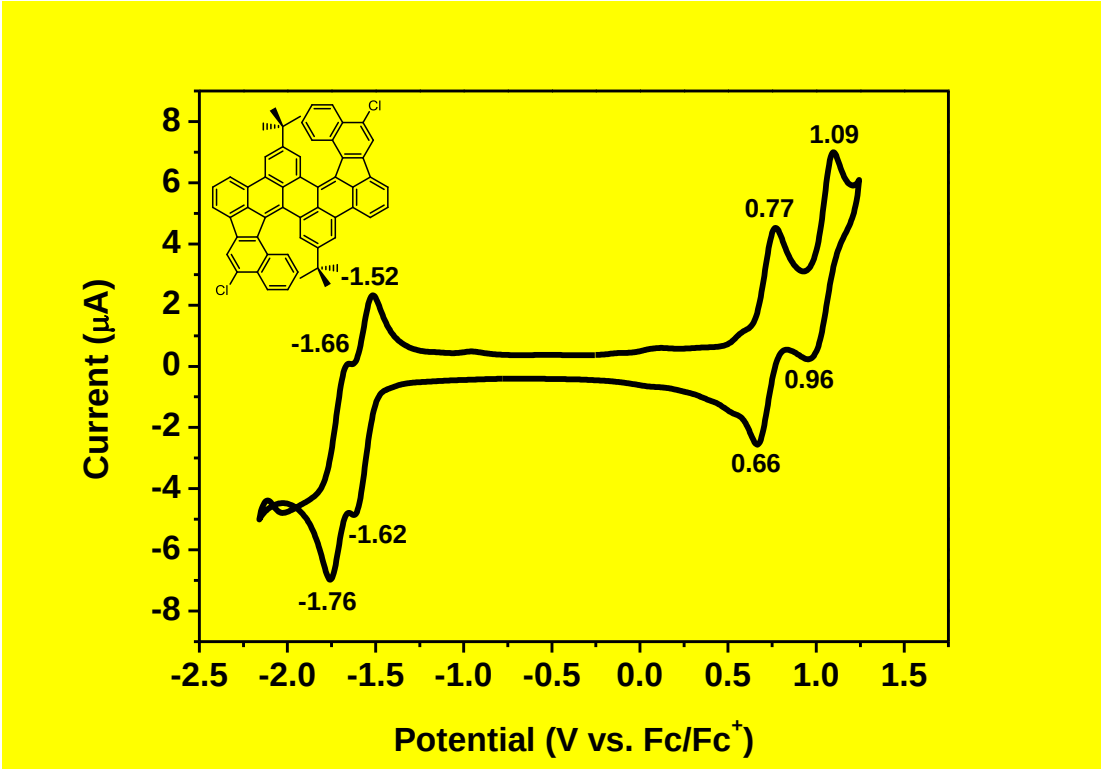

Figure S88. Cyclic voltammogram of compound **7** measured in 0.1 M nBu$_4$NClO$_4$ in CH_2Cl_2 at room temperature. The scan speed was 100 mV/s, and ferrocene/ferrocenium (Fc/Fc$^+$) was used as internal reference.

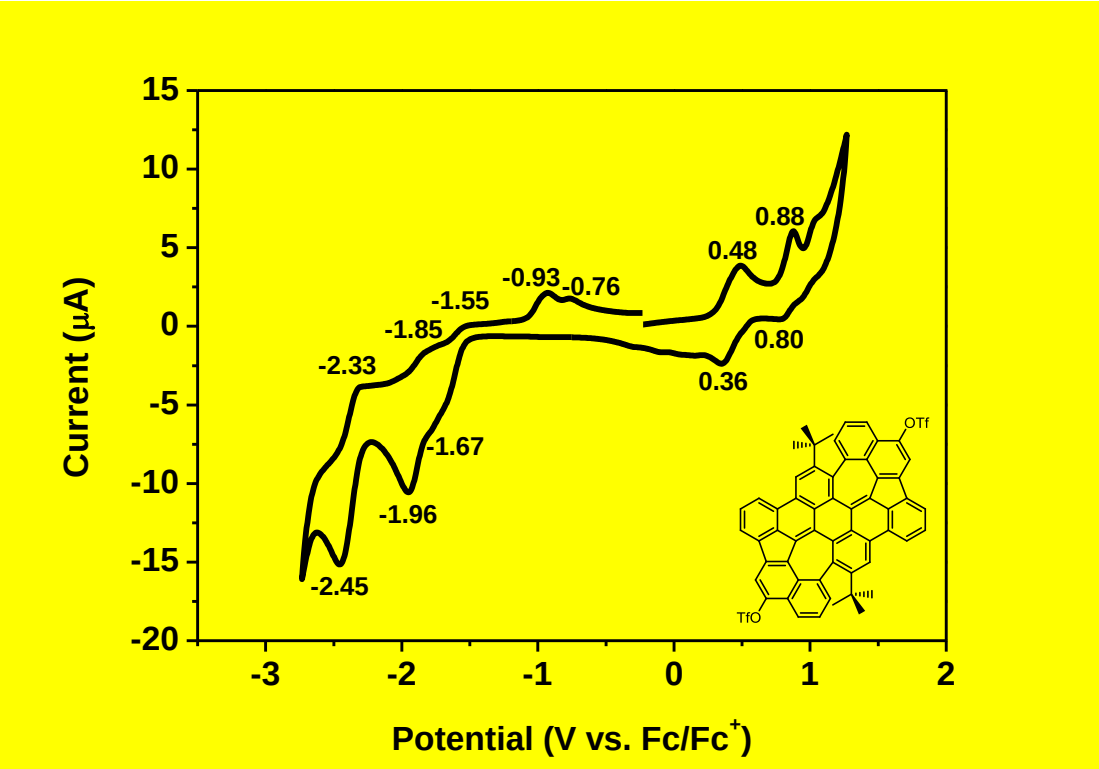

Figure S89. Cyclic voltammogram of compound **8** measured in 0.1 M nBu$_4$NClO$_4$ in CH$_2$Cl$_2$ at room temperature. The scan speed was 100 mV/s, and ferrocene/ferrocenium (Fc/Fc$^+$) was used as internal reference.

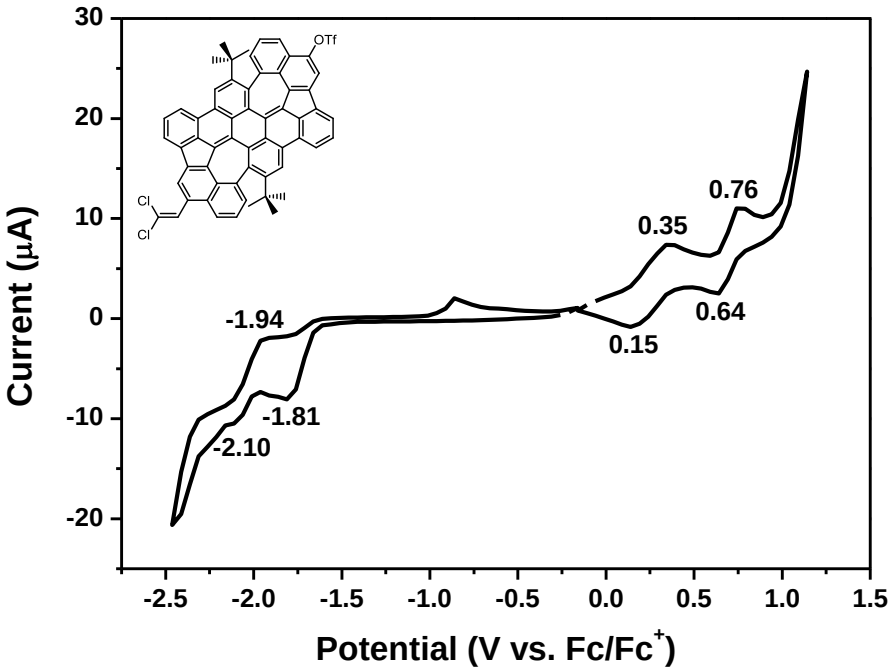

Figure S90. Cyclic voltammogram of compound **9** measured in 0.1 M nBu$_4$NClO$_4$ in CH$_2$Cl$_2$ at room temperature. The scan speed was 100 mV/s, and ferrocene/ferrocenium (Fc/Fc$^+$) was used as internal reference.

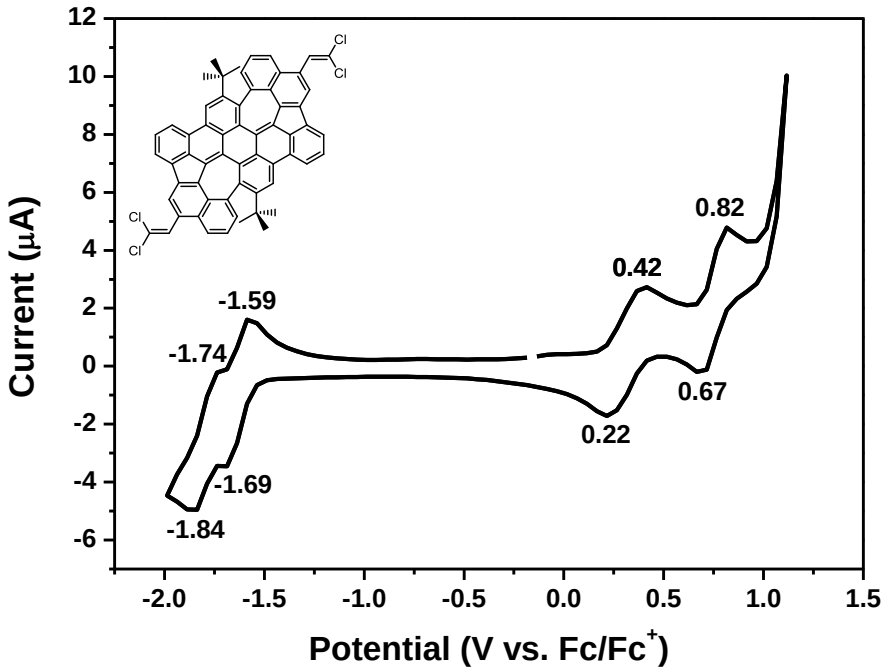

Figure S91. Cyclic voltammogram of compound **10** measured in 0.1 M nBu$_4$NClO$_4$ in CH_2Cl_2 at room temperature. The scan speed was 100 mV/s, and ferrocene/ferrocenium (Fc/Fc$^+$) was used as internal reference.

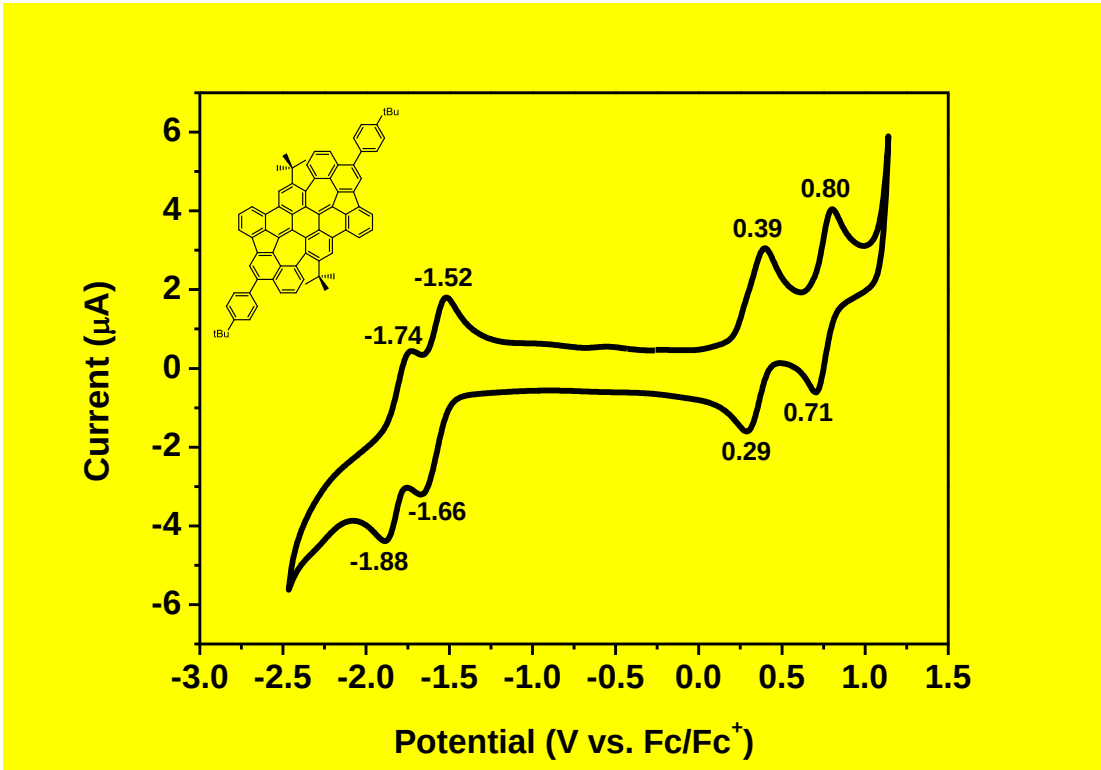

Figure S92. Cyclic voltammogram of compound **11** measured in 0.1 M nBu$_4$NClO$_4$ in CH_2Cl_2 at room temperature. The scan speed was 100 mV/s, and ferrocene/ferrocenium (Fc/Fc$^+$) was used as internal reference.

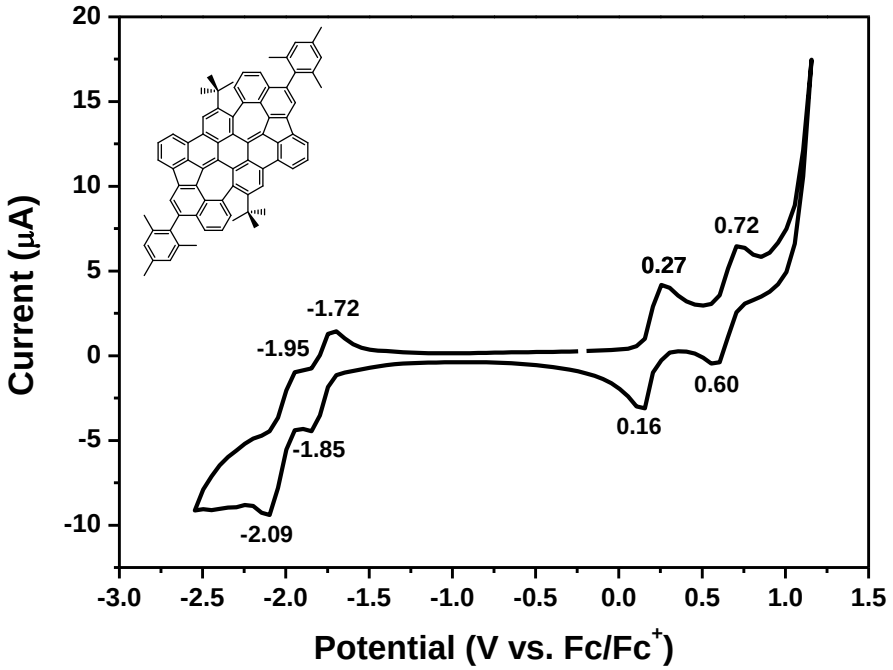

Figure S93. Cyclic voltammogram of compound **12** measured in 0.1 M nBu$_4$NClO$_4$ in CH_2Cl_2 at room temperature. The scan speed was 100 mV/s, and ferrocene/ferrocenium (Fc/Fc$^+$) was used as internal reference.

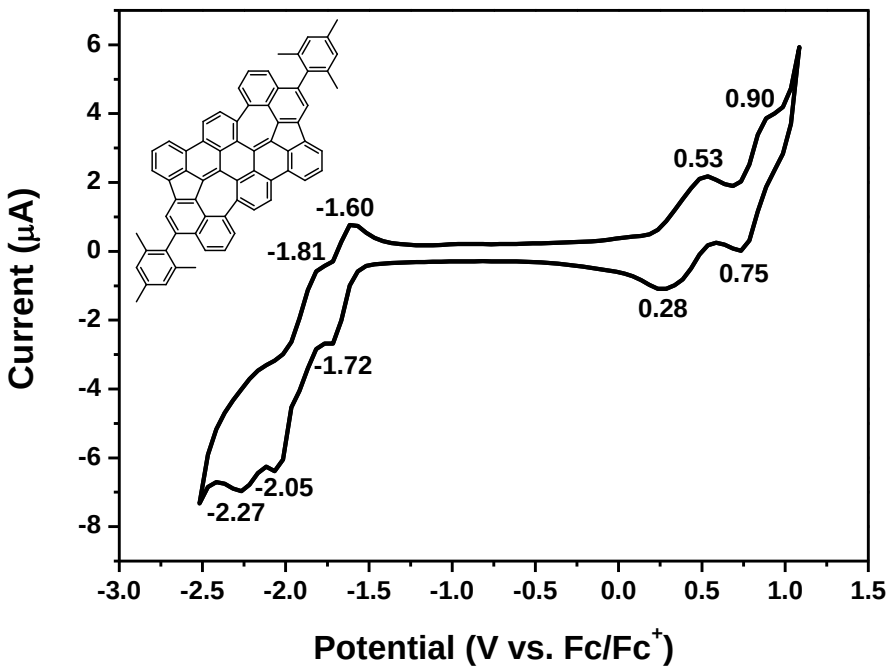

Figure S94. Cyclic voltammogram of compound **13** measured in 0.1 M nBu$_4$NClO$_4$ in CH_2Cl_2 at room temperature. The scan speed was 100 mV/s, and ferrocene/ferrocenium (Fc/Fc$^+$) was used as internal reference.

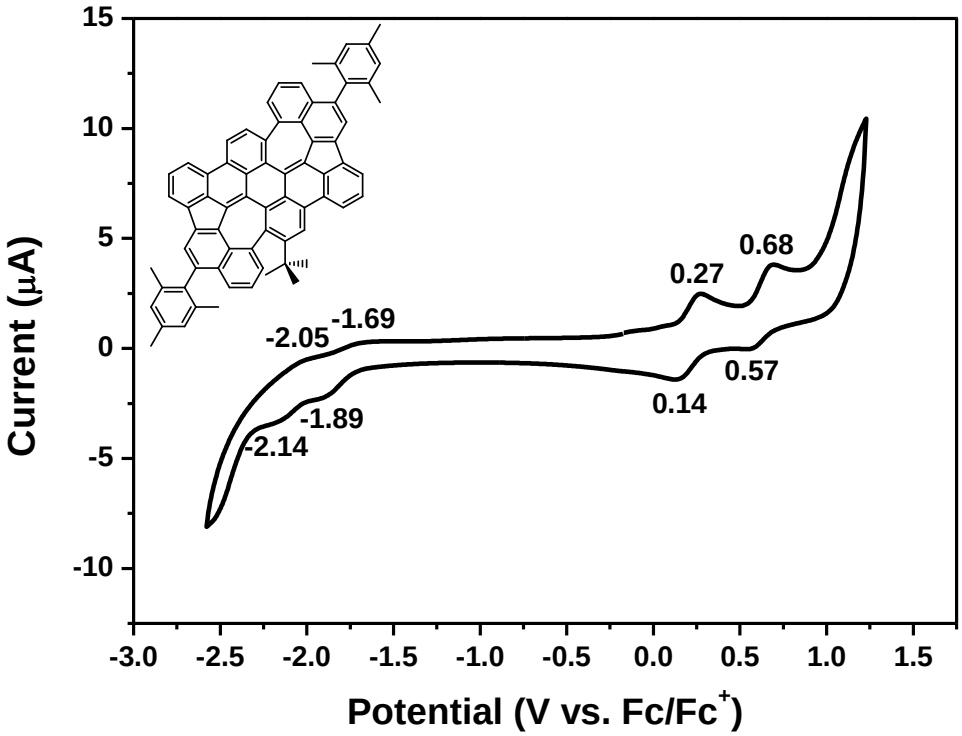

Figure S95. Cyclic voltammogram of compound **14** measured in 0.1 M nBu$_4$NClO$_4$ in CH_2Cl_2 at room temperature. The scan speed was 100 mV/s, and ferrocene/ferrocenium (Fc/Fc$^+$) was used as internal reference.

8. DFT calculations

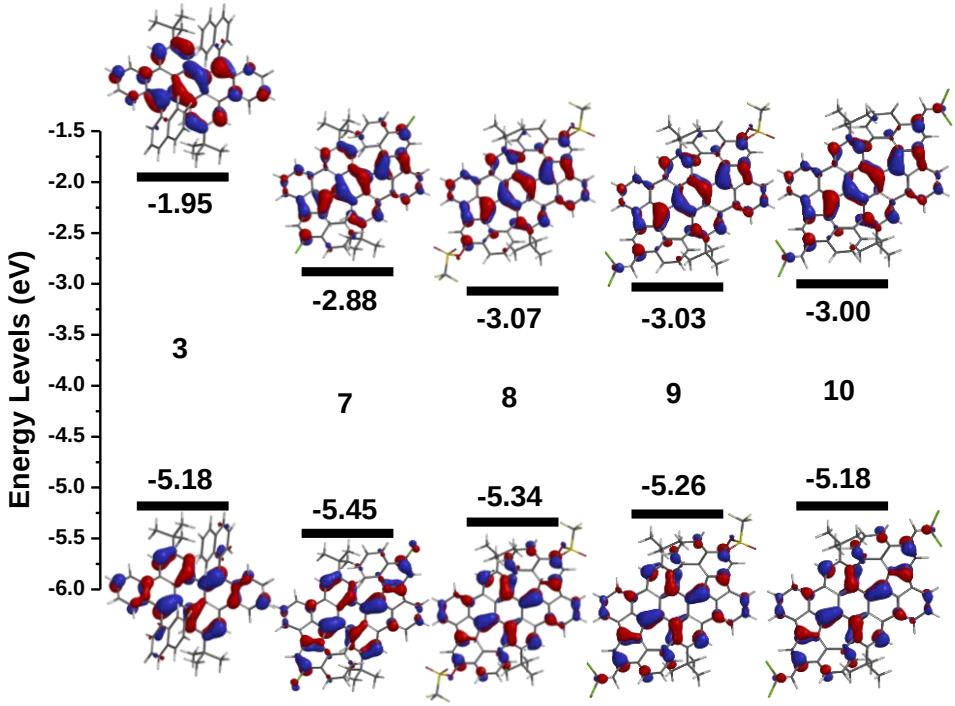

Figure S96. DFT calculations of molecular orbitals and energy levels at B3LYP/6-311G* of compounds **3**, **7-10**.

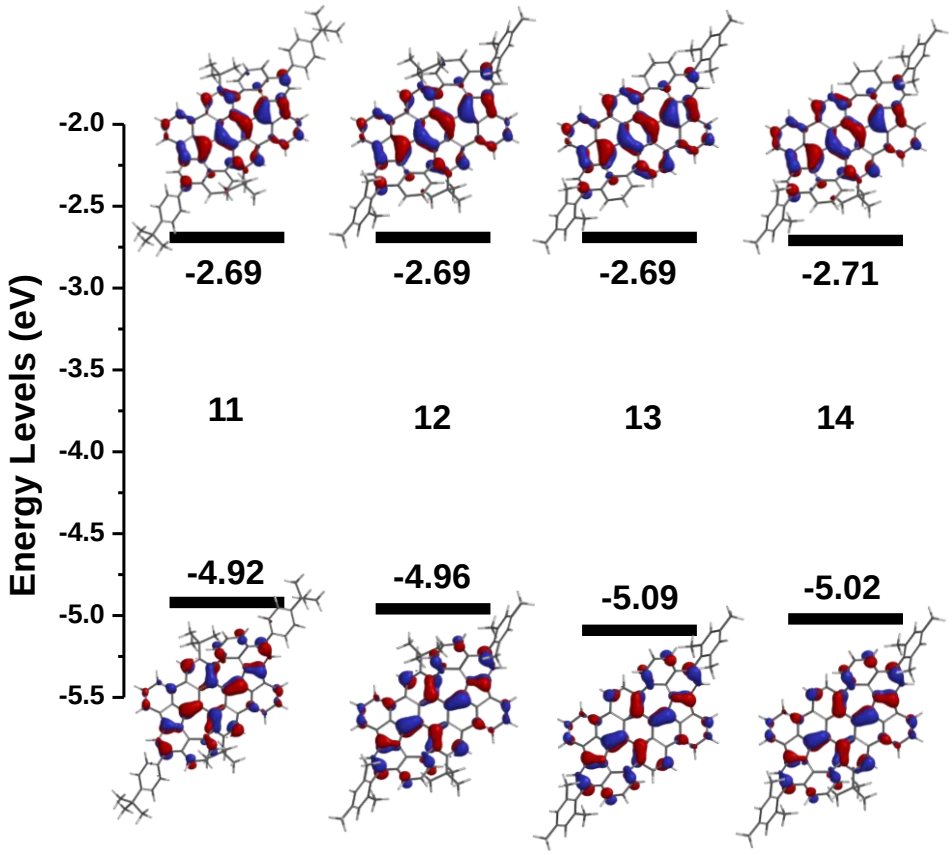

Figure S97. DFT calculations of molecular orbitals and energy levels at B3LYP/6-311G* of compounds **11-14**.

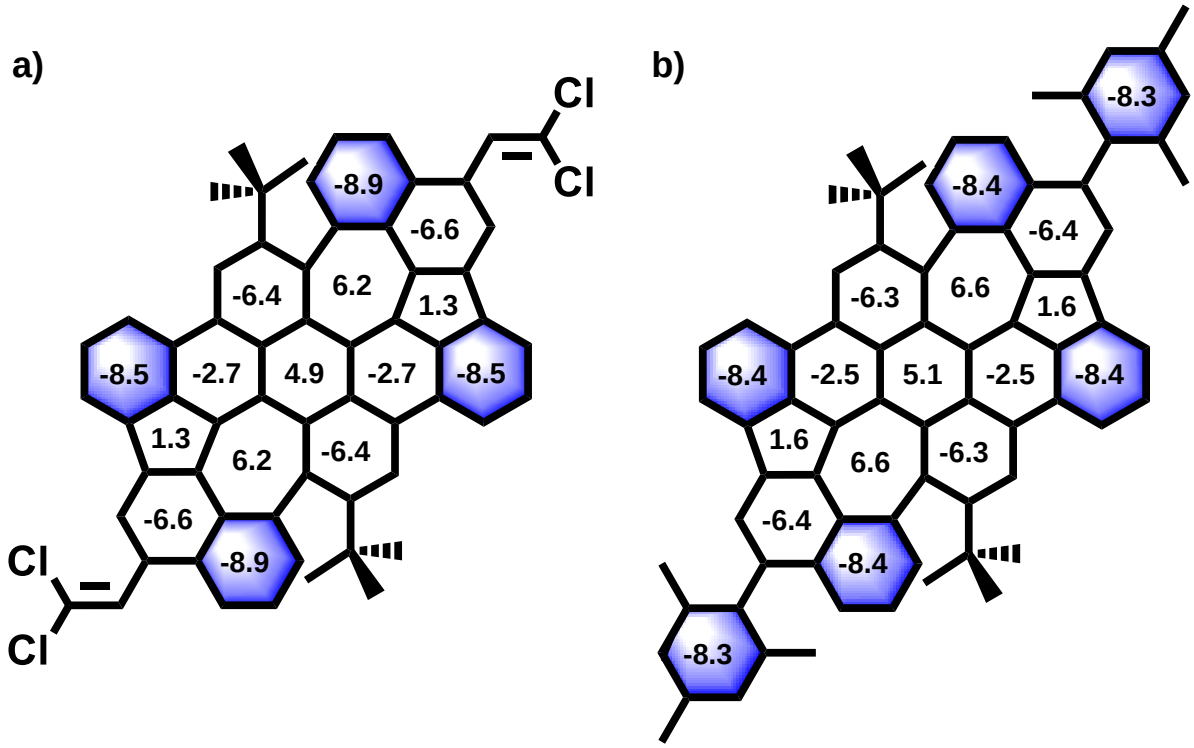

Figure S98. DFT calculated NICS(0) values of PAH **10** and **12** at B3LYP/6-31G* level. Blue-colored rings show clear benzenoid character.

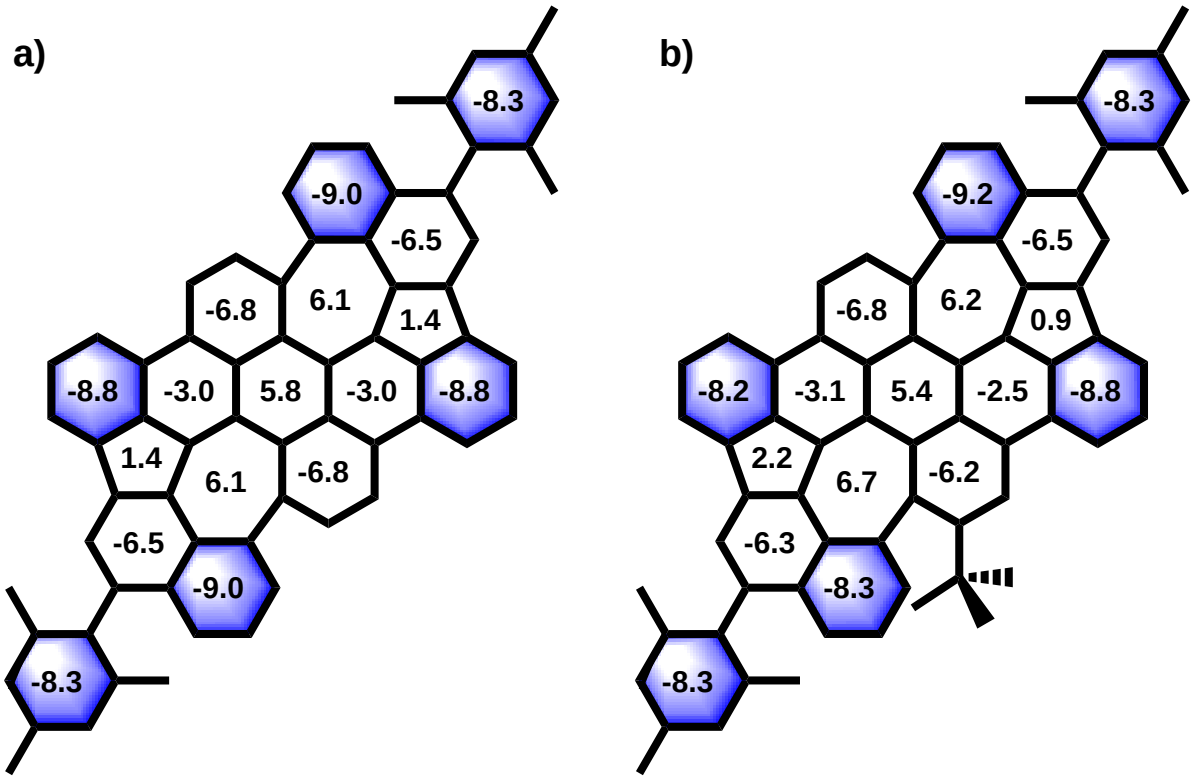

Figure S99. DFT calculated NICS(0) values of PAH **13** and **14** at B3LYP/6-31G* level. Blue-colored rings show clear benzenoid character.

Table S1. Summary of photophysical and electrochemical characterization of all new compounds.

Compd	$\lambda_{max}^{p\text{-band}}$ (log ε)/ nm[a]	λ_{em} (λ_{ex})/ nm[a]	E_g^{opt}/eV[b]	E_{HOMO}^{CV}/ eV[c]	E_{LUMO}^{CV}/ eV[d]	E_g^{cv} / eV	E_{HOMO}^{DFT}/ eV[d]	E_{LUMO}^{DFT}/ eV[d]	Φ/%
3	429 (4.47)	466 (407)	2.7	-5.33	-2.57	2.76	-5.18	-1.95	57.4±1.5
7	542 (4.61)	570, 614 (509)	1.9	-5.43	-3.32	2.11	-5.45	-2.88	15.8±1.0
8	628 (4.55)	648 (280)	1.9	-5.06	-3.29	1.77	-5.34	-3.07	19.8±1.0
9	636 (4.44)	662 (280)	1.8	-4.95	-3.17	1.78	-5.26	-3.03	26.5±1.0
10	644 (4.58)	671 (282)	1.8	-5.00	-3.27	1.73	-5.18	-3.00	23.6±1.0
11	641 (4.55)	667 (594)	1.8	-4.99	-3.33	1.66	-4.92	-2.69	28.4±1.0
12	633 (4.43)	658 (277)	1.8	-4.95	-3.09	1.86	-4.96	-2.69	25.4±0.9
13	618 (4.38)	647 (268)	1.9	-5.03	-3.22	1.81	-5.09	-2.69	17.9±0.2
14	630 (4.39)	657 (272)	1.8	-4.95	-3.07	1.88	-5.02	-2.71	22.3±0.5

[a]Measured in $CHCl_3$ at room temperature. [b]Estimated from absorption onset. [c]Measured in 0.1 M nBu_4NClO_4 in CH_2Cl_2 ~~or oDCB~~ at room temperature. The scan speed was 100 mV/s, and ferrocene/ferrocenium (Fc/Fc^+) was used as internal reference. $E_{HOMO}^{CV} = -(E_{onset}^{ox} + 4.8\ eV)$. $E_{LUMO}^{CV} = -(E_{onset}^{red} + 4.8\ eV)$.[d]Calculated at B3LYP/6-311G* level.

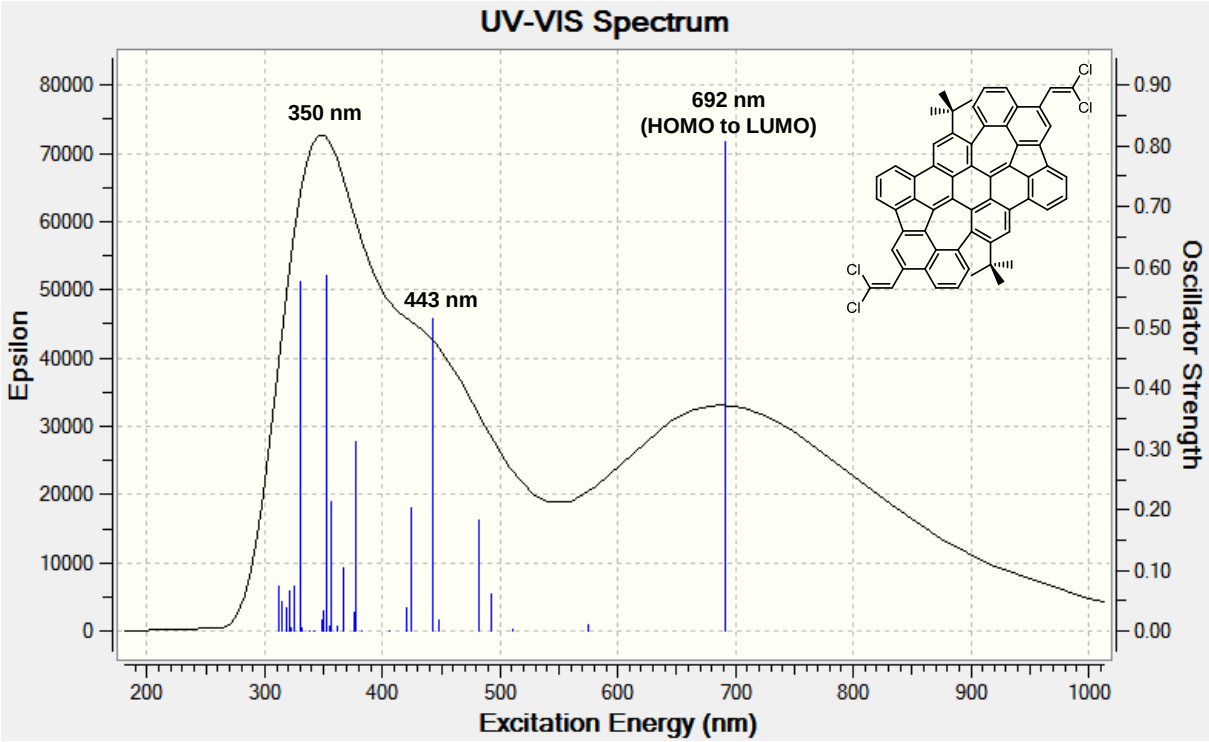

Figure S100. Calculated UV/Vis absorption spectrum of compound **10** based on TDDFT at the B3LYP/6-311G* level. The solvent chloroform was simulated using the polarized continuum model (PCM).

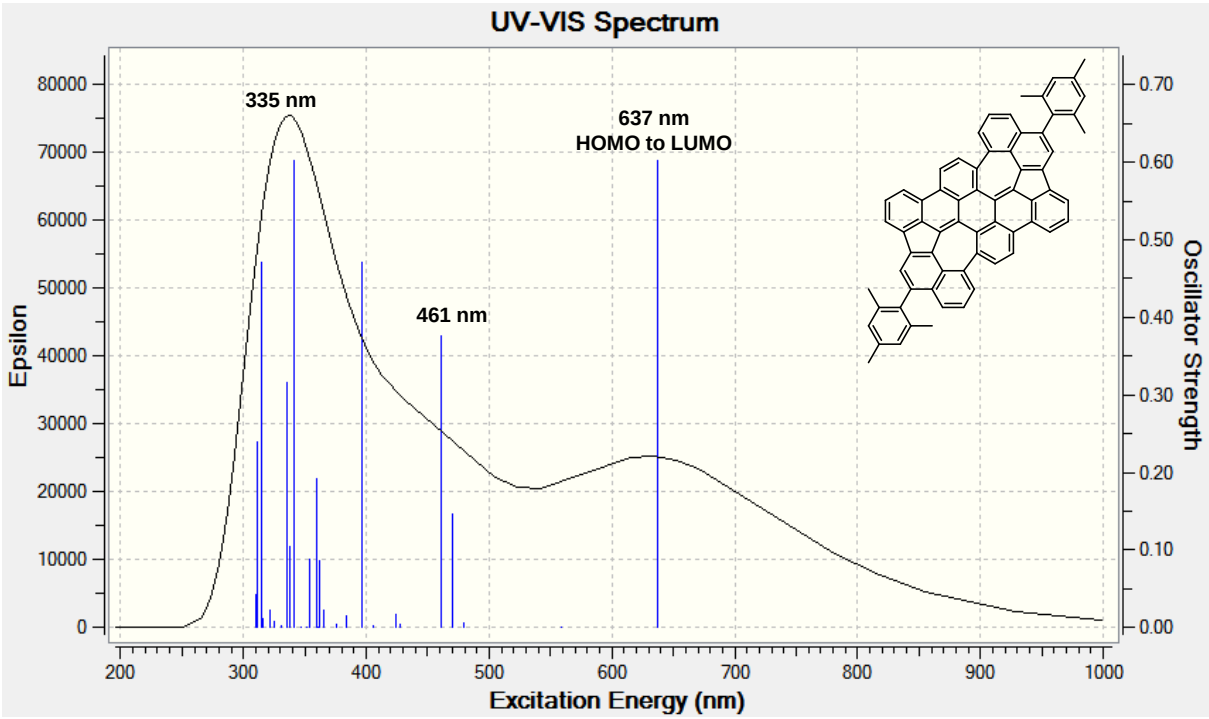

Figure S101. Calculated UV/Vis absorption spectrum of compound **13** based on TDDFT at the B3LYP/6-311G* level. The solvent chloroform was simulated using the polarized continuum model (PCM).

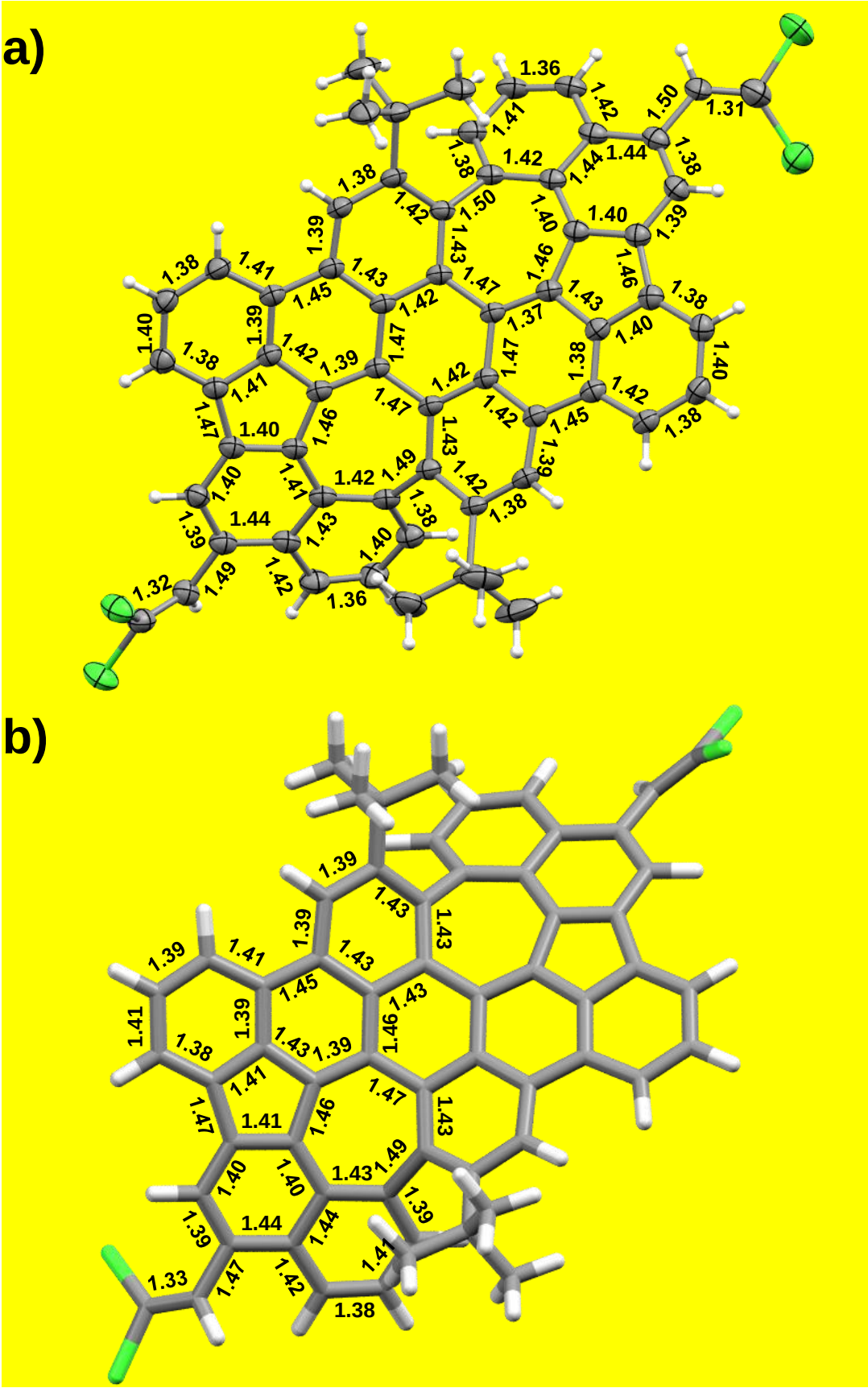

Figure S102. Comparison of bond lengths between the X-ray single crystal diffraction data (a) and the DFT (B3LYP/6-311G*) optimized model (b) of compound **10**. Bond lengths are given in Å.

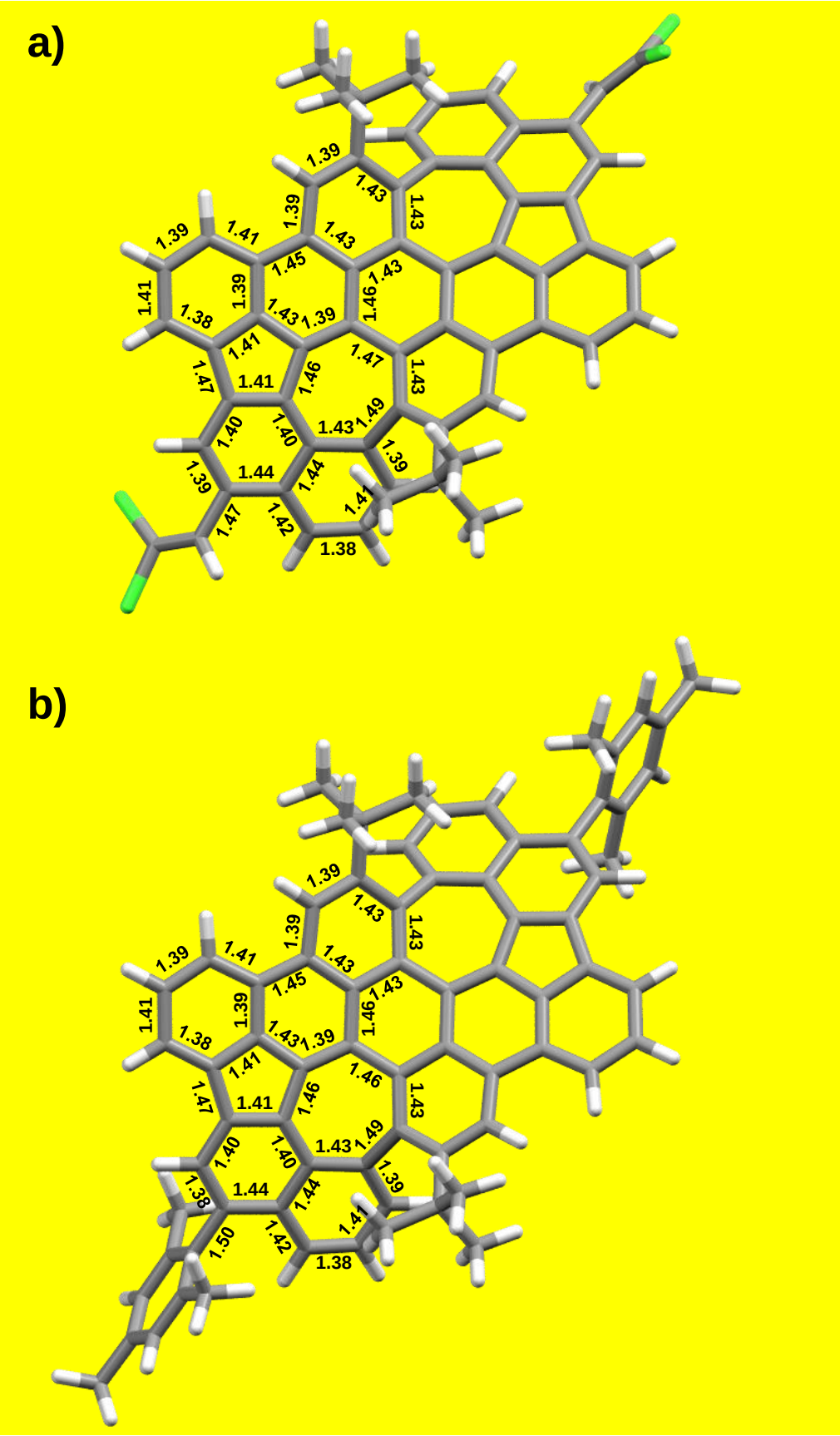

Figure S103. Comparison of bond lengths between the DFT (B3LYP/6-311G*) optimized model of compound **10** (a) and compound **12** (b). Bond lengths are given in Å.

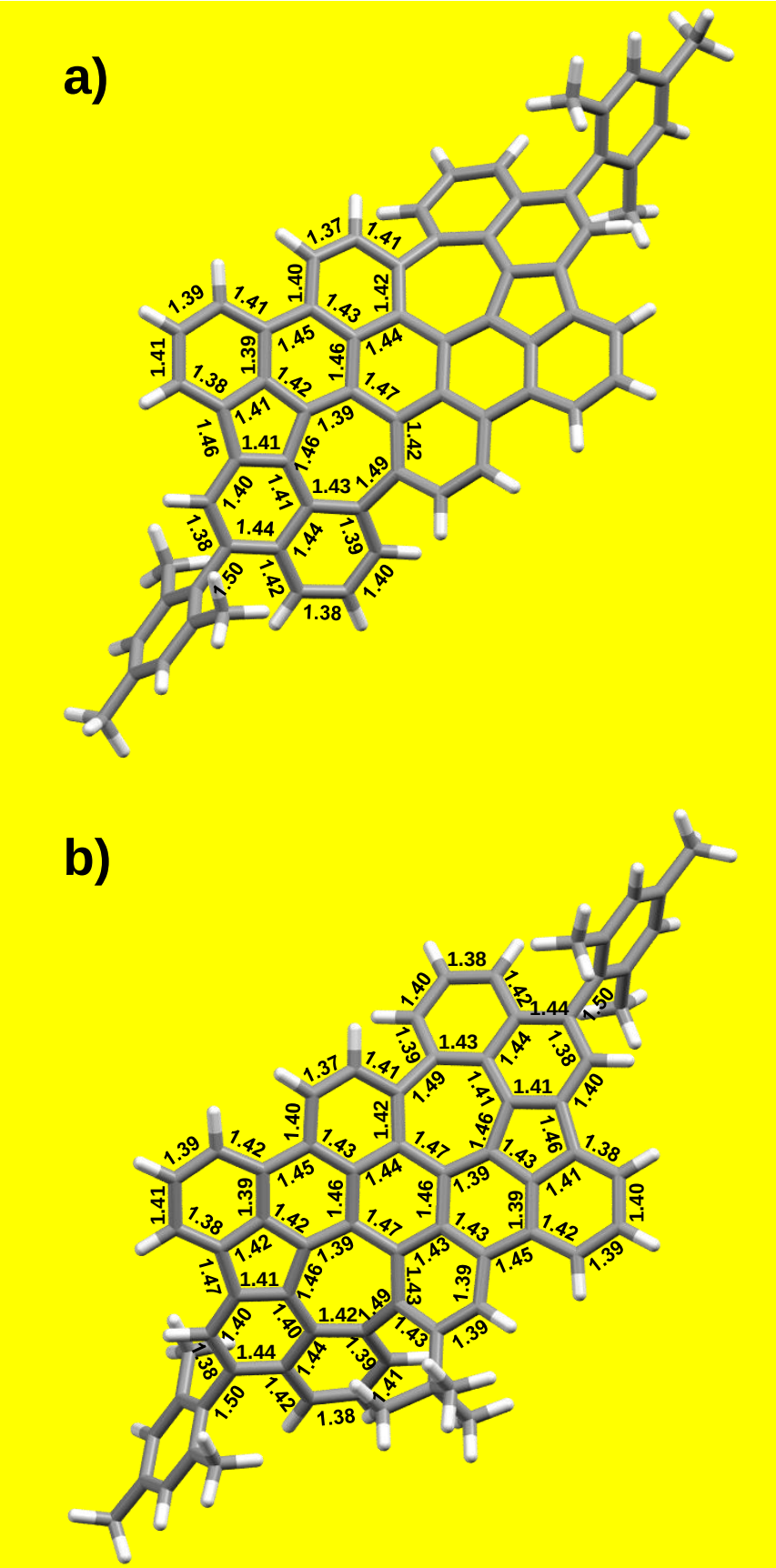

Figure S104. Bond lengths of the DFT (B3LYP/6-311G*) optimized models of two de-tert-butylated compounds **13** (a) and **14** (b). Bond lengths are given in Å.

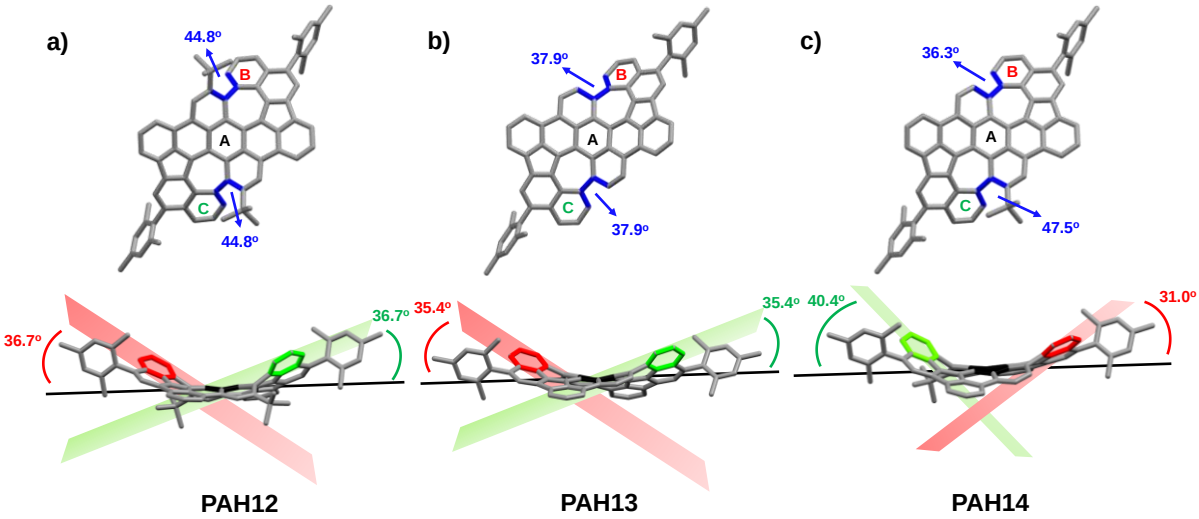

Figure S105. Curvature analysis of the DFT optimized models of compound **12** and two de-tert-butylated compounds **13** (a) and **14** (b). Values shown in upper figures are dihedral angles of indicated C-C bonds. Values shown in lower figures are angles between the plane of peripheral six-membered ring (B or C) with the plane of the central ring (A).

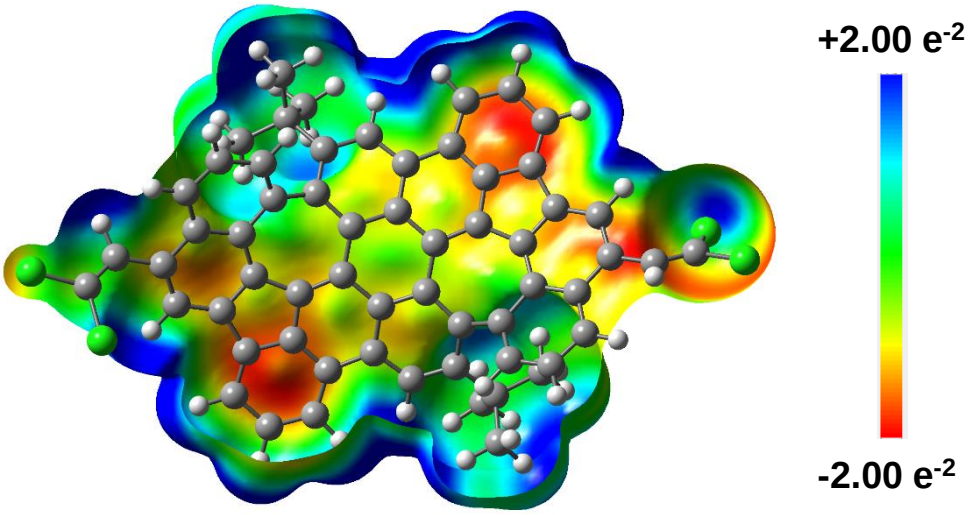

Figure S106. Electrostatic potential map of compound **10** drawn at the contour level of 0.0015 e·Å^{-3} calculated at the UB3LYP-GD3BJ/6-311G* level.

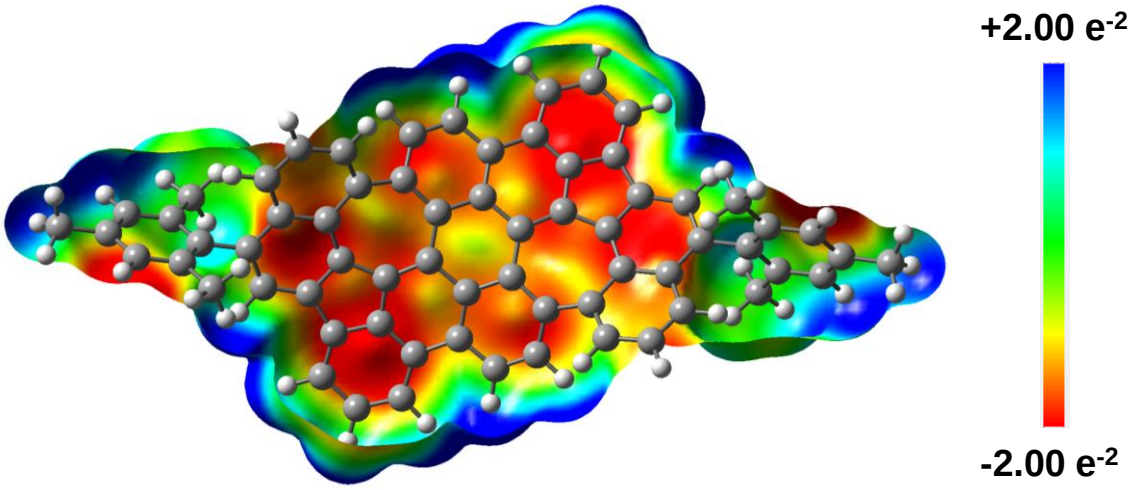

Figure S107. Electrostatic potential map of compound **13** drawn at the contour level of 0.0015 e·Å^{-3} calculated at the UB3LYP-GD3BJ/6-311G* level.

9. X-ray crystallographic structure determination

Table S1. Crystal data and structure refinement for **7**. (**CCDC 1922726**)

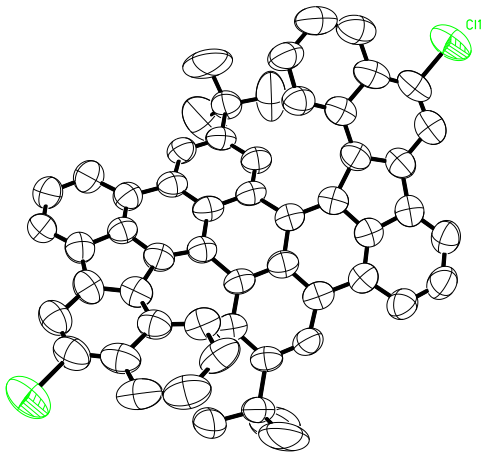

Empirical formula	$C_{56}H_{38}Cl_2$
Formula weight	781.76
Temperature	297(2) K
Wavelength	1.54178 Å
Crystal system	monoclinic
Space group	P2/c
Z	8
Unit cell dimensions	a = 28.3050(11) Å α = 90 deg.
	b = 14.9503(4) Å β =113.096(3) deg.
	c = 21.8942(8) Å γ = 90 deg.
Volume	8522.3(5) $Å^3$
Density (calculated)	1.22 g/cm^3
Absorption coefficient	1.65 mm^{-1}
Crystal shape	polyhedron
Crystal size	0.120 x 0.090 x 0.022 mm^3
Crystal colour	red
Theta range for data collection	2.2 to 55.1 deg.
Index ranges	$-29 \le h \le 30$, $-12 \le k \le 15$, $-22 \le l \le 23$
Reflections collected	48910
Independent reflections	10725 (R(int) = 0.0659)
Observed reflections	5842 ($I > 2\sigma(I)$)
Absorption correction	Semi-empirical from equivalents
Max. and min. transmission	1.23 and 0.76
Refinement method	Full-matrix least-squares on F^2
Data/restraints/parameters	10725 / 2544 / 1046
Goodness-of-fit on F^2	1.56
Final R indices (I>2sigma(I))	R1 = 0.134, wR2 = 0.354
Largest diff. peak and hole	0.95 and -0.63 $eÅ^{-3}$

Table S2. Crystal data and structure refinement for **10**. (**CCDC 1922727**)

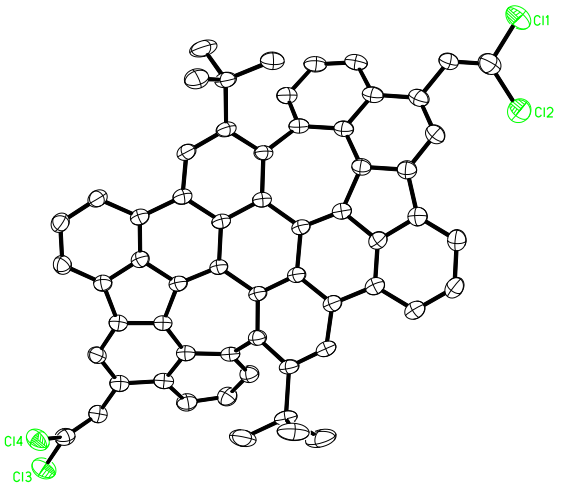

Empirical formula	$C_{60}H_{36}Cl_4$	
Formula weight	898.69	
Temperature	200(2) K	
Wavelength	1.54178 Å	
Crystal system	monoclinic	
Space group	C2/c	
Z	8	
Unit cell dimensions	a = 28.8347(5) Å	α = 90 deg.
	b = 15.4719(4) Å	β =108.238(1) deg.
	c = 19.7496(4) Å	γ = 90 deg.
Volume	8368.2(3) $Å^3$	
Density (calculated)	1.43 g/cm^3	
Absorption coefficient	2.90 mm^{-1}	
Crystal shape	needle	
Crystal size	0.272 x 0.048 x 0.025 mm^3	
Crystal colour	brown	
Theta range for data collection	3.3 to 72.1 deg.	
Index ranges	$-35 \le h \le 31$, $-18 \le k \le 18$, $-13 \le l \le 23$	
Reflections collected	27323	
Independent reflections	7885 (R(int) = 0.0196)	
Observed reflections	6349 ($I > 2\sigma(I)$)	
Absorption correction	Semi-empirical from equivalents	
Max. and min. transmission	1.43 and 0.77	
Refinement method	Full-matrix least-squares on F^2	
Data/restraints/parameters	7885 / 0 / 583	
Goodness-of-fit on F^2	1.02	
Final R indices (I>2sigma(I))	R1 = 0.052, wR2 = 0.142	
Largest diff. peak and hole	0.47 and -0.72 $eÅ^{-3}$	

Table S3. Crystal data and structure refinement for **14**. (**CCDC 1922728**)

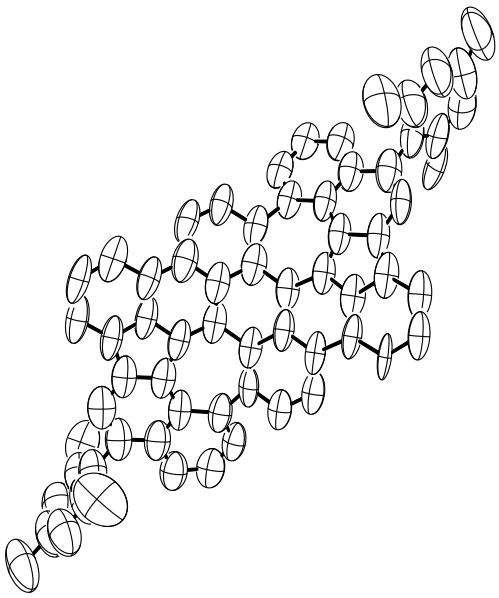

Empirical formula	$C_{66}H_{40}$	
Formula weight	832.98	
Temperature	200(2) K	
Wavelength	1.54178 Å	
Crystal system	monoclinic	
Space group	Pc	
Z	4	
Unit cell dimensions	a = 21.28(3) Å	α = 90 deg.
	b =7.487(6) Å	β =98.1(1) deg.
	c = 29.21(3) Å	γ = 90 deg.
Volume	4606(9) $Å^3$	
Density (calculated)	1.20 g/cm^3	
Absorption coefficient	0.52 mm^{-1}	
Crystal shape	needle	
Crystal size	0.171 x 0.036 x 0.022 mm^3	
Crystal colour	red	
Theta range for data collection	3.9 to 42.5 deg.	
Index ranges	$-18 \le h \le 17$, $-6 \le k \le 6$, $-25 \le l \le 25$	
Reflections collected	12772	
Independent reflections	5238 (R(int) = 0.0616)	
Observed reflections	2602 ($I > 2\sigma(I)$)	
Absorption correction	Semi-empirical from equivalents	
Max. and min. transmission	1.28 and 0.75	
Refinement method	Full-matrix least-squares on F^2	
Data/restraints/parameters	5238 / 3108 / 1009	
Goodness-of-fit on F^2	1.10	
Final R indices (I>2sigma(I))	R1 = 0.082, wR2 = 0.164	
Absolute structure parameter	4.5(10)	
Largest diff. peak and hole	0.18 and -0.14 $eÅ^{-3}$	

10. Temperature dependant ^{1}H NMR of PAH 13

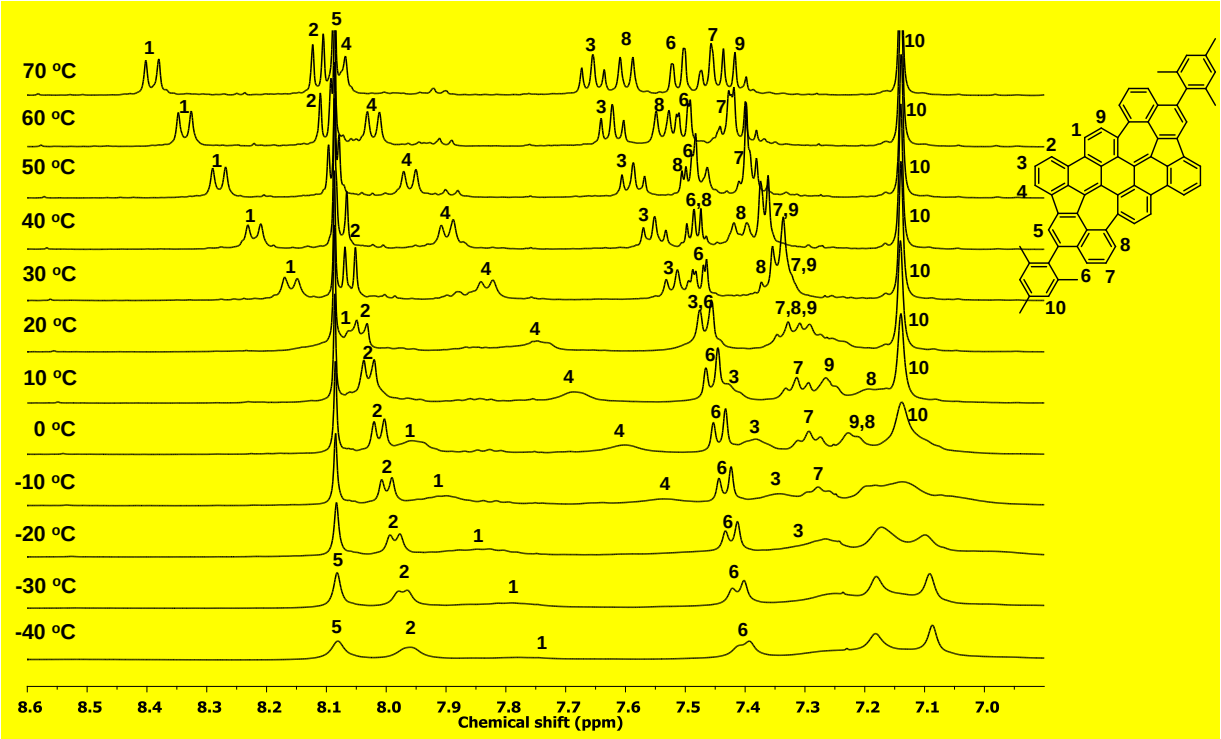

Figure S108. ^{1}H NMR spectra (400 M, $Cl_2CDCDCl_2$, *c*= 2.4 mmol·L^{-1}) of compound **13** at various temperatures.

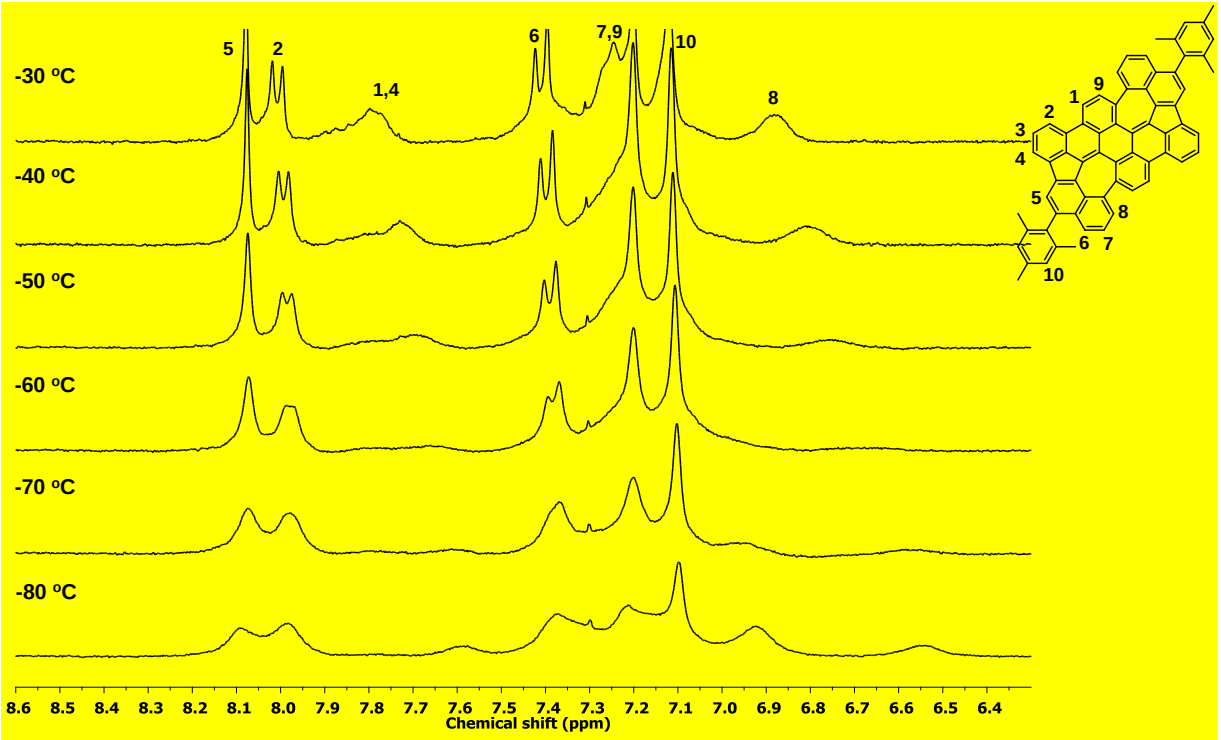

Figure S109. ^{1}H NMR spectra (300 M, CD_2Cl_2, *c*= 2.4 mmol·L^{-1}) of compound **13** at low temperature.

11. Chiral HPLC chromatogram

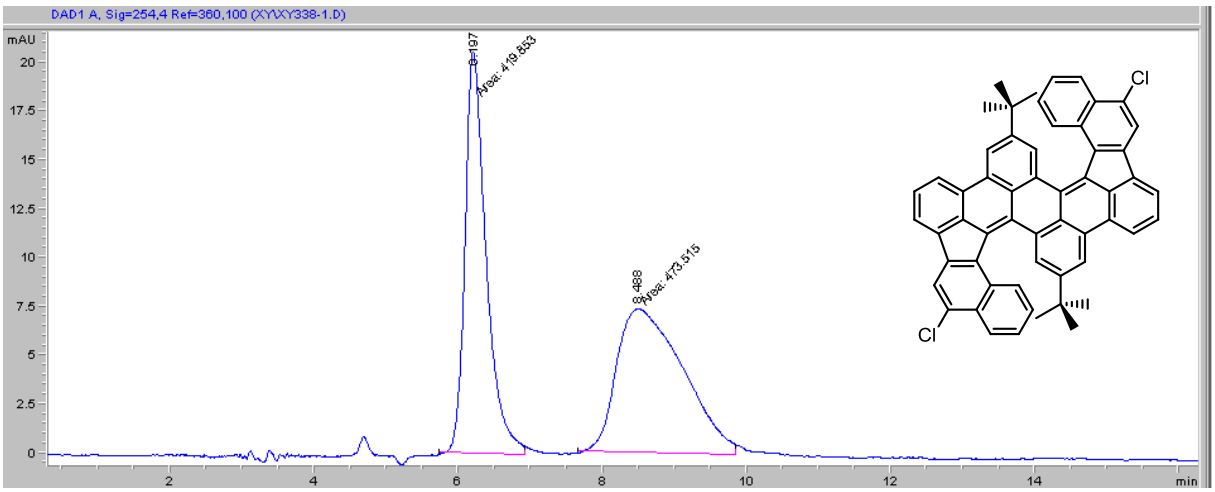

Figure S110. Chiral HPLC chromatogram of compound **7**. The chromatogram was obtained using an analytical column packed with amylose tris(3,5-dimethylphenylcarbamate) (AD-H) coated on 5 µm silica gel with *n*-hexane:isopropanol (99:1) as eluent at a flow rate of 0.7 mL/min.

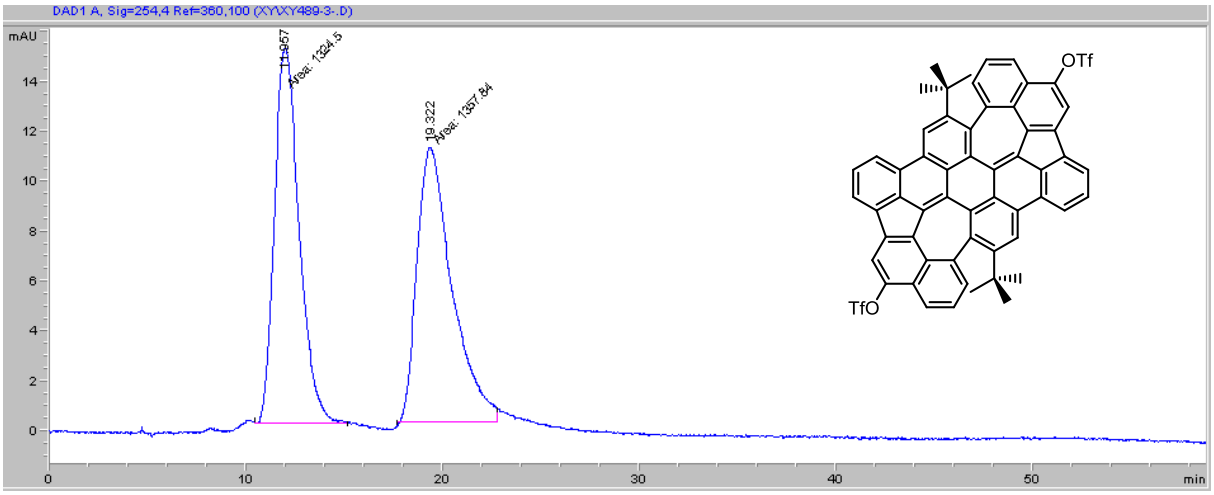

Figure S111. Chiral HPLC chromatogram of PAH **8**. The chromatogram was obtained using an analytical column packed with amylose tris(3,5-dimethylphenylcarbamate) (AD-H) coated on 5 µm silica gel with *n*-hexane:isopropanol (99:1) as eluent at a flow rate of 0.7 mL/min.

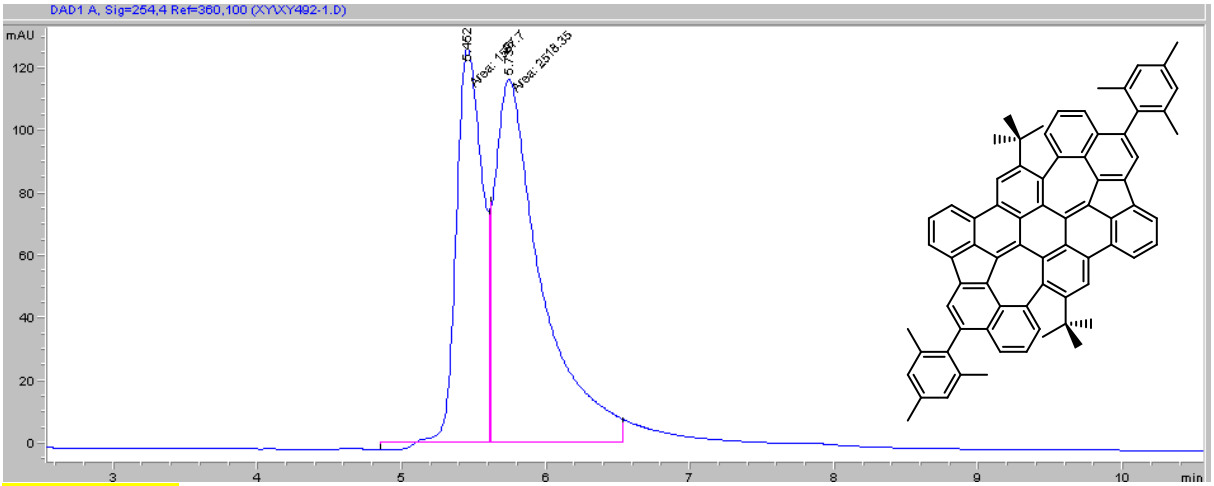

Figure S112. Chiral HPLC chromatogram of PAH **12**. The chromatogram was obtained using an analytical column packed with amylose tris(3,5-dimethylphenylcarbamate) (AD-H) coated on 5 µm silica gel with *n*-hexane:isopropanol (99:1) as eluent at a flow rate of 0.7 mL/min.

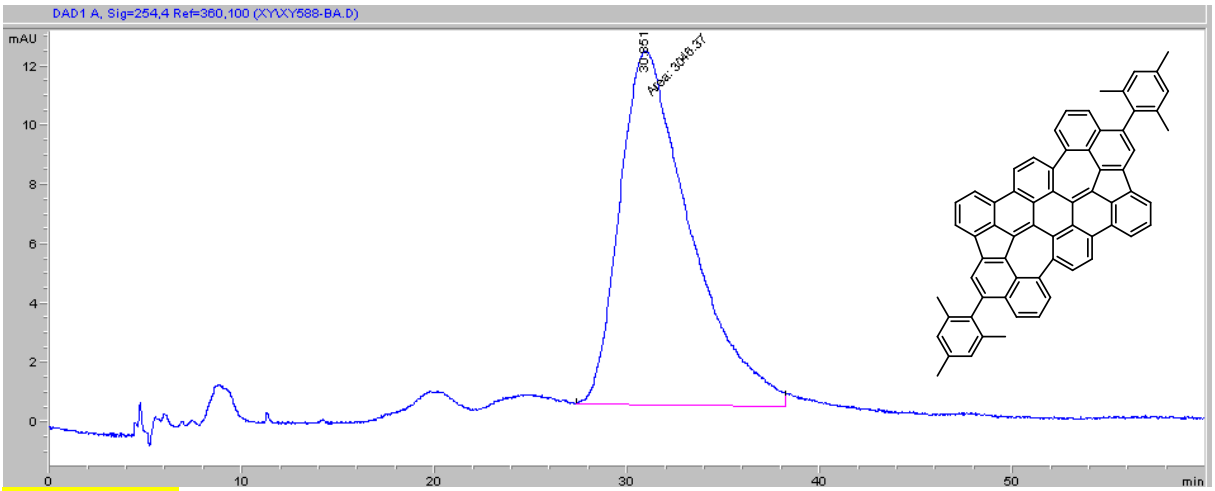

Figure S113. Chiral HPLC chromatogram of PAH **13**. The chromatogram was obtained using an analytical column packed with amylose tris(3,5-dimethylphenylcarbamate) (AD-H) coated on 5 µm silica gel with *n*-hexane:isopropanol (99:1) as eluent at a flow rate of 0.7 mL/min.

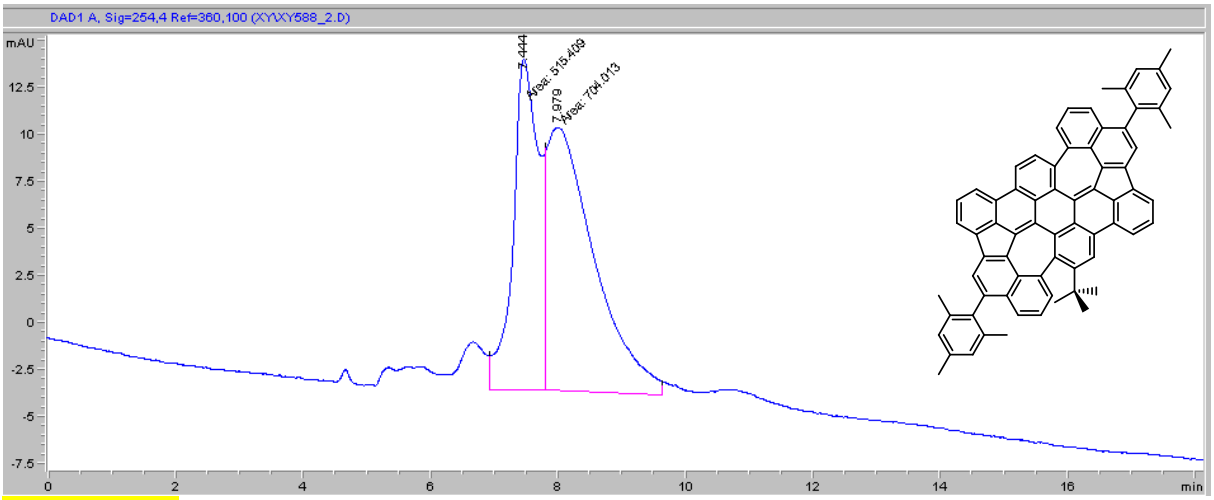

Figure S114. Chiral HPLC chromatogram of PAH **14**. The chromatogram was obtained using an analytical column packed with amylose tris(3,5-dimethylphenylcarbamate) (AD-H) coated on 5 µm silica gel with *n*-hexane:isopropanol (99:1) as eluent at a flow rate of 0.7 mL/min.

12. References

[S1] C. Würth, M. Grabolle, J. Pauli, M. Spieles, U. Resch-Genger, *Nat. Protocols* **2013**, *8*, 1535-1550.

[S2] G. Zhang, F. Rominger, U. Zschieschang, H. Klauk, M. Mastalerz, *Chem. Eur. J.* **2016**, *22*, 14840-14845.

[S3] M. J. Frisch, G. W. Trucks, H. B. Schlegel, G. E. Scuseria, M. A. Robb, J. R. Cheeseman, G. Scalmani, V. Barone, G. A. Petersson, H. Nakatsuji, X. Li, M. Caricato, A. V. Marenich, J. Bloino, B. G. Janesko, R. Gomperts, B. Mennucci, H. P. Hratchian, J. V. Ortiz, A. F. Izmaylov, J. L. Sonnenberg, Williams, F. Ding, F. Lipparini, F. Egidi, J. Goings, B. Peng, A. Petrone, T. Henderson, D. Ranasinghe, V. G. Zakrzewski, J. Gao, N. Rega, G. Zheng, W. Liang, M. Hada, M. Ehara, K. Toyota, R. Fukuda, J. Hasegawa, M. Ishida, T. Nakajima, Y. Honda, O. Kitao, H. Nakai, T. Vreven, K. Throssell, J. A. Montgomery Jr., J. E. Peralta, F. Ogliaro, M. J. Bearpark, J. J. Heyd, E. N. Brothers, K. N. Kudin, V. N. Staroverov, T. A. Keith, R. Kobayashi, J. Normand, K. Raghavachari, A. P. Rendell, J. C. Burant, S. S. Iyengar, J. Tomasi, M. Cossi, J. M. Millam, M. Klene, C. Adamo, R. Cammi, J. W. Ochterski, R. L. Martin, K. Morokuma, O. Farkas, J. B. Foresman, D. J. Fox, *Gaussian 09, Revision D.01*, Gaussian Inc., Wallingford, CT, **2013**.